SYNTHESIS AND STUDY OF MODIFIED-NANOCRYSTALLINE CELLULOSE EFFECTIVE FOR SO_2 CAPTURE

Raheleh Zafari

Thesis submitted to the University of Ottawa
in partial Fulfillment of the requirements for the
Master of Applied Science

Department of Chemical and Biological Engineering
Faculty of Engineering
University of Ottawa

© Raheleh Zafari, Ottawa, Canada, 2021

ABSTRACT

One of today's world's main challenges is access to a clean environment. The release of hazardous and toxic gases from burning fossil fuels is of critical concern due to these gases' destructive effects on the nearby atmosphere. Among these, acid rain is one of the most severe consequences of air pollution caused by sulfur dioxide (SO_2) gas and still needs to be better addressed. One of the solutions is the adsorption-based technologies because of their ease of use, possible high adsorption capacity, minimum environmental impact, low cost, and efficient sorbate recovery possibilities. Gas separation via adsorption is not yet widely employed commercially since it needs regenerable, high-durable, high-performance, and cost-effective adsorbents. One of the common methods of absorbing acid gases is the use of amino absorbents that have disadvantages such as create many waste materials challenging to regenerate, wastewater, and waste gas. Therefore, incorporating amine groups on the surface of solids to overcome the problem of regeneration has attracted considerable attention in gas uptake**.**

In this project, we proposed to functionalize nanocrystalline cellulose (NCC) using a solvent-free method to boost their SO_2 interactions and thus their adsorption capability. Therefore, a commercial NCC material was modified using ethylenediamine (EDA) in a green and straightforward amination approach in order to tune its surface basicity and obtain an efficient green-biobased adsorbent. Since the substitution process of amines with hydroxyl groups on the cellulose surface is carried out through dangerous halogen solvents, we used the solvent-free one-step method and investigated the synthetic parameters.

Amination conditions of NCC adsorbents were optimized via the effects of the amination temperature, the amination time, and the amount of EDA on their physical properties and their performance for SO_2 adsorption. The sorbents were characterized using attenuated total reflection-Fourier-transform infrared spectroscopy (ATR-FTIR), solid carbon nuclear magnetic resonance (^{13}CNMR), X-ray diffraction (XRD), thermogravimetric analysis (TGA), and scanning electron microscopy- energy-dispersive X-ray spectroscopy (SEM-EDS) to see if EDA was incorporated into the NCC and investigate the changes in thermal stability of adsorbents by changing synthesis conditions. Sorbents were then tested for SO_2 capture at the same conditions of room temperature

(RT), atmospheric pressure, and a flow rate of 20 ml/min, which was selected based on previous studies to optimize flow rate in the same research group. The optimal conditions to create an effective sulfur dioxide adsorbent were found to be 70 ^{o}C for 8 hours of amination. At ideal conditions, the NCC modified had an SO_2 adsorption capacity value of 0.030 mg/100 mg. The promising properties of EDA-NCC in terms of adsorption capacity (showing a significant increase in capacity when compared to the NCC at atmospheric pressure and ambient temperature) make them potential adsorbent candidates.

In addition, the impacts of SO_2 capture operating conditions on adsorption capacity were evaluated. By varying the adsorption temperature from room temperature to 60 °C and the feed flow rate from 10 to 30 ml min^{-1}, fixed-bed breakthrough studies for SO_2 adsorption onto NCC and modified-NCC adsorbent (prepared at 70^{o}C, 3hr, and EDA/NCC=25) were carried out. Over the range of operating parameters studied, the greatest SO_2 capacity and breakthrough time values were obtained with adsorbent at room temperature and 20 ml min^{-1} input flow rate. As expected, due to the exothermic nature of the adsorption process, the amount of SO_2 adsorbed at equilibrium decreased with increasing temperature. It was also observed that as the flow rate increases, the breakthrough time decreases due to the higher flow rate of the feed gas was accompanied by the faster transport of the adsorbate molecules and leading to a shorter breakthrough time, as expected.

Finally, another EDA functionalization method was tested, using a two-step method. First, cellulose was functionalized using citric acid (CA), and then the EDA was incorporated via carboxylic acid functional groups in the CA to obtain both amide and amine groups on the NCC's surface. This approach aimed to compare EDA deposition on cellulose surface via a different method by adding one more functional group and evaluating their performance in SO_2 gas adsorption. It was concluded that oxygenated functional groups and groups with low alkalinity, such as carboxylic acid and amide, can negatively affect gas adsorption. These results were concluded by comparing two adsorbents, one containing only amine groups and the other adsorbent containing amide and carboxylic acid groups in addition to the amine group, although the amine content of the two adsorbents was different. Future research will explore the mechanisms and capturing phenomena to improve capturing capacity and process applicability as well as the material optimal regeneration operating conditions.

RÉSUMÉ

L'un des principaux défis mondiaux d'aujourd'hui est l'accès à un environnement propre. La libération de gaz dangereux et toxiques provenant de la combustion de combustibles fossiles est une préoccupation majeure en raison des effets destructeurs de ces gaz sur l'atmosphère voisine. Parmi ceux-ci, les pluies acides sont l'une des conséquences les plus graves de la pollution atmosphérique causée par le dioxyde de soufre (SO_2) et constituent encore une problématique de nos jours. Une solution réside dans les technologies basées sur l'adsorption en raison de leur facilité d'utilisation, de leur capacité d'adsorption élevée, de leur faible impact environnemental, de leur faible coût et des possibilités efficaces de récupération de l'adsorbat. La séparation des gaz par adsorption n'est pas encore largement utilisée commercialement, car elle nécessite des adsorbants régénérables, hautement durables, performants et rentables. L'une des méthodes courantes d'absorption des gaz acides est donc l'utilisation d'absorbants aminés qui présentent toutefois des inconvénients tels que la création de nombreux déchets difficiles à régénérer, d'eaux usées et de gaz résiduaires. Par conséquent, l'incorporation de groupes amines à la surface d'adsorbants solides pour surmonter le problème de la régénération a attiré une attention considérable dans l'absorption de gaz.

Dans ce projet, nous avons proposé de fonctionnaliser la cellulose nanocristalline (NCC) en utilisant une méthode sans solvant pour améliorer l'interaction avec le SO_2 et donc sa capacité d'adsorption. Par conséquent, un matériau NCC commercial a été modifié à l'aide d'éthylènediamine (EDA) dans une approche d'amination verte et directe afin d'ajuster sa basicité de surface et d'obtenir un adsorbant bio-sourcé efficace. Étant donné que le processus de substitution des amines par des groupes hydroxyles à la surface de la cellulose est généralement effectué à l'aide de solvants halogènes dangereux, nous avons utilisé la méthode en une étape sans solvant à plus haute température et étudié les paramètres de synthèse.

Les conditions d'amination des adsorbants NCC ont été optimisées en étudiant les effets de la température d'amination, du temps d'amination et de la quantité d'EDA sur leurs propriétés physiques et leurs performances pour l'adsorption du SO_2. Les absorbants ont été caractérisés par réflexion totale atténuée-spectroscopie infrarouge à transformée de Fourier (ATR-FTIR), résonance magnétique nucléaire du carbone solide (^{13}CNMR), diffraction des rayons X (XRD), analyse thermogravimétrique (TGA) et microscopie électronique à balayage-énergie-

spectroscopie à rayons X dispersifs (SEM-EDS) pour voir si l'EDA a été incorporé dans le NCC et étudier les changements de stabilité thermique des adsorbants en changeant les conditions de synthèse. Les absorbants ont ensuite été testés pour la capture du SO_2 dans les mêmes conditions de température ambiante (RT), de pression atmosphérique et un débit de 20 ml/min, qui a été sélectionné sur la base d'études précédentes pour optimiser le débit, effectuées dans le groupe de recherche. Les conditions optimales pour créer un adsorbant de dioxyde de soufre efficace se sont avérées être de 70 °C pendant 8 heures d'amination. Dans des conditions idéales, une capacité d'adsorption de SO_2 de 0.030 mg/100 mg a été obtenue. Les propriétés prometteuses de l'EDA-NCC en termes de capacité d'adsorption (montrant une augmentation significative de la capacité par rapport au NCC à pression atmosphérique et température ambiante) en font des potentiels candidats comme adsorbants.

De plus, les impacts des conditions opératoires de captage du SO_2 sur la capacité d'adsorption ont été évalués. En faisant varier la température d'adsorption de la température ambiante à 60 °C et le débit d'alimentation de 10 à 30 ml min^{-1}, des études de percée en lit fixe pour l'adsorption de SO_2 sur NCC et adsorbant NCC modifié (préparé à 70ºC, 3h et EDA /NCC=25) ont été réalisées. Sur la gamme des paramètres de fonctionnement étudiés, les plus grandes valeurs de capacité de SO_2 et de temps de percée ont été obtenues avec l'adsorbant à température ambiante et un débit d'entrée de 20 ml min^{-1}. Comme prévu, en raison de la nature exothermique du processus d'adsorption, la température affecte de manière significative la quantité d'adsorbat. Par conséquent, à une pression donnée, la quantité de SO_2 adsorbée à l'équilibre diminue avec l'augmentation de la température. Il a également été observé que lorsque le débit augmente, le temps de percée diminue en raison du débit plus élevé du gaz d'alimentation s'accompagnant d'un transport plus rapide des molécules d'adsorbat et conduisant à un temps de percée plus court, comme prévu.

Enfin, une autre méthode de fonctionnalisation EDA a été testée, en utilisant une méthode en deux étapes. Tout d'abord, la cellulose a été fonctionnalisée à l'aide d'acide citrique (CA), puis l'EDA a été incorporé via des groupes fonctionnels d'acide carboxylique dans le CA pour obtenir à la fois des groupes amide et amine à la surface de la NCC. Cette approche visait à comparer le dépôt d'EDA sur la surface de la cellulose via une méthode différente en ajoutant un groupe fonctionnel supplémentaire et en évaluant leurs performances dans l'adsorption de gaz SO_2. Il a été conclu que les groupes fonctionnels oxygénés et les groupes à faible alcalinité, tels que l'acide carboxylique

et l'amide, peuvent affecter négativement l'adsorption des gaz. Ces résultats ont été conclus en comparant deux adsorbants, l'un ne contenant que des groupes amine et l'autre adsorbant contenant des groupes amide et acide carboxylique en plus du groupe amine, bien que la teneur en amine des deux adsorbants soit différente. Les recherches futures exploreront les mécanismes et les phénomènes de capture pour améliorer la capacité de capture et l'applicabilité du procédé ainsi que les conditions de fonctionnement optimales de la régénération des matériaux.

Dedication

I dedicate this thesis to my *parents* and *siblings* for their endless support, guidance, and love and to my *friends* and *colleagues* who helped me to proceed in my education and life.

Statement of Contributions

I declare that I am the first author of all the chapters written in this thesis. I acknowledge the supervision of Prof. Clémence Fauteux-Lefebvre on the work described in this thesis, her editorial comments on the written document, and her scientific guidance in preparing and performing laboratory experiments. **Chapter 1** is the introduction to the thesis work and a brief description of the problems, thesis objectives, and an overview of the thesis. **Chapter 2** presents the literature review which provides a detailed insight into the problem and the steps taken to mitigate sulfur dioxide. It moves forward with an introduction to the solution suggested in this thesis work, functionalization, and applications. **Chapters 3 and 4** are written in paper format and intended to be submitted to scientific journals. **Chapter 5** concludes the thesis work and provides some prospective future work.

Chapter 3: Amine-functionalized Nanocrystalline Cellulose based adsorbent efficient for SO_2 capture

Fabrication of all samples, SO_2 capture testing, and physicochemical characterizations of samples were carried out by Raheleh Zafari with Dr. Fauteux-Lefebvre's supervision. The SO_2 setup was built by Dr. Fauteux-Lefebvre's previous students. The idea of using cellulose for SO_2 capture applications was first proposed by Dr. Fauteux-Lefebvre and developed by Raheleh Zafari. Synthesis of sorbents carried out at Prof. Tom Baker's lab in science faculty along with Fernanda G. Mendonça (Postdoc researcher) guidance. The article was written by Raheleh Zafari. Finally, Dr. C. Fauteux-Lefebvre, critically reviewed and revised the article. Prof. Tom Baker and Fernanda G. Mendonça will participate in the analysis of the results and review of the paper.

Chapter 4: Modifying the surface of Nanocrystalline Cellulose with mixed functional groups: An efficient adsorbent for Sulfur Dioxide Capture

Fabrication of modified NCC, testing them for SO_2 capture application, and physicochemical characterizations of samples were carried out by Raheleh Zafari with Dr. Fauteux-Lefebvre's supervision. The article was written by Raheleh Zafari. Finally, Dr. C. Fauteux-Lefebvre critically reviewed and revised the article.

Acknowledgements

I would like to express my earnest gratitude to Prof. Clémence Fauteux-Lefebvre for her scientific guidance and support, and her mentorship throughout the duration of my study. The project would not have been successful without her continuous motivation, discussions, and time, effort, and support.

I also wish to thank Professor R. Tom Baker and his postdoc Fernanda G. Mendonça for their general guidance, assistance, and support throughout the duration of this research.

I would also like to thank the support staff member, Franco Ziroldo, for his technical and mechanical support. I would also like to thank the administrative staff, Francine Petrin, Frantz Célestin, and Chantal Dube.

I would like to thank Dr. Yun Liu for helping us out with the SEM and EDXS analysis, along with training of analytical devices for ATR-FTIR and TGA**.** I would like to thank Jeffrey Ovens and Peter Pallister for their training and valuable guidance on XRD and NMR.

I want to thank my friends and colleagues in Clémence's research group: Tanushree Sankar Sanyal and Xinlong Chen.

I am thankful to the Natural Sciences and Engineering Research Council of Canada, to Celluforce Inc., and to the University of Ottawa for their financial support.

TABLE OF CONTENTS

LIST OF FIGURES

LIST OF TABLES

ABBREVIATIONS

ATR-FTIR Attenuated total reflectance-Fourier transform infrared spectroscopy	**HCl** Hydrochloric acid
CA Citric acid	**NaOH** Sodium hydroxide
CA-NCC Citric acid modified nano crystalline cellulose	**NCC** Nanocrystalline Cellulose
DMF Dimethyl formamide	**NMR** Nuclear magnetic resonance spectroscopy
EDA-NCC Ethylenediamine modified nanocrystalline cellulose	**ppm** Parts per million
EDA Ethylenediamine	**SEM** Scanning electron microscopy
EDS Electron dispersive spectroscopy	**SO_2** Sulfur dioxide
EIA Energy Information Administration	**TGA** Thermogravimetric analysis
	XRD X-ray diffraction

1 INTRODUCTION

1.1. Overview

Despite the collective efforts and agreements to decrease greenhouse gas generation around the world, electricity generation from fossil fuels is still increasing with a predicted average annual raise of 0.2% from 2011 to 2040, according to the United States Energy Information Administration (EIA)[1]. Even if there is increased use of natural gas and alternative energy sources, coal continues to be the primary source for electricity production in many countries (Figure 1.1). In 2019, coal demand for power generation and industries dropped by 5% and 11%, respectively. However, with the economy forecast to revive significantly in 2021, energy demand is expected to rise by 7%, putting requests 2% higher than in 2019. As power demand rebounds, coal consumption is predicted to grow by over 9%, contributing the most to demand[2].

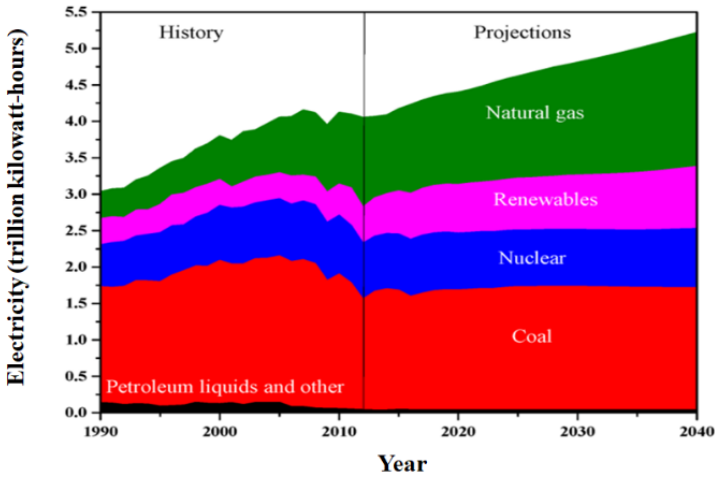

Figure 1.1 Electricity generation by fuel for 1990-2040 (10^{12} kwh) in the US[1]

The burning of fossil fuels causes the emissions of various pollutants, and among them, sulfur dioxides and nitrous oxides have major negative short-term environmental impacts and cause health diseases. 87% of emitted sulfur oxide (SO_x) and 67% of emitted nitrous oxide (NO_x) come from fossil-fuel power plants that release flue gas streams[1]. Sulfur dioxide (SO_2), a colorless and non-flammable gas, is the most poisonous and damaging SO_x species discharged into the environment. In addition to the combustion of sulfur-containing fossil fuels, major sources of SO_2

emissions are the smelting of sulfide ores and oil refining[3]. Apart from its disadvantages, SO_2 has a wide range of uses, including being a crucial intermediate in the production of sulphuric acid, pulp, and paper. SO_2 can also be used as a food preservative and disinfectant agent in the food industry, as a catalyst, co-catalyst, or solvent in the petroleum industry, and as a flotation depressant in the processing of sulfide ores[4]. On the other hand, when captured through desulphurization processes or produced on purpose, it can be mitigated or converted to other compounds, for example, to produce H_2SO_3 (sulfurous acid) and sulphuric acid (H_2SO_4). Nonetheless, its persistence and toxicity in the environment are a source of public concern, and reducing SO_2 levels is critical for environmental preservation[1],[5].

SO_2 gas is designed as the primary source of atmospheric contamination and is thought to be causing increasingly serious environmental and health issues. The negative impacts of SO_x emissions have prompted researchers to investigate and develop methods for purifying flue gas streams[6]. Since 2000, Canada has been reducing gas emissions through a variety of initiatives, including reducing the amount of sulfur in fuels and implementing a Canada-wide Acid Rain policy[7]. In 2010, for example, the total SO_2 gas emissions were roughly 57% below the established national capacity of 3.5 million short tonnes[7]. While Canada has been successful in lowering acid pollution, parts across the country, particularly in the east, have not yet been able to prevent acid deposition and are at a critical level of acid pollution[8]. In addition, as mentioned above, worldwide emissions are still increasing.

The impact of SO_x contamination on downstream carbon dioxide (CO_2) capture systems is another key application for SO_x removal. Although the removal of SO_x impurities is vital, the significant impact of this unwanted acid gas on CO_2 capture systems is another factor that must be carefully considered and for which very low SO_2 concentrations are required[9].

1.2. **Desulphurization technologies**

Generally, four major procedures for toxic gases like CO_2 and SO_2 removal have been used in industry: absorption, adsorption, cryogenic distillation, and membrane separation[10]. Absorption is the most common industrial technique, while adsorption is more actively explored and used to increase efficiency.

The flue gas desulfurization (FGD) technologies regroup the most common industrial SO_2 removal methods, primarily wet and semi-wet absorption-based, including limestone-gypsum and organic amine methods [1,5]. These approaches are generally irreversible and create many waste materials challenging to regenerate, wastewater, and waste gas. These traditional SO_2 removal technologies have the advantage of large-scale setup and maturity. Still, in addition to waste produced, the energy costs are high, and they generally cannot achieve very low concentrations (i.e., ppm level)[11]. There are regenerable adsorbent-based technologies using solid materials like zeolites, activated carbons, metal organic frameworks (MOF)s and are currently attracting interest [6]. In terms of cost and waste output, regenerable-based technologies outperform their non-renewable equivalents. Although one can accomplish this by using new adsorbents, one of the significant barriers to the proliferation of such technologies is the development of efficient materials, which are still in their early stages of development[8].

As a result, developing alternative, lower-cost, energy-efficient SO_2 removal solutions are critical. Compared to traditional absorption with liquid solvents, adsorption separation and purification of gas mixtures is a viable option because of its ease of use, possible high adsorption capacity, minimum environmental impact, low cost, and efficient sorbate recovery possibilities.[12]. In particular, pressure-swing adsorption (PSA) has several appealing features, including its application over a wide range of temperature and pressure settings, low energy requirements, and cheap capital investment costs.[13]. Over the last three decades, there has been a tremendous increase in research and commercial applications of PSA techniques for removing SO_2 from diverse flue-gas mixes. Adsorption separation for SO_2 capture in flue-gas applications would undoubtedly benefit from developing a readily regenerated and durable adsorbent with fast adsorption/desorption kinetics, high selectivity, and high adsorption capacity.[14].

1.3. **Research objectives**

This project aims to build a high-performance sorbent for SO_2 capture made up of modified nanocrystalline cellulose (NCC), with the surface modification of NCC to enhance its interaction with SO_2 and increase adsorption capacity. NCC has been chosen because it is the most abundant natural polymer, is a low-cost versatile material, offers crystalline structure, and can be functionalized through the hydroxyl groups. Since SO_2 is an acidic gas, we used ethylene diamine, which has a basicity property to functionalize the surface of cellulose, with solvent-free

functionalization method. The hypothesis is that in this case, acid-base or electrophilic-nucleophilic interaction occurs between the acidic SO_2, and the amine base groups. The following are the thesis's specific goals:

- Functionalize NCC with ethylenediamine (EDA) through a non-toxic, simple, and one-step method;
- Functionalize NCC using citric acid pre-treatment and EDA in a two-step method;
- Optimize the amination conditions of NCC adsorbents to maximize their SO_2 adsorption capacities;
- Measure the adsorption capacity and study the breakthrough curves of SO_2 onto the ammonia modified and untreated NCC adsorbents;
- Study the effect of different temperatures and flow rates in the gas stream for SO_2 capture.

1.4. Thesis organization

There are five chapters in this thesis. The first chapter provides an overview as well as research objectives. The Literature Review in Chapter 2 covers the current state-of-art technologies used to reduce SO_2 levels, followed by an introduction to cellulose and its characteristics, and then cellulose functionalization. The third and fourth chapters are written in an article format. The manufacturing, characterization, and assessment of EDA-NCC adsorbents for SO_2 capture are discussed in Chapter 3. Chapter 4 examines the performance of an adsorbent for SO_2 removal and focuses on EDA-NCC fabrication using a new approach with the citric acid pre-treatment. The results of Chapters 3 and 4 can be used to evaluate the suitability of amine-functionalized cellulose for SO_2 capture. The general conclusions of this research project are presented in Chapter 5, along with recommendations for future research.

2 LITERATURE REVIEW

2.1 The ideal adsorbent for SO_2

The previous section discussed some scenarios in which SO_2 removal is required and some existing capturing technologies. The "adsorption-based" procedures will be the emphasis of this thesis. A sorbent and a sorbate are needed for any sorption (adsorption or absorption) based process. Pressure/Vacuum or Temperature Swing Adsorption (PSA, VSA, or TSA) are all adsorption procedures that need an adsorbent[15],[8].

2.1.1 Targeted properties

There are various factors to consider while selecting an adsorbent. In this section, some of the most typical requirements for a "good" adsorbent are described for the case of SO_2 capture. In terms of SO_2 removal, the adsorbent serves as a "host" for the gas. Hence its SO_2 capacity is critical. When an adsorbent's SO_2 capacity is limited, the entire process becomes inefficient since the adsorbent must be regenerated frequently to remove adsorbed SO_2 from the adsorbent. Adsorbents with a high SO_2 capacity are attractive because they can improve SO_2 capture efficiency and save costs.

On the other hand, having the largest SO_2 capacity (SO_2 capacity at saturation) may not be necessary for particular processes, primarily when very low outlet concentration is aimed. The material's working capacity, under specific process conditions, is then often more critical than its maximal capacity.

SO_2 capacity of an adsorbent that may be retained and reused after the adsorption/desorption process is known as its cyclic capacity. The adsorbent's SO_2 capacity should ideally remain constant throughout its lifetime. If the adsorbent is not stable under operating conditions, it may lose its SO_2 capacity as the number of cycles increases. The loss of SO_2 capacity affects the effectiveness of the SO_2 removal process, diminishes the adsorbent's lifetime, and can increase the cost of SO_2 capture. Because of the shorter lifespan, the adsorbent will need to be replaced more regularly, and there will be an increase in waste material production. The production of heavily adsorbed (chemisorbed) SO_2, or SO_2 trapped inside the material, is another way the SO_2 capacity decreases with the number of cycles. As a result, these SO_2 molecules are unable to be desorbed. Both types of SO_2 are challenging to remove and can raise the cost of production[17].

SO_2 capture at point sources almost has the SO_2 in a mixture with other gases. For instance, flue gas from a coal power plant can contain SO_2 in a mixture with mainly N_2. If adsorption processes are used to remove SO_2 from flue gas, it is important that the adsorbent can separate SO_2 from these other gases. Adsorption of the other gas will compromise the SO_2 uptake, decreasing the SO_2 removal efficiency. Furthermore, the desorbed gas will not be pure SO_2. Ideally, the adsorbent should exclusively adsorb SO_2 and adsorb no other sorbates. This means that the adsorbent should also be hydrophobic, as the adsorption of water will also lower the SO_2 uptake[18].

Any industrial process should always be maintained as inexpensive as possible. The cost of capturing SO_2 can be evaluated as a function of capital and operating costs. As a result, these costs should be maintained to a bare minimum. Heat exchangers, dehydration units, compressors, and adsorption units are typical capital expenses for an adsorption system. Because a big amount of adsorbent is normally required to fill the adsorbers, the cost of the adsorbent contributes significantly to the cost of SO_2 capture. A low-cost adsorbent necessitates a low-cost raw material for its production. It is worth noting that the link between the cost of SO_2 capture and the cost of the adsorbent is influenced by the adsorbent's qualities. For example, a hypothetical adsorbent with much higher SO_2 removal efficiency and a longer lifetime than zeolite may nonetheless be more cost-efficient than low-cost SO_2 capture with zeolite despite having a higher production cost. In summary, regardless of its qualities, the adsorbent cost should be optimized[19].

Finally, the material's thermal and mechanical stability is critical when it comes to adsorbents. For SO_2 capture, an adsorbent must be able to resist the operating conditions and environment it is subjected to. Heat exchangers commonly chill flue gas before it reaches the adsorption unit in a coal-fired power station. As a result, an adsorbent must be structurally sound efficient at this temperature. Moreover, for SO_2 capture application, room temperature could be an appropriate operational temperature[19].

2.2 Classification of adsorbents

Adsorption technologies for depollution have gained interest in recent years due to their comparatively simple design and ease of operation for the elimination of toxic gases. Metal oxides [50], zeolites [23], activated carbon (AC), carbon nanotubes (CNT)[63], graphene oxides

(GO)[63], , metal-organic framework (MOF)[39], polymers, bio-adsorbents, and other adsorbents have all been studied for SO_2 capture so far[20]. Nanomaterials have gained prominence as potential adsorbents for environmental toxins over the last decade, drawing more attention to the subject[21]. Nanostructured materials often offer higher adsorption capabilities and binding affinities than their macroscale counterparts as adsorbents[22]. Because of the small size, high specific surface area, and dominance of interfacial processes, they have specific nanoscale properties.

Furthermore, the possibility to tune surface properties via nanomaterial surface modification opens the door to new possibilities in environmental cleanup. Furthermore, nanoparticles are an option to be investigated; nevertheless, they should be handled with caution for safety reasons [22]. Figure 2.1 shows some of the most used materials as possible adsorbents following their classes for environmental remediation.

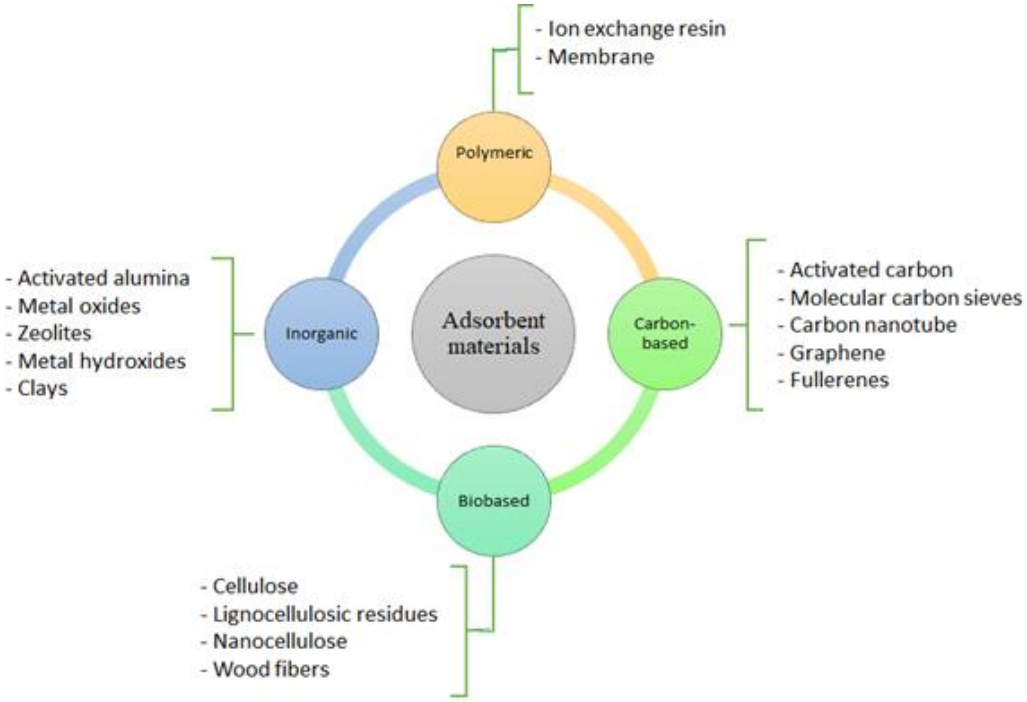

Figure 2.1 The most frequently used adsorbent materials for environmental remediation[22]**.**

2.3 Solid adsorbent materials for SO_2

2.3.1 Zeolites

The development of innovative technologies to remove and capture sulfur gases (H_2S and SO_2) in porous materials like zeolites is of interest to scientists all over the world. Zeolites are porous pure silica or aluminosilicate frameworks produced by SiO_4^- tetrahedra or a combination of SiO_4 and AlO_4^- tetrahedra sharing a vertex whose framework are open structures with cations positioned within the material's pores (Fig 2.2) and have been used in catalysis, gas separation, and ionic exchange applications[23].

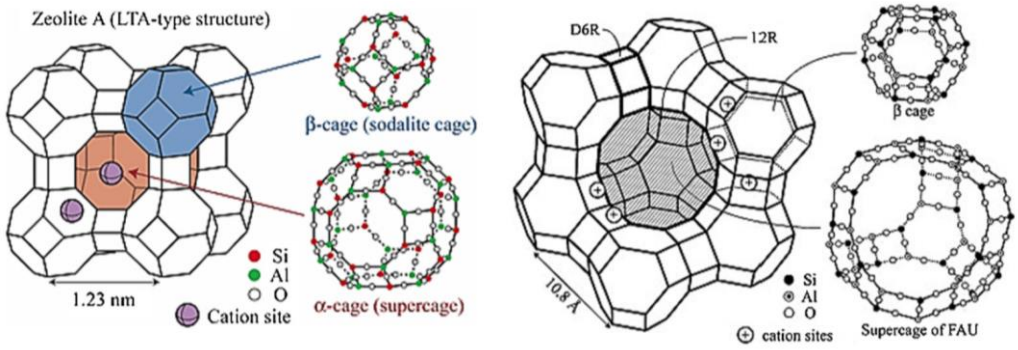

Figure 2.2 the framework structure of zeolite A (LTA-type structure)[24]

The use of zeolite X, zeolite Y, and silicate for SO_2 capture has yielded excellent results. Kopac et al. [25] studied molecular sieve 13X for SO_2 adsorption at temperatures ranging from 250°C to 400°C and found that it has a significant adsorption capability at 250°C. When Kopac and colleagues[26] tested zeolite 4A over the temperature range of 250-445 °C, they found that it had a higher SO_2 adsorption capability than zeolite 5A[27].

The adsorption of SO_2 onto the clinoptilolite-rich zeolite tuff was studied by Alver et al.[28]. At two different temperatures (273 K and 293 K), the natural form and its cation-exchanged (Na^+, K^+, Ca^{2+}, and Mg^{2+}) form were examined up to 100 kPa pressure. The uptake of SO_2 onto synthetic and natural zeolite adsorbents increased in the order of Ca-G < natural-G < Mg-G < K-G < Na-G at both temperatures, according to the quantitative study[29].

The adsorption temperature and SO_2 concentration are the two most essential operating parameters affecting zeolites' adsorption capability, but gas moisture is also important. Muhammad et al.[30] showed that zeolitic tuff (ZT) adsorbent maintained its stability in a dry gas environment, but the adsorption was weakened to the moisture. Interaction with SO_2 at high temperatures (400°C and 650°C) disrupts their structure, which impairs their adsorptive behavior. Even though zeolites may be regenerated several times, their applicability is limited due to low adsorptive site density and pore size limits.

Finally, it is worth noting that sulfur dioxide is a Lewis acid with an electron acceptor site on the S atom, which is highly important for surface interaction with materials. Marcu and Sandulescu[31] investigated the adsorption mechanism of SO_2 on zeolite Y at temperatures ranging from 25°C to 200 °C by assessing the sample with and without adsorbed SO_2 using Infra-red (IR) spectroscopy and total Lewis' acidity measurements. The results of IR and acidity tests on samples revealed that the SO_2 molecules are most likely adsorbed by hydrogen bonding to one or two conveniently located surface hydroxyl groups (Figure 2.3). SO_2 removal capacities of various zeolites are summarized in Table 2.1.

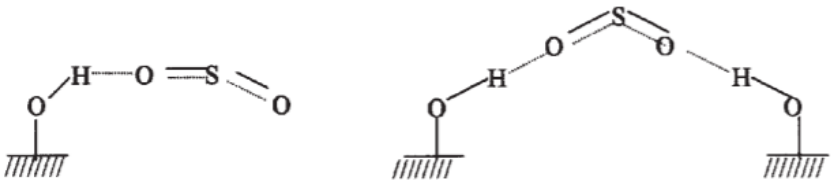

Figure 2.3 Sulfur dioxide adsorption mechanism on Y type zeolites through hydroxyl groups available on the Y zeolite surface[31]

Table 2.1 Summary of SO_2 removal capacities using different zeolites

Sorbent	Inlet SO_2 concentration (ppm)	Temperature (K)	Adsorption capacity (mg SO_2/g sorbent)	Reference
Fly ash/ CaO	2000	360	0.37(mol/mol)	[32]
NaX	10000	363	82.64	[33]
K-NaX			101.86	
Ca-NaX			62.78	
NH_4Y	200	298	19	[34]
13X	500	303	87.91	[35]
5A			87.63	
Raw-Clinoptilolite	2700	298	8.30	[36]
Fe-Clinoptilolite			21.90	
ZX-WS		373	34.59	[37]
ZX-DS			37.80	
ZX-WS-WV			48.05	

2.3.2 Metal and metal oxides

Metal oxides are another solid material for desulfurization procedures that has been extensively explored. Metal oxides have long been known to be good at removing sulphur gases from the flue gas stream. Adsorption of SO_2 and subsequent oxidation of SO_2 to SO_3 are carried out by metals. This reaction is significant because SO_3 may have a stronger affinity for the surface than SO_2.

Many metal oxides can trap gases, but only a few are effective in removing SO_2. Single oxides, mixed oxides, and supported oxides were categorized by Mathieu et al.[50] into three categories. Because of the high surface areas and inertness of silica to SO_2, it was proposed that silica-based adsorbents were more promising. When metal oxides were exposed to SO_2, they formed stable metal salts, which resulted in rapid deactivation and, as a result, a reduction in SO_2 removal capability.

Bandosz et al[51]. experimentally studied the uptake of SO_2 on metal oxides of iron and aluminum at ambient temperatures and proposed that when SO_2 is exposed to their surface, significant amounts of sulfite or sulphate are produced. For SO_2 adsorption and oxidation, surface hydroxyls have been suggested as active centers. The unique activities of hydroxyl functional groups on MnO_2 that act between acidic and basic active intermediate sites, or electrophilic- nucleophilic sites, are responsible for their unique activities for various catalytic redox reactions and can directly capture and oxidize SO_2 into sulphate, according to experimental and theoretical results.

The efficiency and products produced can also be influenced by the geometric features of adsorbents. Differences in the reactivity of the surface oxygen and the quantity of defect sites were responsible for the SO_2 interactions with different CeO_2 nano-shapes. SO_2 bonds stronger to CeO_2 rods with high basicity and more flaws than to CeO_2 cubes and octahedra. The greater desorption temperature of SO_2 on rods than cubes and octahedral proves the surface basicity effect and the existence of defect sites on the SO_2 binding strength on CeO_2[52].

Despite this, most adsorbents did not show promising SO_2 adsorption ability. To boost adsorption effectiveness, functional groups and metals added to the pore surface have been studied extensively. When compared to activated carbons (ACs) without metal, CuO and CeO_2 activated carbons (ACs) performed better in SO_2 capture. According to Patarin et al.[53], an MCM-41 adsorbent containing two metal oxides of CuO and CeO_2 along with LiCl additive had a high adsorption capacity of 130 mg SO_2/g at 673 K from initial concentration of 250 ppm SO_2. In Table 2.2, SO_2 removal capacities of various metal oxides are shown.

Table 2.2 Summary of SO_2 adsorption capacity of some metal oxides

Sorbent	Inlet SO_2 concentration (ppm)	Temperature (K)	Adsorption capacity (mg SO_2/g)	Reference
Fe_3O_4	-	298	40.50	[54]
δ-MnO_2	205 (ppb)	298	18.83	[55]
MgO	-	298	140.70	[56]
MnO_x	1000	498	0.21 (mol/mol)	[57]
$ZnAl_2O_4$	200	298	84.56	[58]
NiAlO	-	473	35.87	[59]

Unfortunately, despite their properties and results, compared with other dry FGD sorbents such as CaO and $CaCO_3$, SO_2 removal capacities of metal oxides and zeolites can be considered weak. The regeneration of these sorbents also suffered from the production of sulfates during the adsorption reaction.

2.3.3 Metal Organic Framework (MOF)

Because of their tailorable surface chemical functions and exceptional surface areas, MOFs have recently been the subject of significant investigation for effective gas separation technologies. More than 6000 MOF have been registered in the Cambridge Structural Database up to this date[38]. Metal ions or clusters are bonded together by organic linkers via strong covalent interactions to form these three-dimensional compounds. Unlike zeolites and carbon-based materials, investigations on the application of MOFs for SO_x and NO_x adsorption are not common[39]. Even though significant research has been done on gas separations in MOFs, very little has been done on the sequestration of SO_2, which frequently results in severe structural degradation of the material and/or irreversible uptake. Because of their chemical composition, ligand functionality, cavity size, ease of synthesis, and comparatively low-cost reactivation, MOFs have a few advantages over traditional porous materials[39], [40].

For SO_2 adsorption at high temperatures, benzenetricarboxylate MOFs containing copper as the core cation and $BaCl_2$ as a second component (Ba/Cu-BTC) demonstrated enhanced absorption.

In a combination of SO_2, N_2, and CH_4, fluorinated MOF (FMOF-2) is produced from 2,2-bis (4-carboxyphenyl) hexafluoropropane and zinc nitrate hexahydrate was shown to have a high adsorption capacity and selectivity for SO_2[41].

The instability of MOF coordination compounds, when exposed to wet flue gas, is a key disadvantage of employing them as adsorbents. The corrosive and poisonous characteristics of SO_2 cause structural damage as well as irreversible SO_2 adsorption. MOF uses have also been constrained by the expensive cost of organic precursors.

Snapshots of the structures of MOF materials with adsorbed SO_2 were investigated to better understand the adsorption behavior of SO_2 in these MOF materials at the molecular level. In Figure 2.4, two snapshots of SO_2 adsorption in IRMOF-10 are shown as an example. According to the mechanism of gas adsorption in IRMOF-10, the gas molecules first occupy the zinc corner regions, which are the most energetically favorable adsorption locations, as shown in Figure (2.4a). At mild pressures, the organic units begin adsorbing adsorbate molecules. Finally, the adsorbate molecules fill the holes' interior spaces. (Figure 2.4b)[40]. The structures of the IRMOF-10 model with SO_2 were optimized using a DFT calculation, as shown in Figure (2.4c). Three aromatic CH groups surround the adsorbed SO_2 molecule, forming three hydrogen bond interactions between the O (-) of SO_2 and the H (+) of the CH groups. One SO_2 O (-) connects with two H (+) of CH groups, whereas the other O (-) interacts with one H (+) of a CH group. This points to weak hydrogen bonding interactions with IRMOF-10, which is in line with IRMOF-10's low isosteric temperatures of adsorption[42].

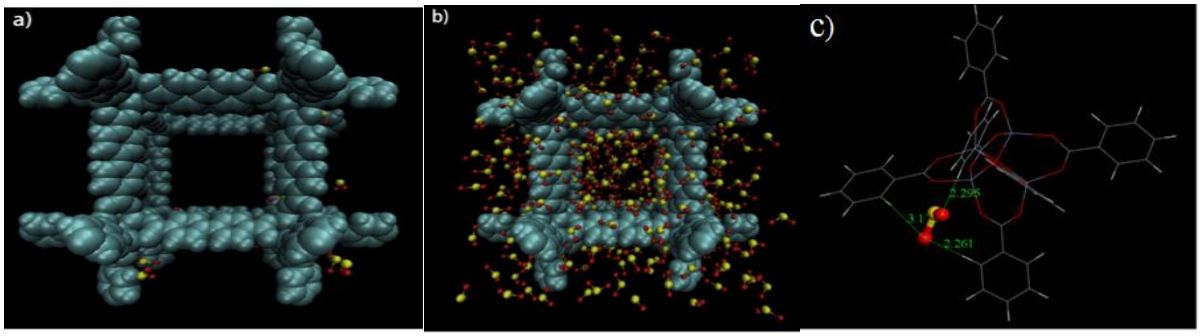

Figure 2.4. Snapshots of the structures of IRMOF-10 with adsorbed SO_2 at two pressures: (a) P = 10^4 Pa and (b) P = 10^6 Pa, View of the adsorption site of the SO_2 molecule within the unit cell of IRMOF-10(c). [42]

At 293 K, Brandt et al. utilized MOF-177, which had a strong SO_2 absorption of 25.7 mmol g^{-1}. The SO_2 adsorption capacity of mmen-MIL-101 (Cr) produced by Zhang et al[43]. was as high as 4.27 mmol g^{-1}, but MOF stability is a serious issue that prevents its use[44]. Summary of some MOFs for SO_2 capture is shown in Table 2.3.

Table 2.3 Summary of SO_2 removal capacity of MOFs

MOFs	Inlet SO_2 concentration (ppm)	Temperature (K)	Adsorption capacity (mg SO_2/g)	Reference
MFM-601	2500	298	1082.61	[45]
NPC-1	2000	298	118.10	[46]
NPC-2			102.60	
CTF-CSU41	1300	298	429.20	[46]
NPC-1	2000	298	156.72	[47]
NPC-2			112.86	
NPC-3			156.23	
MFM-170	2500	298	1121.05	[48]
MFM-305	2500	273	579.74	[48]
MFM-305-CH_3			338.88	
MOF-177	1000	293	1646.34	[49]
NH_2-MIL-125(Ti)			691.85	
MIL-160			461.23	

2.3.4 Carbon-based Materials

Carbon-based materials are an excellent candidate for adsorption applications in general. Some important qualities are resistance to acidic and basic conditions, low cost, low density, recycling capabilities, simple synthesis procedures, affinity with chemicals, regenerability, mechanical strength, diffusion characteristics, stability, and availability[60]. Activated carbon [73], carbon

monoliths [69], carbon nanotubes, and graphene-based products [63] are some of the most well-known examples of carbon-based products that have been studied for their potential applications in a variety of sectors. Biomass and other types of waste materials can be used to make carbon-based adsorbents at very low costs[61].

2.3.5 Activated carbon

Carbon-based adsorbents, like metal oxide and zeolite materials, have been widely researched in the past for SO_x and NO_x adsorption. This is because of the positive properties of this family of adsorbents, which include high adsorption capacity, rapid adsorption kinetics, regenerability, low cost, and thermal and mechanical stability. Most of the operations that create SO_2 in product streams take place at high temperatures (up to 100 °C), and the stream must be cooled before separation. As a result, finding an adsorbent with a high adsorption capacity at relatively high temperatures can significantly reduce the costs[61]. Modification of the activated carbon's surface chemical properties is well known to have a significant impact on its SO_2 adsorption performance. Researchers have integrated several basic nitrogen functional groups onto the carbon surface for SO_2 removal from gaseous mixtures, inspired by current liquid-phase amine scrubbing technology. To regenerate the solid adsorbent, this method is predicted to take advantage of the strong chemical interactions between SO_2 and the connected basic nitrogen functions, as well as the low energy needs.

It has been demonstrated that SO_2 can be oxidized to SO_3 over activated carbon, with sulfuric acid (H_2SO_4) forming as a result of the subsequent reaction with water. Because this causes the surface to become acidic, activated carbons with a basic surface are recommended for effective SO_2 removal. Karatepe et al[61]. employed lignite-based activated carbon for adsorptive removal of SO_2 at a concentration of 4800 ppm at 25 °C. SO_2 adsorption values as high as 5.55 mmol/g have been observed, leading to the conclusion that carbonaceous adsorbents with larger micropore volume, rather than surface area, are the best choices for SO_2 removal. Moreover, these researchers noticed that phenolic and lactone groups contained in the structure of activated carbon play a major role in SO_2 adsorption. The simultaneous removal of SO_x and NO_x by carbon-based materials has lately attracted attention, and the results of such investigations indicate that both gases co-adsorb over activated carbon surfaces in a synergistic manner. Activated carbon reacts differently when exposed to pure or mixed gases, as several research groups have previously demonstrated. While

NO_x facilitates SO_2 adsorption, activated carbon has a higher affinity for SO_x than NO_x. This is due to the fact that SO_2 has a higher permanent dipole moment and polarizability than NO_x, resulting in more surface dispersion and electrostatic interactions[62].

Guo et al[63]. recently investigated the simultaneous adsorption of SO_2 and NO on activated carbon at 120 °C by assessing the effects of different SO_2 and NO concentrations on the adsorption capacity. When the NO content is relatively high (i.e., >200 ppm), it has been demonstrated that NO improves SO_2 adsorption, principally through boosting SO_2 chemisorption over the activated carbon surface. On the other hand, as the SO_2 concentration rises (i.e., >700 ppm), the NO adsorption capacity decreases, owing to the obstruction of accessible adsorption sites for NO conversion to NO_2. The maximum total adsorption capacity for the gases was obtained at an SO_2/NO ratio of 1.7, according to the authors. Martine et al[16]. used two types of AC to test SO_2 capture with SO_2 levels less than 100 ppm: granulated activated carbon and PAN fiber. When a low concentration of SO_2 in the air (2.5 ppm) was used, the amount of SO_2 adsorbed per gram of AC decreased, but when a high concentration of SO_2 in the air (>1000 ppm) was used, the amount of SO_2 adsorbed per gram of AC increased. The irreversible adsorption of SO_2 was followed by oxidation, showing that the mechanism was not physisorption.

Because of the interaction of their basic sites with acidic SO_2, amine-treated porous chemo-sorbents have received a lot of interest. Few studies have been published on the use of amine functional groups to boost SO_2 adsorption capability. Zhi et al.[64] evaluated the SO_2 adsorption capacity of a triethanolamine-impregnated SBA-15 adsorbent, for example. Furthermore, utilizing diamine-anchored Merrifield resins, Yu et al[65]. obtained high SO_2 adsorption capacity of up to 6.40 mmol/g of adsorbent. The mechanism of SO_2 adsorption with various types of amine groups has not been widely researched to our knowledge, even though it appears promising. There is currently a scarcity of data on the influence of amine groups on SO_2 adsorption efficiency. Table 2.4 shows some ACs modified with metals and through the surface and their adsorption capacity.

Table 2.4 Summary of SO_2 adsorption capacity of activated carbons modified with metal or on the surface

AC Precursor	Modifier	Inlet SO_2 concentration (ppm)	Temperature (K)	Adsorption capacity (mg SO_2/g)	Reference
Bituminous coal	Manganese	2000	353	154	[66]
Coconut shell	Vanadium	200	298	0.803	[67]
	Manganese			0.339	
	Copper			0.436	
Lyocell fiber	Copper	40	298	1830.5	[68]
Commercial AC	Manganese + cerium	2700	353	113	[69]
Ceramic monolith	Cobalt	300	373	123.1	[70]
Sewage sludge	Chitosan	2000	343	35.80	[71]
Waste tires	KOH	2500	318	21	[72]
Mesoporous carbon	Melamine	400	308	13.72	[73]
Fly ash	KOH	40	298	7	[74]

2.4 Nano Crystalline Cellulose (NCC)

Cellulose, a common biopolymer, is made up of repeating glucose units (Figure 2.5). Strong acids hydrolyze glucoside structures, breaking only the most accessible glycosidic link and releasing nanocrystalline cellulose, or nano celluloses. They are highly crystalline, renewable, biodegradable, non-hazardous, thermally and mechanically stable, and industrially accessible on massive scales. They also have a large specific surface area and adjustable surface chemistry[75].

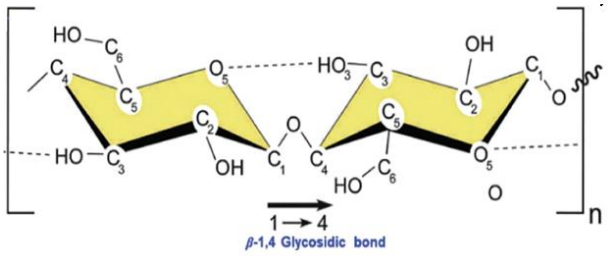

Figure 2.5 Chemical structure of cellulose and β 1–4 glycosidic bonds[76]

NCCs exhibit a high degree of crystallinity, with a diameter of less than 100 nm and a length of less than 500 nm and are the result of the formation of hydrogen bonds between the glucose monomer units in the cellulose structure. Acid hydrolysis procedures require extremely harsh reaction conditions, which usually necessitate concentrated acid. The amorphous areas of cellulose are more readily invested by acid during the hydrolysis process than the crystalline sections, resulting in the amorphous regions degrading first and the crystalline regions maintain. Finally, NCCs that look like whiskers are created. Figure 2.6 depicts how amorphous sections of cellulose are destroyed during acid hydrolysis, and Table 2.5 compares nanofiber and cellulose nanocrystals generated using two distinct methods[76].

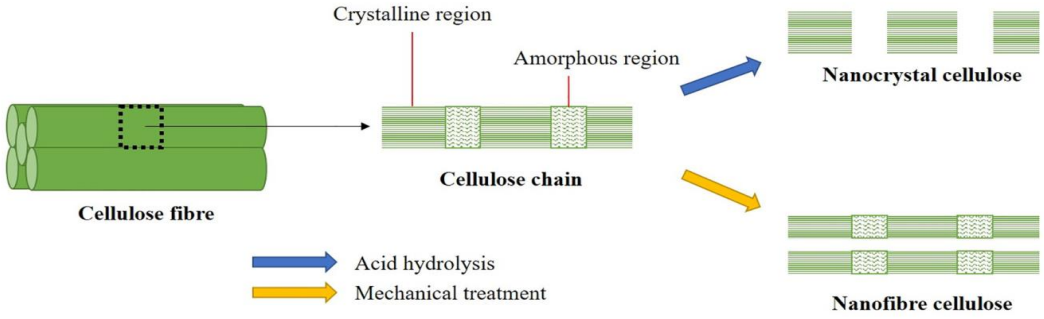

Figure 2.6 Schematic of nanocellulose isolation[77]**.**

Table 2.5 Type of cellulose and its properties. Adapted from [78]

Nanocellulose type	Extraction method	Dimensions	Characteristics
CNF	Mechanical treatment	Network-structured nanofibers	Low crystallinity
		Diameter range between 5 nm and 60 nm	longer length
			Low aspect ratio
NCC	Acid hydrolysis	Rod-shaped crystal-like particle	High crystallinity
		Diameter range between 5 nm and 70 nm	Shorter length
		Length range between100 nm ad 250 nm	Low aspect ratio

2.5 Chemical modification of NCC surface

Because of its surface hydroxyl groups, cellulose is widely utilized as an adsorbent. These groups are amenable to chemical alteration, allowing for increased adsorption capacity. Surface modifications of cellulose can be divide into three categories: surface modification as a result of cellulose treatment or extraction, electrostatic adsorption to the cellulose surface, and molecule covalent attachment or cellulose surface derivatization utilizing hydroxyl groups for selective modification[81]. Several surface modifications approaches have been thoroughly investigated, with some examples depicted in Figure 2.7. For example, various chemical processes have been used to incorporate alkaline centers from nitrogen-containing molecules such as amino ethanethiol and ethylenediamine. The surface chemistry of nanocellulose can be modified chemically through physical interactions, and biological techniques, due to the highly hydrophilic nature of nanocellulose due to the presence of OH groups on its surface[82]. Surface functionalization of nanocellulose can be done during the preparation process or after its manufacture. These changes result in the acquisition of desired qualities, which improve their effectiveness for a specific application. The surface of a nano cellulosic material can be manipulated to change how it interacts with foreign molecules by including any chemical functionality. Different chemical changes have been carried out to enable the adsorption of different types of contaminants due to the abundance of hydroxyl groups on the surface of cellulose[83], [84].

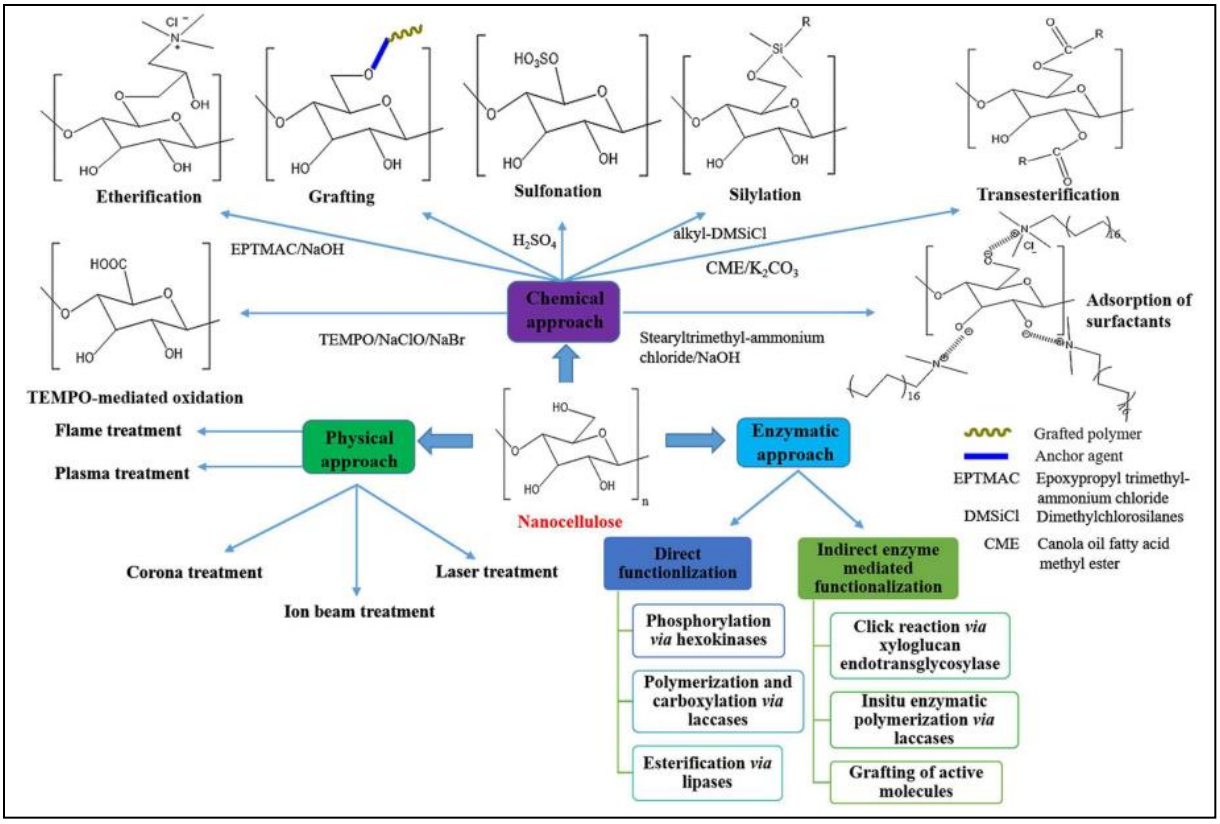

Figure 2.7 Schematic representation of the most commonly used surface modification routes of nanocellulose[85]

One of the disadvantages of the heterogeneous sorbent, as previously said, is its cost. There have been several experiments using cellulose for acid gas capture since it is abundant in nature, low-cost, has a crystalline structure, and can be functionalized through the hydroxyl groups. Because SO_2 is a stronger acid than CO_2, some adsorbents used for CO_2 capture may provide a clue because there is more research on CO_2 capture.

Toyoko Imae et al.[86] hybridized poly (amidoamine) dendrimers (organoclay) with oxidized cellulose nanofibers to improve CO_2 gas adsorption and found that increasing the amount of organoclay enhanced the adsorption capacity. However, because the affinity of gases for clays was insufficient, gases were easily removed from the clays (Figure 2.8).

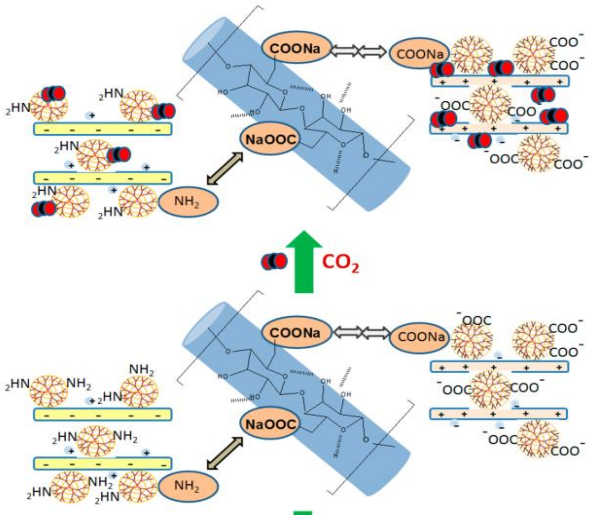

Figure 2.8 . Schematic of CO_2 adsorption on Organoclay- oxidized cellulose nanofibers[86]

A carbon nanofibre (CNF) aerogel grafted with Aminopropyl triethoxysilane (APS) was used in another investigation to absorb CO_2 (Figure 2.9). Because of the higher nitrogen content, it seemed logical to improve the CO_2 adsorption capacity by increasing the concentration of APS. The thermal stability and crystallinity of modified CNFs were both affected by the effective amine loading on the polymer surface, and the CO_2 adsorption capacity was also affected by the APS concentration[87].

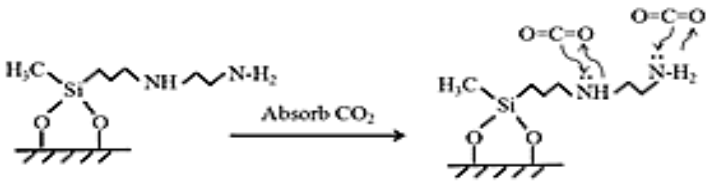

Figure 2.9. Schematic description of grafted aerogel and CO_2 adsorption[87]

Gebald et al.[88] studied CO_2 capture using amine-modified cellulose from Air. At a CO_2 concentration of 506 ppm, 1.39 mmol CO_2/g adsorb after 12 hours at 25°C, according to the

findings. Silva Filho et al[89] used microcrystalline cellulose that had been directly treated with ethylenediamine as an adsorbent for the removal of Amitriptyline drug from aqueous solution. The cellulose was modified by ethylenediamine in two phases. In the first step, cellulose was chlorinated by a halogenation reaction to increasing its reactivity and subsequently reacted with an amine [90]. Halogenation reaction, in addition to not being economically affordable and viable, also generates toxic intermediates, which are dangerous to the environment.

In a one-step and direct method, which is the goal of this project, the temperature would provide the energy needed to overcome the energy barrier and converts the reactants into products. The alkalinity of the cellulose from alcohol groups and in ethylenediamine from amine groups is vital to finding out what products are shaped. Many different types of adsorption materials have been explored to improve capture capacity so far. Improved selectivity and adsorption rate at lower temperatures, as well as long-term stability and regeneration, are the primary difficulties. Cost, physical properties, thermal and chemical stability, and unique technical designs are all important factors to consider. Therefore, we purpose to discover the most effective functionalization approach, which can improve SO_2 capture capacity. We also are aware of environmental impact, commercialization, and their future.

2.6 References

[1] F. Rezaei, A. A. Rownaghi, S. Monjezi, R. P. Lively, and C. W. Jones, "SOx/NOx Removal from Flue Gas Streams by Solid Adsorbents: A Review of Current Challenges and Future Directions," *Energy and Fuels*, vol. 29, no. 9, pp. 5467–5486, 2015, doi: 10.1021/acs.energyfuels.5b01286.

[2] International Energy Agency, "Global Energy Review 2021," *Glob. Energy Rev. 2020*, pp. 1–36, 2021, [Online]. Available: https://iea.blob.core.windows.net/assets/d0031107-401d-4a2f-a48b-9eed19457335/GlobalEnergyReview2021.pdf.

[3] P. R. Arghya Sardar, "SO_2 Emission Control and Finding a Way Out to Produce Sulphuric Acid from Industrial SO_2 Emission," *J. Chem. Eng. Process Technol.*, vol. 06, no. 02, 2015, doi: 10.4172/2157-7048.1000230.

[4] E. J. Emmett and M. C. Willis, "The Development and Application of Sulfur Dioxide Surrogates in Synthetic Organic Chemistry," *Asian J. Org. Chem.*, vol. 4, no. 7, pp. 602–611, 2015, doi: 10.1002/ajoc.201500103.

[5] Y. Sun, E. Zwolińska, and A. G. Chmielewski, "Abatement technologies for high concentrations of NO x and so2 removal from exhaust gases: A review," *Crit. Rev. Environ. Sci. Technol.*, vol. 46, no. 2, pp. 119–142, 2016, doi: 10.1080/10643389.2015.1063334.

[6] D. J. Eatough, F. M. Caka, and R. J. Farber, "The Conversion of SO2 to Sulfate in the Atmosphere," *Isr. J. Chem.*, vol. 34, no. 3–4, pp. 301–314, 1994, doi: 10.1002/ijch.199400034.

[7] E. and climate change Canada, "Key Commitments and Progress: SO2 Emission Reductions." https://ec.gc.ca/air.

[8] M. A. Hanif, N. Ibrahim, and A. Abdul Jalil, "Sulfur dioxide removal: An overview of regenerative flue gas desulfurization and factors affecting desulfurization capacity and sorbent regeneration," *Environ. Sci. Pollut. Res.*, vol. 27, no. 22, pp. 27515–27540, 2020, doi: 10.1007/s11356-020-09191-4.

[9] Z. Y. Chen, C. Chen, Y. Zhang, Z. M. Xia, K. F. Yan, and X. Sen Li, "Carbon dioxide and sulfur dioxide capture from flue gas by gas hydrate based process," *Energy Procedia*, vol. 142, pp. 3454–3459, 2017, doi: 10.1016/j.egypro.2017.12.229.

[10] D. Aaron and C. Tsouris, "Separation of CO_2 from flue gas: A review," *Sep. Sci. Technol.*, vol. 40, no. 1–3, pp. 321–348, 2005, doi: 10.1081/SS-200042244.

[11] S. O. R. Program, "SO_2 Scrubbing Technologies : A Review," vol. 20, no. 4, pp. 219–228, 2001.

[12] J. S. Heslin and B. F. Hobbs, "A probabilistic production costing analysis of s02 emissions reduction strategies for ohio: Emissions, cost, and employment tradeoffs," *J. Air Waste Manag. Assoc.*, vol. 41, no. 7, pp. 956–966, 1991, doi: 10.1080/10473289.1991.10466893.

[13] K. C. Chong, S. O. Lai, H. S. Thiam, H. C. Teoh, and S. L. Heng, "Recent progress of

oxygen/nitrogen separation using membrane technology," *J. Eng. Sci. Technol.*, vol. 11, no. 7, pp. 1016–1030, 2016.

[14] OEHHA. The Office of Environmental Health Hazard Assessment, "Science Discussion Document On The Development Of Air Standards For Sulphur Dioxide July 2016 Standards Development Branch Ministry of the Environment and Climate Change Executive Summary," no. July, 2016.

[15] D. H. Everett, "Manual of Symbols and Terminology for Physicochemical Quantities and Units, Appendix II: Definitions, Terminology and Symbols in Colloid and Surface Chemistry," *Pure Appl. Chem.*, vol. 46, pp. 577–638, 2019, doi: 10.1351/pac197231040577.

[16] U. Narkiewicz, A. Pietrasz, I. Pełech, and W. Arabczyk, "Removal of SO 2 from gases on carbon materials," *Polish J. Chem. Technol.*, vol. 14, no. 1, pp. 41–45, 2012, doi: 10.2478/v10026-012-0057-6.

[17] S. Bari, "Effect of carbon dioxide on the performance of biogas/diesel duel-fuel engine," *Renew. Energy*, vol. 9, no. 1-4 SPEC. ISS., pp. 1007–1010, 1996, doi: 10.1016/0960-1481(96)88450-3.

[18] X. Xu, C. Song, R. Wincek, J. M. Andresen, B. G. Miller, and A. W. Scaroni, "Separation of CO2 from Power Plant Flue Gas Using a Novel CO2 'Molecular Basket' Adsorbent," *ACS Div. Fuel Chem. Prepr.*, vol. 48, no. 1, pp. 162–163, 2003.

[19] M. T. Ho, G. W. Allinson, and D. E. Wiley, "Reducing the cost of CO2 capture from flue gases using pressure swing adsorption," *Ind. Eng. Chem. Res.*, vol. 47, no. 14, pp. 4883–4890, 2008, doi: 10.1021/ie070831e.

[20] S. Y. Lee and S. J. Park, "A review on solid adsorbents for carbon dioxide capture," *J. Ind. Eng. Chem.*, vol. 23, pp. 1–11, 2015, doi: 10.1016/j.jiec.2014.09.001.

[21] A. M. Ealias and M. P. Saravanakumar, "A review on the classification, characterisation, synthesis of nanoparticles and their application," *IOP Conf. Ser. Mater. Sci. Eng.*, vol. 263, no. 3, pp. 0–15, 2017, doi: 10.1088/1757-899X/263/3/032019.

[22] N. Mahfoudhi and S. Boufi, "Nanocellulose as a novel nanostructured adsorbent for environmental remediation: a review," *Cellulose*, vol. 24, no. 3, pp. 1171–1197, 2017, doi: 10.1007/s10570-017-1194-0.

[23] A. Khaleque, M. Alam, M. Hoque, Sh. Mondal, "Zeolite synthesis from low-cost materials and environmental applications: A review," *Environ. Adv.*, vol. 2, no. August, p. 100019, 2020, doi: 10.1016/j.envadv.2020.100019.

[24] T. Abdullahi, Z. Harun, and M. H. D. Othman, "A review on sustainable synthesis of zeolite from kaolinite resources via hydrothermal process," *Adv. Powder Technol.*, vol. 28, no. 8, pp. 1827–1840, 2017, doi: 10.1016/j.apt.2017.04.028.

[25] P. S. Wheatley, A. R. Butler; M. S. Crane, S. Fox, B. Xiao, "NO-releasing zeolites and their antithrombotic properties," *J. Am. Chem. Soc.*, vol. 128, no. 2, pp. 502–509, 2006, doi: 10.1021/ja0503579.

[26] T. Kopaç and S. Kocabaş, "Sulfur dioxide adsorption isotherms and breakthrough analysis on molecular sieve 5A zeolite," *Chem. Eng. Commun.*, vol. 190, no. 5–8, pp. 1041–1054, 2003, doi: 10.1080/00986440302103.

[27] T. Kopaç, E. Kaymakçi, and M. Kopaç, "Dynamic adsorption of SO2 on zeolite molecular sieves," *Chem. Eng. Commun.*, vol. 164, pp. 99–109, 1998, doi: 10.1080/00986449808912360.

[28] A. Ü. Metin, H. Çiftçi, and E. Alver, "Efficient removal of acidic dye using low-cost biocomposite beads," *Ind. Eng. Chem. Res.*, vol. 52, no. 31, pp. 10569–10581, 2013, doi: 10.1021/ie400480s.

[29] B. E. Alver, M. Sakizci, and E. Yörükoğullari, "Adsorption of sulphur dioxide using natural and modified gördes clinoptilolites," *Adsorpt. Sci. Technol.*, vol. 29, no. 4, pp. 413–422, 2011, doi: 10.1260/0263-6174.29.4.413.

[30] M. Al-Harahsheh, R. Shawabkeh, M. Batiha, A. Al-Harahsheh, and K. Al-Zboon, "Sulfur dioxide removal using natural zeolitic tuff," *Fuel Process. Technol.*, vol. 126, no. April 2018, pp. 249–258, 2014, doi: 10.1016/j.fuproc.2014.04.025.

[31] I. Marcu and I. S. Ndulescu, "Study of sulfur dioxide adsorption on Y zeolite," vol. 69, no. 7, pp. 563–569, 2004.

[32] D. O. Ogenga, M. M. Mbarawa, K. T. Lee, A. R. Mohamed, and I. Dahlan, "Sulphur dioxide removal using South African limestone/siliceous materials," *Fuel*, vol. 89, no. 9, pp. 2549–2555, 2010, doi: 10.1016/j.fuel.2010.04.029.

[33] H. Deng, H. Yi, X. Tang, H. Liu, and X. Zhou, "Interactive effect for simultaneous removal of SO2, NO, and CO2 in flue gas on ion exchanged zeolites," *Ind. Eng. Chem. Res.*, vol. 52, no. 20, pp. 6778–6784, 2013, doi: 10.1021/ie303319f.

[34] D. R. S. Pedrolo, L. K. De Menezes Quines, G. De Souza, and N. R. Marcilio, "Synthesis of zeolites from Brazilian coal ash and its application in SO2 adsorption," *J. Environ. Chem. Eng.*, vol. 5, no. 5, pp. 4788–4794, 2017, doi: 10.1016/j.jece.2017.09.015.

[35] H. Deng, H. Yi, X. Tang, Q. Yu, P. Ning, and L. Yang, "Adsorption equilibrium for sulfur dioxide, nitric oxide, carbon dioxide, nitrogen on 13X and 5A zeolites," *Chem. Eng. J.*, vol. 188, pp. 77–85, 2012, doi: 10.1016/j.cej.2012.02.026.

[36] M. Mahmoodi Meimand, N. Javid, and M. Malakootian, "Adsorption of Sulfur Dioxide on Clinoptilolite/Nano Iron Oxide and Natural Clinoptilolite," *Heal. Scope*, vol. In Press, no. In Press, 2019, doi: 10.5812/jhealthscope.69158.

[37] N. Czuma, R. Panek, P. Baran, and K. Zarębska, "The influence of binders for the pelletization of fly ash zeolites on sulfur dioxide sorption properties," *Clay Miner.*, vol. 55, no. 1, pp. 40–47, 2020,

doi: 10.1180/clm.2020.3.

[38] "Cambridge Structural Database." www.ccdc.cam.ac.uk.

[39] C. Reviews, "Introduction to Metal − Organic Frameworks," pp. 673–674, 2012.

[40] H. Frost, T. Düren, and R. Q. Snurr, "Effects of surface area, free volume, and heat of adsorption on hydrogen uptake in metal-organic frameworks," *J. Phys. Chem. B*, vol. 110, no. 19, pp. 9565–9570, 2006, doi: 10.1021/jp060433.

[41] H. Dathe, E. Peringer, V. Roberts, A. Jentys, and J. A. Lercher, "Metal organic frameworks based on Cu2+ and benzene-1,3,5-tricarboxylate as host for SO2 trapping agents," *Comptes Rendus Chim.*, vol. 8, no. 3–4, pp. 753–763, 2005, doi: 10.1016/j.crci.2004.10.018.

[42] X. D. Song, S. Wang, C. Hao, and J. S. Qiu, "Investigation of SO2 gas adsorption in metal-organic frameworks by molecular simulation," *Inorg. Chem. Commun.*, vol. 46, pp. 277–281, 2014, doi: 10.1016/j.inoche.2014.06.003.

[43] L. Li, I. da Silva, D. Kolokolov, X. Han, J. Li, G. Smith, Y. Cheng, L. Daemen, Ch. Morris, J. Harry, "Post-synthetic modulation of the charge distribution in a metal-organic framework for optimal binding of carbon dioxide and sulfur dioxide," *Chem. Sci.*, vol. 10, no. 5, pp. 1472–1482, 2019, doi: 10.1039/c8sc01959b.

[44] T. A. Faculty, J. Karra, and I. P. Fulfillment, "Development of Porous Metal-Organic Frameworks for Gas Adsorption Applications Development of Porous Metal-Organic Frameworks for Gas Adsorption Applications," *Biomol. Eng.*, no. December, 2011.

[45] J. H. Carter, X. Han, F. Moreau, I. da Silva, A. Nevin, H. G.W. Godfrey, Ch. Tang, S. Yang, M. Schröder, "Exceptional Adsorption and Binding of Sulfur Dioxide in a Robust Zirconium-Based Metal-Organic Framework," *J. Am. Chem. Soc.*, vol. 140, no. 46, pp. 15564–15567, 2018, doi: 10.1021/jacs.8b08433.

[46] Y. Fu, Zh. Wang, S. Li, X. He, Ch. Pan, J. Yan, G. Yu, "Functionalized Covalent Triazine Frameworks for Effective CO_2 and SO_2 Removal," *ACS Appl. Mater. Interfaces*, vol. 10, no. 42, pp. 36002–36009, 2018, doi: 10.1021/acsami.8b13417.

[47] A. Wang, R. Fan, X. Pi, S. Hao, X. Zheng, and Y. Yang, "N-Doped Porous Carbon Derived by Direct Carbonization of Metal-Organic Complexes Crystal Materials for SO2 Adsorption," *Cryst. Growth Des.*, vol. 19, no. 3, pp. 1973–1984, 2019, doi: 10.1021/acs.cgd.8b01925.

[48] L. Li, I. da Silva, D. Kolokolov, X. Han, J. Li, G. Smith, Y. Cheng, L. Daemen, Ch. Morris, J. Harry, "Post-synthetic modulation of the charge distribution in a metal-organic framework for optimal binding of carbon dioxide and sulfur dioxide," *Chem. Sci.*, vol. 10, no. 5, pp. 1472–1482, 2019, doi: 10.1039/c8sc01959b.

[49] P. Brandt, A. Nuhnen, M. Lange, J. Möllmer, O. Weingart, and C. Janiak, "Metal-Organic Frameworks with Potential Application for SO2 Separation and Flue Gas Desulfurization," *ACS Appl. Mater. Interfaces*, vol. 11, no. 19, pp. 17350–17358, 2019, doi: 10.1021/acsami.9b00029.

[50] Y. Mathieu, L. Tzanis, M. Soulard, J. Patarin, M. Vierling, and M. Molière, "Adsorption of SOx by oxide materials: A review," *Fuel Process. Technol.*, vol. 114, pp. 81–100, 2013, doi: 10.1016/j.fuproc.2013.03.019.

[51] H. Wu, W. Cai, M. Long, H. Wang, Zh. Wang, Ch. Chen, X. Hu, X. Yu, Xiao, "Sulfur Dioxide Capture by Heterogeneous Oxidation on Hydroxylated Manganese Dioxide" *Environ. Sci. Technol.*, vol. 50, no. 11, pp. 5809–5816, 2016, doi: 10.1021/acs.est.5b05592.

[52] U. Tumuluri, M. Li, B. G. Cook, B. Sumpter, S. Dai, and Z. Wu, "Surface Structure Dependence of SO2 Interaction with Ceria Nanocrystals with Well-Defined Surface Facets," *J. Phys. Chem. C*, vol. 119, no. 52, pp. 28895–28905, 2015, doi: 10.1021/acs.jpcc.5b07946.

[53] Y. Mathieu, M. Soulard, J. Patarin, and M. Molière, "Mesoporous materials for the removal of SO 2 from gas streams," *Fuel Process. Technol.*, vol. 99, pp. 35–42, 2012, doi: 10.1016/j.fuproc.2012.02.005.

[54] X. M. Pham, D. Pham, N. Hanh, T. Dang Thi, L. Thuy Giang, H. Phuong, N.T. Anh, L. Hac Thi,"An initial evaluation on the adsorption of so_2 and NO_2 over Porous Fe_3O_4 Nanoparticles Synthesized by Facile Scalable Method," *J. Chem.*, vol. 2019, no. 2, 2019, doi: 10.1155/2019/9742826.

[55] W. Yang, J. Zhang, Q. Ma, Y. Zhao, Y. Liu, and H. He, "Heterogeneous Reaction of SO2 on Manganese Oxides: The Effect of Crystal Structure and Relative Humidity," *Sci. Rep.*, vol. 7, no. 1, pp. 1–14, 2017, doi: 10.1038/s41598-017-04551-6.

[56] Q. Zhang, Q. Tao, H. He, H. Liu, and S. Komarneni, "An efficient SO_2-adsorbent from calcination of natural magnesite," *Ceram. Int.*, vol. 43, no. 15, pp. 12557–12562, 2017, doi: 10.1016/j.ceramint.2017.06.130.

[57] X. Ma, J. Li, M. A. Rankin, L. M. Croll, and J. R. Dahn, "Highly porous MnOx prepared from $Mn(C_2O_4)\cdot 3H_2O$ as an adsorbent for the removal of SO_2 and NH_3," *Microporous Mesoporous Mater.*, vol. 244, pp. 192–198, 2017, doi: 10.1016/j.micromeso.2016.10.019.

[58] L. Zhao, S. Bi, J. Pei, X. Li, R. Yu, J. Zhao, Ch. Martyniuk, "Adsorption performance of SO_2 over $ZnAl_2O_4$ nanospheres," *J. Ind. Eng. Chem.*, vol. 41, pp. 151–157, 2016, doi: 10.1016/j.jiec.2016.07.019.

[59] L. Zhao, X. Li, Z. Qu, Q. Zhao, S. Liu, and X. Hu, "The NiAl mixed oxides: The relation between basicity and SO2 removal capacity," *Sep. Purif. Technol.*, vol. 80, no. 2, pp. 345–350, 2011, doi: 10.1016/j.seppur.2011.04.035.

[60] D. J. Babu, D. Puthusseri, F.G. Kühl, Sh. Okeil, M. Bruns, M. Hampe, J. Schneider, "SO_2 gas adsorption on carbon nanomaterials: A comparative study," *Beilstein J. Nanotechnol.*, vol. 9, no. 1, pp. 1782–1792, 2018, doi: 10.3762/bjnano.9.169.

[61] K. Silas, W. A. W. A. K. Ghani, T. S. Y. Choong, and U. Rashid, "Carbonaceous materials modified catalysts for simultaneous SO2/NOx removal from flue gas: A review," *Catal. Rev. - Sci. Eng.*, vol. 61, no. 1, pp. 134–161, 2019, doi: 10.1080/01614940.2018.1482641.

[62] M. M. Sabzehmeidani, S. Mahnaee, M. Ghaedi, H. Heidari, and V. A. L. Roy, "Carbon based materials: a review of adsorbents for inorganic and organic compounds," *Mater. Adv.*, vol. 2, no. 2, pp. 598–627, 2021, doi: 10.1039/d0ma00087f.

[63] X. Zhang, H. Zheng, G. Li, J. Gu, and J. Shao, "Ammoniated and activated microporous biochar for enhancement of SO 2 adsorption," *J. Anal. Appl. Pyrolysis*, vol. 156, no. March, p. 105119, 2021, doi: 10.1016/j.jaap.2021.105119.

[64] Y. Zhi, Y. Zhou, W. Su, Y. Sun, and L. Zhou, "Selective adsorption of SO2 from flue gas on triethanolamine-modified large pore SBA-15," *Ind. Eng. Chem. Res.*, vol. 50, no. 14, pp. 8698–8702, 2011, doi: 10.1021/ie2004658.

[65] X. Yu, J. Hao, Z. Xi, T. Liu, Y. Lin, and B. Xu, "Investigation of low concentration SO 2 adsorption performance on different amine-modified Merrifield resins," *Atmos. Pollut. Res.*, vol. 10, no. 2, pp. 404–411, 2019, doi: 10.1016/j.apr.2018.08.015.

[66] L. Yang, X. Jiang, Z. S. Yang, and W. J. Jiang, "Effect of MnSO4on the removal of so2by manganese-modified activated coke," *Ind. Eng. Chem. Res.*, vol. 54, no. 5, pp. 1689–1696, 2015, doi: 10.1021/ie503729a.

[67] C. H. Chiu, H. Lin, T. Kuo, Sh. Chen, T. Chang, K. Su, Kai-H. Hsi, "Simultaneous control of elemental mercury/sulfur dioxide/nitrogen monoxide from coal-fired flue gases with metal oxide-impregnated activated carbon," *Aerosol Air Qual. Res.*, vol. 15, no. 5, pp. 2094–2103, 2015, doi: 10.4209/aaqr.2015.03.0176.

[68] B. C. Bai, C. W. Lee, Y. S. Lee, and J. S. Im, "Metal impregnate on activated carbon fiber for SO2 gas removal: Assessment of pore structure, Cu supporter, breakthrough, and bed utilization," *Colloids Surfaces A Physicochem. Eng. Asp.*, vol. 509, pp. 73–79, 2016, doi: 10.1016/j.colsurfa.2016.08.038.

[69] N. J. Fang, J. X. Guo, S. Shu, J. J. Li, and Y. H. Chu, "Influence of textures, oxygen-containing functional groups and metal species on SO2 and NO removal over Ce-Mn/NAC," *Fuel*, vol. 202, pp. 328–337, 2017, doi: 10.1016/j.fuel.2017.04.035.

[70] K. Silas, W. A. W. A. K. Ghani, T. S. Y. Choong, and U. Rashid, "Breakthrough studies of Co3O4 supported activated carbon monolith for simultaneous SO2/NOx removal from flue gas," *Fuel Process. Technol.*, vol. 180, no. May, pp. 155–165, 2018, doi: 10.1016/j.fuproc.2018.08.018.

[71] X. Fan and X. Zhang, "Simultaneous removal of SO2 and NO with activated carbon from sewage sludge modified by chitosan," *Appl. Mech. Mater.*, vol. 253–255, no. PART 1, pp. 960–964, 2013, doi: 10.4028/www.scientific.net/AMM.253-255.960.

[72] A. Nieto-Márquez, E. Atanes, J. Morena, F. Fernández-Martínez, and J. L. Valverde, "Upgrading waste tires by chemical activation for the capture of SO2," *Fuel Process. Technol.*, vol. 144, pp. 274–281, 2016, doi: 10.1016/j.fuproc.2016.01.009.

[73] X. Song, X. Ma, G. Ning, and J. Gao, "Pitch-Based Nitrogen-Doped Mesoporous Carbon for Flue

Gas Desulfurization," *Ind. Eng. Chem. Res.*, vol. 56, no. 16, pp. 4743–4749, 2017, doi: 10.1021/acs.iecr.7b00054.

[74] A. Azetsu, H. Koga, A. Isogai, and T. Kitaoka, "Synthesis and catalytic features of hybrid metal nanoparticles supported on cellulose nanofibers," *Catalysts*, vol. 1, no. 1, pp. 83–96, 2011, doi: 10.3390/catal1010083.

[75] M. Kaushik and A. Moores, "Review: Nanocelluloses as versatile supports for metal nanoparticles and their applications in catalysis," *Green Chem.*, vol. 18, no. 3, pp. 622–637, 2016, doi: 10.1039/c5gc02500a.

[76] J. Tang, J. Sisler, N. Grishkewich, and K. C. Tam, "Functionalization of cellulose nanocrystals for advanced applications," *J. Colloid Interface Sci.*, vol. 494, pp. 397–409, 2017, doi: 10.1016/j.jcis.2017.01.077.

[77] H. Ibrahim, N. Sazali, W. Norharyati, W. Salleh, M. Nizam, and Z. Abidin, "Materials Today : Proceedings A short review on recent utilization of nanocellulose for wastewater remediation and sgas separation," *Mater. Today Proc.*, no. xxxx, 2020, doi: 10.1016/j.matpr.2020.09.245.

[78] A. Sheikhi, J. Hayashi, J. Eichenbaum, M. Gutin, N. Kuntjoro, D. Khorsandi, A. Khademhosseini, "Recent advances in nanoengineering cellulose for cargo delivery," *J. Control. Release*, vol. 294, no. June 2018, pp. 53–76, 2019, doi: 10.1016/j.jconrel.2018.11.024.

[79] R. S. Varma, "Biomass-Derived Renewable Carbonaceous Materials for Sustainable Chemical and Environmental Applications," *ACS Sustain. Chem. Eng.*, vol. 7, no. 7, pp. 6458–6470, 2019, doi: 10.1021/acssuschemeng.8b06550.

[80] E. J. Foster, R. J. Moon, U. P. Agarwal, M. Bortner, J. Bras, Ch. Sana, C.Kathleen, M. Clift., "Current characterization methods for cellulose nanomaterials," *Chem. Soc. Rev.*, vol. 47, no. 8, pp. 2609–2679, 2018, doi: 10.1039/c6cs00895j.

[81] E. Lam, K. B. Male, J. H. Chong, A. C. W. Leung, and J. H. T. Luong, "Applications of functionalized and nanoparticle-modified nanocrystalline cellulose," *Trends Biotechnol.*, vol. 30, no. 5, pp. 283–290, 2012, doi: 10.1016/j.tibtech.2012.02.001.

[82] M. L. Foresti, A. Vázquez, and B. Boury, "Applications of bacterial cellulose as precursor of carbon and composites with metal oxide, metal sulfide and metal nanoparticles: A review of recent advances," *Carbohydr. Polym.*, vol. 157, pp. 447–467, 2017, doi: 10.1016/j.carbpol.2016.09.008.

[83] R. S. Varma, "Biomass-Derived Renewable Carbonaceous Materials for Sustainable Chemical and Environmental Applications," *ACS Sustain. Chem. Eng.*, vol. 7, no. 7, pp. 6458–6470, 2019, doi: 10.1021/acssuschemeng.8b06550.

[84] M. Gopiraman, H. Bang, G. Yuan, Ch. Yin, K. Song, J. Lee, I. Chung, R. Karvembu, I. Kim, "Noble metal/functionalized cellulose nanofiber composites for catalytic applications," *Carbohydr. Polym.*, vol. 132, pp. 554–564, 2015, doi: 10.1016/j.carbpol.2015.06.051.

[85] D. Trache, A. Tarchoun, M. Derradji, T. Hamidon, N. Masruchin, N. Brosse, M.H. Hussin, Nanocellulose: From Fundamentals to Advanced Applications, vol. 8, no. May. 2020.

[86] K. J. Shah and T. Imae, "Selective Gas Capture Ability of Gas-Adsorbent-Incorporated Cellulose Nanofiber Films," *Biomacromolecules*, vol. 17, no. 5, pp. 1653–1661, 2016, doi: 10.1021/acs.biomac.6b00065.

[87] Y. Wu, Y. Zhang, N. Chen, S. Dai, H. Jiang, and S. Wang, "Effects of amine loading on the properties of cellulose nanofibrils aerogel and its CO2 capturing performance," *Carbohydr. Polym.*, vol. 194, no. February, pp. 252–259, 2018, doi: 10.1016/j.carbpol.2018.04.017.

[88] C. Gebald, J. A. Wurzbacher, P. Tingaut, T. Zimmermann, and A. Steinfeld, "Amine-based nanofibrillated cellulose as adsorbent for CO2 capture from air," *Environ. Sci. Technol.*, vol. 45, no. 20, pp. 9101–9108, 2011, doi: 10.1021/es202223p.

[89] R. D. S. Bezerra, R.C. Leal, M. S. da Silva, A. Morais, Th. Marques, J. Osajima, "Direct modification of microcrystalline cellulose with ethylenediamine for use as adsorbent for removal amitriptyline drug from environment," *Molecules*, vol. 22, no. 11, 2017, doi: 10.3390/molecules22112039.

[90] E. C. Silva Filho, L. C. B. Lima, K. S. Sousa, M. G. Fonseca, and F. A. R. Pereira, "Calorimetry studies for interaction in solid/liquid interface between the modified cellulose and divalent cation," *J. Therm. Anal. Calorim.*, vol. 114, no. 1, pp. 57–66, 2013, doi: 10.1007/s10973-012-2868-3.

3 Amine-functionalized Nanocrystalline Cellulose based adsorbent efficient for SO_2 capture

Raheleh Zafari[a], Fernanda G. Mendonça[b], R. Tom Baker[b], Clémence Fauteux-Lefebvre[a*]

[a]Department of Chemical and Biological Engineering, University of Ottawa,161 Louis Pasteur St, ON, Canada, K1N 6N5

[b]Department of Chemistry and Biomolecular Sciences and Centre for Catalysis Research and Innovation, University of Ottawa, Ottawa, Ontario K1N 6N5, Canada

Abstract

Adsorbents made from cellulose derivatives have widely been used to remove contaminants such as toxic gases, medications, colours, and metals due to their availability, cost-effectiveness, and non-contaminating nature. In this regard, we chemically modified cellulose nanocrystals with ethylenediamine (EDA) in the absence of solvent to create amine-functionalized cellulose as a new green adsorbent for SO_2 capture. The effective surface modification was confirmed using X-ray diffraction (XRD), elemental analysis, Fourier Transform Infrared Spectroscopy (FTIR), thermogravimetry analysis (TGA), solid-state Nuclear Magnetic Resonance of ^{13}C (^{13}C-NMR), scanning electron microscopy (SEM), and energy-dispersive x-ray spectroscopy (EDS). The effect of functionalization time, functionalization temperature, and the amount of EDA in the adsorbent structure on the SO_2 capture capacity have been studied. During these investigations, the highest adsorption capacity of 0.0293 mg_{SO2}/100 $mg_{sorbent}$ was reported using the sorbent prepared at 70^oC for 8 hr at constant room temperature, atmospheric pressure, and a flow rate of 20 ml/min. Furthermore, the performance of this adsorbent was studied at various temperatures and flow rates. We concluded that there is a significant increase in capture capacity by decreasing temperature, confirming the adsorption behavior.

Keywords: Amine-functionalization; nano cellulose; SO_2 capture; adsorption

3.1 Introduction

Sulfur dioxide (SO_2) released from coal-fired burning plants is dangerous to the atmosphere and social well-being. Its central role in generating acid rain is currently one of the most severe global environmental hazards[1]. Scientists are examining and developing approaches to purify flue gas streams due to the harmful effects of SO_x emissions. Several advancements have been achieved in the removal of SO_2 from industrial exhaust gases. Adsorption-catalysis technology has been successfully used to remove SO_2 from flue gas and has been shown to be particularly promising [2],[3]. The dry desulfurization method effectively avoids generating large amounts of by-products, unlike wet desulfurization technologies[4]. Although a wet process using a Ca or Na compound such as $Ca(OH)_2$, $CaCO_3$, Na_2CO_3, and $NaHCO_3$ has been utilized to eliminate SO_2, dry processes have attracted significant concerns from the scientific community[5].

These conventional and wet technologies have advantages of large-scale establishment and maturity, although they consume much energy and could rarely achieve deficient concentrations (i.e., ppm level)[3]. Therefore, dry-based technologies have benefits over wet-based counterparts in respect to cost and waste production. They are inexpensive and facilitate the recycling of SO_2. Using a porous adsorbent to remove SO_2 is the simplest and most cost-effective way among these. In such an adsorption process, SO_2 is adsorbed as gas molecules through physical adsorption, which occurs largely at room temperature, and the saturated adsorbent is recycled through SO_2 desorption, which is accomplished by raising the temperature or lowering the pressure. Nevertheless, this can happen by employing innovative adsorbents, and one of the main barriers to the expansion of such technologies is still the development of efficient and productive materials and remains in the initial phases of development[3,4],[7], [8].

One of the drawbacks of a heterogenous sorbent is its cost. Since cellulose is the most abundant natural polymer, low-cost, versatile material, offering crystalline structure and functionalizing through the hydroxyl groups, some studies used cellulose, for instance, for CO_2 capture from air capture or volatile organic compounds (VOCs)[9],[10]. Previous studies have shown that the gas capture capacity of cellulose could be significantly improved by modification with amine functional groups. Several methods can load functional groups onto the surface of cellulosic material [11-15]. As SO_2 is a stronger acid than CO_2, some adsorbents used for CO_2 capture could also give indications of suitable properties for SO_2 capture.

For example, Bernard and et al.[11] investigated amine-modified cellulose for CO_2 capture. In another study, amine-based nano-fibrillated cellulose was investigated for CO_2 Capture from Air. The results demonstrated that at a CO_2 concentration of 506 ppm, 61.16 mg CO_2/g adsorb after 12 h at 25^oC. In another study, cellulose nanofiber (CNF) aerogel was grafted with Aminopropyl triethoxysilane (APS) to adsorb CO_2. It was expected that the CO_2 adsorption capacity increased with increasing the concentration of APS grafted on the CNF aerogels due to the higher nitrogen content. However, with a higher concentration of APS grafted on the CNF aerogels, the thermal stability and the crystallinity of modified CNFs decreased slightly. It was also shown that the CO_2 adsorption capacities depended on the effective amine loading on the polymer surface[12],[13]. Finally, amine-modified cellulose has been applied for the adsorption of other pollutants. For example, Silva Filho et al, [14],[15], modified microcrystalline cellulose with ethylenediamine without using chlorinated solvent at 70^oC for 3 hr and EDA/NCC=25 and utilized this adsorbent to remove amitriptyline drug from the environment. Using halogenated solvents allows functionalization at a low temperature of around 40^oC; however, solvents are dangerous and toxic. Therefore, it is hypothesized that increasing temperature instead of using dangerous solvents could probably overcome energy barriers and make the reaction less hazardous for the environment, which is also the purpose of this research.

This study aims to investigate the effect of amine groups on the surface of nanocrystalline cellulose (NCC) and compare it with pure NCC for SO_2 capture. Building on previous studies on ethylenediamine functionalization at higher temperature for other applications [14],[15], this work aims at proposing optimized functionalization conditions for SO_2 capture application without the use armful solvents. Seven adsorbents were prepared at different condition of functionalization time (3, 5.5, 8), functionalization temperature (70, 85, 100^oC) and ethylenediamine (EDA) amount (EDA/NCC=15, 25, 40 molar ratio) to study the effect of amine groups on the SO_2 capture performance[15], [16]. They were prepared without any chlorinated solvent, which is very toxic. The introduction of amine groups could increase the alkalinity NCC and increase the hydrogen bonding sites, thereby inhibiting the volatility of EDA. Physical properties of the as-prepared EDA-NCCs, such as thermal stability, crystallinity, were characterized systematically. Then, SO_2 adsorption capacities were measured at different temperatures and flow rates to study their effect on adsorption capacity. This work would share a novel strategy for green SO_2 adsorption technology and related applications.

3.2 Experimental Procedure

3.2.1 Materials

The spray-dried powder form of the NCCs (BET: 0.7661 ± 0.0134 m²/g) was obtained by CelluForce Inc. (Windsor, Quebec). 0.7661 ± 0.0134 m²/g Laboratory grade ethylenediamine was purchased from Sigma-Aldrich. Distilled water was used to wash the adsorbents. Ar and SO_2 (35 ppm SO_2 in Ar) gas cylinders were received from Messer, and all the gases were of purity greater than 99.99%.

3.2.2 Synthesis of Amine-functionalized NCC

NCC was functionalized with amine groups using a solvent-free and environmentally friendly technique. The cellulose was activated in inert environment using a Schlenk line by flowing nitrogen gas at 110 °C for 1 hour and then producing a vacuum for 30 minutes before the reaction. 1 g of cellulose was modified with ethylenediamine by varying the ratios of EDA/NCC, the contact time and the temperature in a three-neck flask. The resulting material was centrifugated (6000 rpm for 5 min) and washed with distilled water. The product was then separated from the supernatant and dried for 12 hours at 60°C. A design of experiment to evaluate the effect of parameters with a synthesis time (3, 5.5, and 8 hours), temperature (70, 85, and 100 ^{o}C), and stoichiometry (15, 25, and 40 molar ratios of EDA/NCC) was performed. The synthesis conditions of the adsorbents are shown in Table 3.1. The naming of adsorbents based on synthesis conditions are given in the whole text as adsorbent (temperature, time, EDA/NCC ratio).

Table 3.1 Synthesis condition of the sorbents

Sample	Temperature (^{o}C)	Time (hr)	EDA/NCC ratio
NCC	-	-	-
EDA-NCC	70	3	25
EDA-NCC	70	5.5	25
EDA-NCC	70	8	25
EDA-NCC	85	3	25
EDA-NCC	100	3	25
EDA-NCC	70	3	15
EDA-NCC	70	3	40

3.2.3 Characterizations

Attenuated Total Reflection-Fourier Transform Infrared (ATR-FTIR) spectra of the modified NCC were obtained using a Nicolet 6700 FTIR (Thermo Scientific) with a diamond crystal. To determine the type of functional groups in the samples, all scans are captured at a resolution of 4 cm^{-1} in a range of wave numbers between 400 and 4000 cm^{-1}. Carbon Nuclear Magnetic Resonance (^{13}C NMR) spectra of samples obtained using a single crystal solid state probe on a Bruker AVANCE III 200 NMR spectrometer. This approach is also used to confirm the type of functional groups and the compound's overall structure. X-Ray Diffraction (XRD) using The Rigaku Ultima IV Diffractometer was performed to examine the crystallinity structure of the material. At room temperature, the XRD test is performed with Cu K radiation (=1.5418) at 40 kV and 44 mA, with 0.02° step width and 1°/min scan speed, with a 2θ range of 5° to 60°. Scanning electron micrograph produced from the top surface of samples using the Zeiss Gemini SEM 500 is used to assess their morphology at various magnifications and micron scales. To learn more about elemental analysis, EDS was used in conjunction with SEM. Thermogravimetric analysis (TGA) was performed using a Perkin Elmer Pyris to determine the structural stability of compounds as temperature changes. The samples (4–7 mg) were placed in a platinum pan and heated up to 700°C at 10°C/min rate under nitrogen purge (20 ml/min).

3.2.4 SO_2 Adsorption Set-up

The sorbents were tested for their ability to adsorb SO_2 via a simulation of a stream containing the toxic gas. Figure 3.1. displays a detailed schematic of the SO_2 setup. A cylinder graded at 35 ppm of SO_2 in argon was used. SO_2 capture study was carried out in a fixed-bed quartz reactor tube. The reactor is put inside a tubular furnace (2.5mm ID, 3.5 mm OD, and a total heating length of 450 mm). A rotameter controlled the flow rates of Ar and SO_2 in Ar. The furnace temperature was controlled using an electrical heater and a temperature controller and measured using a K-type thermocouple. An SO_2 detector, Drager X-am 2500 detector, attached at the quartz tube outlet, detected the amount of SO_2 not captured by the prepared material and recorded the SO_2 concentration at a minute interval. Because SO_2 can be harmful even at low concentrations, the setup is placed within a fume hood. The sample (50 mg) is put in the reactor sandwiched in quartz wool, with an adsorbent length bed of approximately 20 mm. Before each run, the adsorbent sample (approximately 50 mg) was purged for 30 min online under a 15 $ml.min^{-1}$ flow pure argon at room temperature and atmospheric pressure to purge the sample from adsorbed water and other physisorbed species. Since the specific surface area of cellulose was very small, we hypothesized that argon could not be adsorbed through internal penetration [30]. During this time, the temperature was increased to the specific operating temperature to be tested. When it reached steady-state, pure Ar was stopped and, the SO_2/Ar mixture (35 ppm SO_2 in Ar) was fed at the inlet of the quartz tube at a specific volumetric flow rate to be tested, considering argon is inert.

A blank experiment was performed for each set of operating conditions and used as the baseline to correct and normalized all experiments. The system reached a saturation when the outlet concentration read on the Drager detector was constant or until the effluent concentration was equal to the input concentration, i.e., $c_t/c_0=1$, indicating that thermodynamic equilibrium was attained. The data is exported from the USB to an Excel file via Gas Vision Software. The read concentration at maximum (when reaching saturation) for the repeated blank experiments was 25 ppm and used as the inlet concentration. It is different from the supplier-provided information, which was 35 ppm, attributed to experimental errors. The results were then normalized using the blank experiments. Additionally, experiments with blank samples showed that the reactor system was inert in adsorbing gas. Because the amount of outlet SO_2 gas quickly reached 25 ppm and did not change after a long time. This indicates that the whole system is ineffective in adsorbing gas.

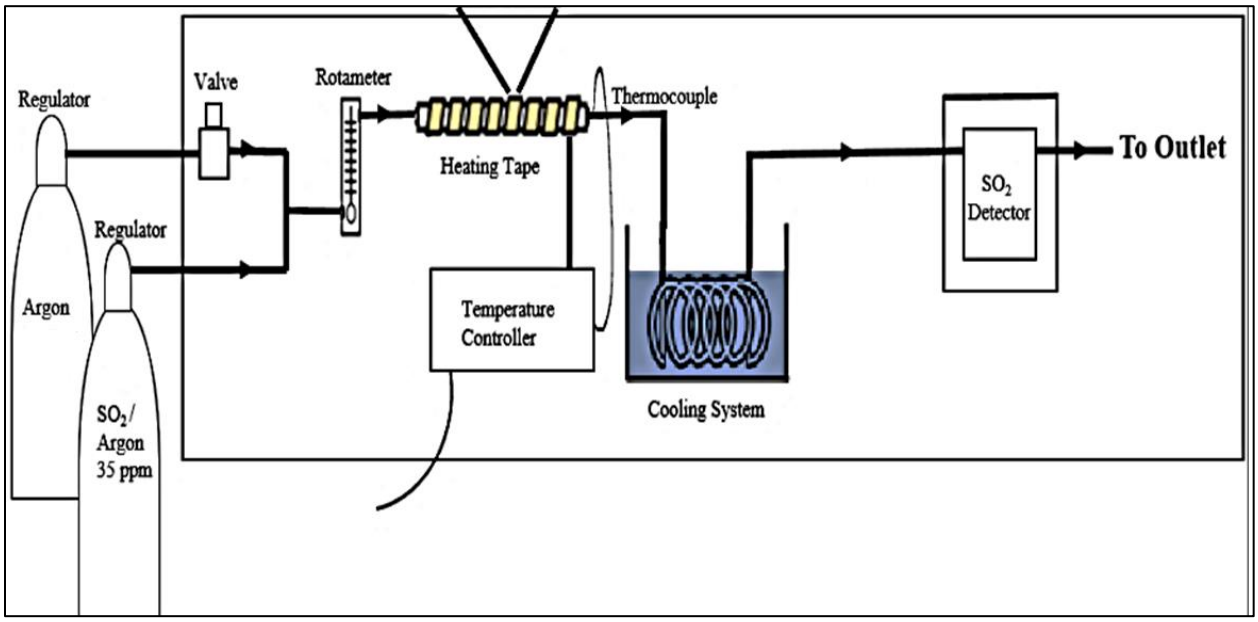

Figure 3.1 Detailed schematic of the SO_2 setup

In this study, the setup itself was tested with three different conditions to assess the adsorption results. First, the SO_2/Ar was fed through an empty tube containing no traces of the adsorbent or any other material. The fresh NCC from the supplier was tested as well. Finally, the synthesized sorbents were tested. At the end of each run, argon gas was fed to purge the system. the SO_2 Capture capacity at saturation is determined from below equation 1:

$$Q = \frac{[(\int (C_i - C_o)dt) \times volumetric\ flowrate]}{Mass\ of\ material} \qquad \text{Eq.1}$$

Where Q is adsorption capacity (mg SO_2/mg adsorbent) and C_i and C_o are the amounts of SO_2 at the inlet and outlet, respectively, and *t* is time. A detailed description of the calculations is given in Appendix 1. The flow rate of the reaction was varied from 10 mL/min to 30 mL/min, and the mass of material was taken as 50 mg.

3.3 Results and discussions

The proposed surface reaction mechanism for the functionalization of cellulose with EDA at low and high temperatures is depicted in Fig 3.2b. As can be observed, direct reactivity of NCC hydroxy groups with an amine at lower temperatures is likely to be challenging because the basic amine will deprotonate the -OH groups, resulting in a highly unreactive ammonium salt. When the ammonium salt is heated to a temperature above 70^{o}C, water is driven off, forming the final product [17].

As mentioned in the previous section, several methods incorporate amine sites on the cellulose surface. In most methods, an intermediate chlorination step using thionyl chloride ($SOCl_2$) is applied to enhance the reactivity of hydroxyl groups and then increase the incorporated amine groups (Fig 3.2 a)[15]. In this study, cellulose is directly functionalized using ethylenediamine (EDA) without chlorination step, making this process less hazardous to the environment and more cost-effective. To see if the amine incorporation was successful, physiochemical characterization of aminated NCCs was performed and described.

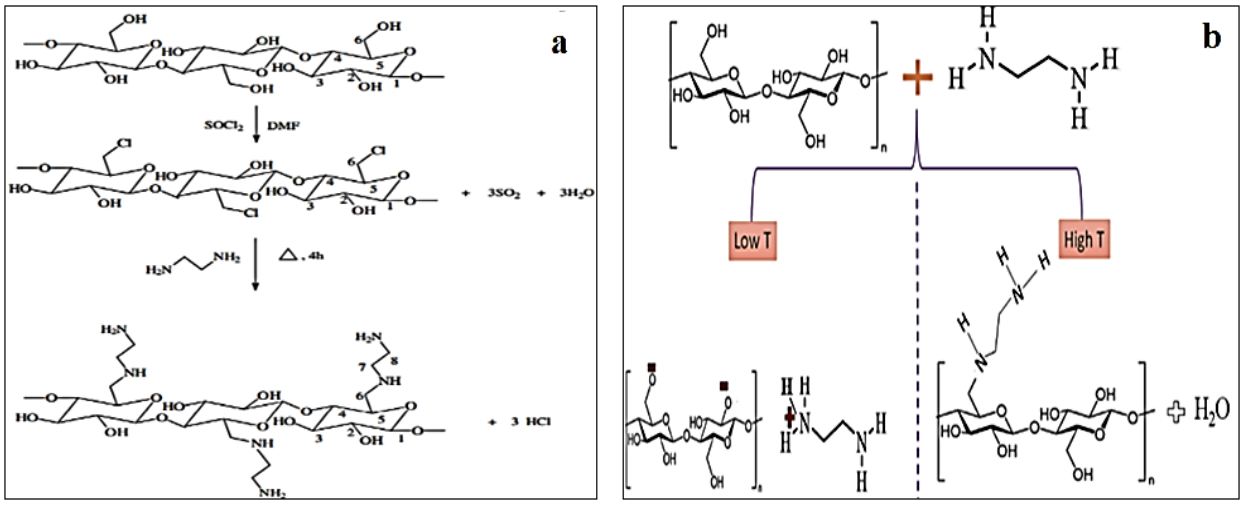

Figure 3.2. a) Schematic of modification via an intermediate chlorination step b) the proposed surface reaction of NCC and EDA at low and high temperature, [18].

3.3.1 Physiochemical Characterization of Aminated NCCs

ATR-FTIR spectroscopy was used to demonstrate the presence of primary amine groups in NCC. The FTIR spectrum of EDA-modified NCCs is shown in Figure 3.3. When comparing the FTIR

spectra of EDA-NCC to NCC, the characteristic cellulose peaks are visible at 1080 cm^{-1} related to C-O-C stretching vibrations, 1490 cm^{-1} attributed to carbonyl groups at the reducing end of NCC, the characteristic peak for hydroxyl groups from 3500 to 3200 cm^{-1} and at 3400 cm^{-1} assigned to C-H stretching vibration characteristic for the aliphatic[19]. For the functionalized NCCs, a distinctive peak between 3500 and 3200 cm^{-1} and a peak extending from 1640 to 1500 cm^{-1} should be present[20]. The FTIR spectrum of EDA-modified NCCs presents several bands like those in the FTIR spectrum of untreated NCC. The distinctive N-H peak between 3500 and 3200 cm^{-1} was hidden by the high O-H absorption of cellulose, thus preventing observation of the absorption bands corresponding to the amino groups.

Nevertheless, significant changes are observed after cellulose modification by ethylenediamine, such as the appearance of two bands, one around 3364 cm^{-1}, related to the N–H stretching of primary amines and another one at 1575 cm^{-1} (between 1640 and 1500 cm^{-1}), corresponding to N–H deformation primary amines[19], [20]. Although the O-H absorption peak at 3500 -3200 cm^{-1} masked the primary amine peak, the other characteristic peak ranging from 1640 to 1500 cm^{-1} is easily distinguishable from the NCC, as shown in Figure 3.3. The existence of this peak proves that a primary amine was conjugated to the NCC surface[16], [21]–[23].

It is evident that by increasing temperature and EDA, the peak intensity at 1575 cm^{-1} is increased, indicating that the amount of incorporated amine is affected by the synthesis conditions. It is seen that decreases in band intensities at 3500-3200 cm^{-1} occur, which is associated with reducing the number of O–H vibrations due to the substitute of O–H groups by amino groups after the chemical modification.

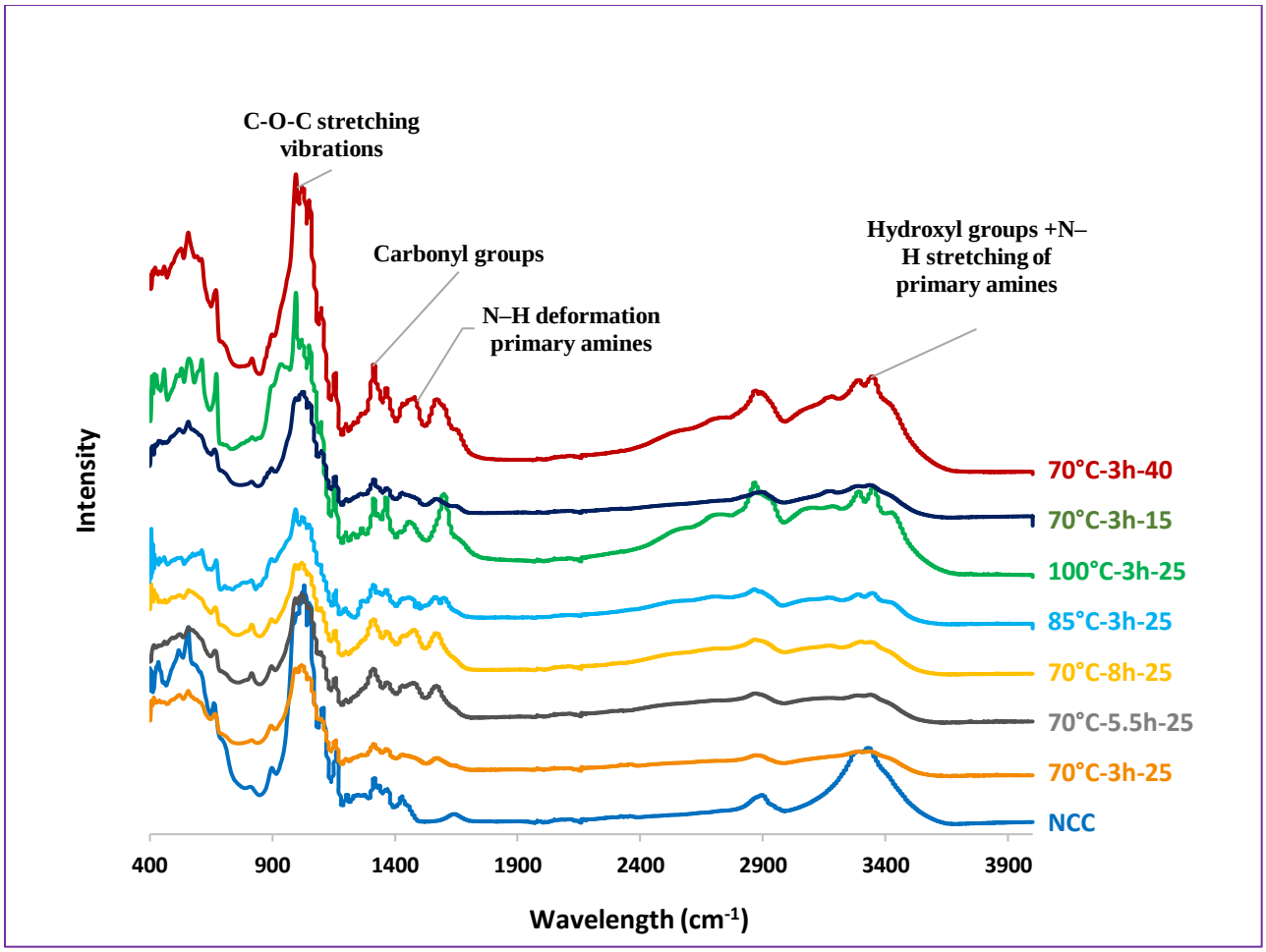

Figure 3.3 ATR-FTIR results of pristine NCC and the modified NCC at different conditions

On the other hand, FTIR spectroscopy cannot discover to which carbon the primary amine is added. The C6 or C2 carbon atoms were thought to be involved in the amine functionalization of the NCC surface, which was investigated using solid ^{13}CNMR.

The pure cellulose's solid-state ^{13}C-NMR spectrum is shown in Figure 3.4. Because it is connected to two oxygen atoms, the C1 (carbon 1) exhibits the largest chemical shift in this spectrum at 105 ppm. C4, coupled to only one oxygen and responsible for the 1,4-glucoside bond, is assigned the signals at 89 and 84 ppm. The signal at 89 ppm denotes a higher crystallinity zone, whereas the at 83 ppm denotes a less crystalline or amorphous carbon. The signals at 75, 73, and 71 ppm are ascribed to C2, C3, and C5, which all have similar chemical environments. Finally, the signals at 65 and 63 ppm are attributed to C6, which has the smallest chemical shift since it is a primary

carbon attached to a hydroxyl and contains the only CH_2 in the cellulose. The signal at 65 ppm corresponds to higher crystallinity regions, while 63 ppm corresponds to lower crystallinity regions[24], [25].

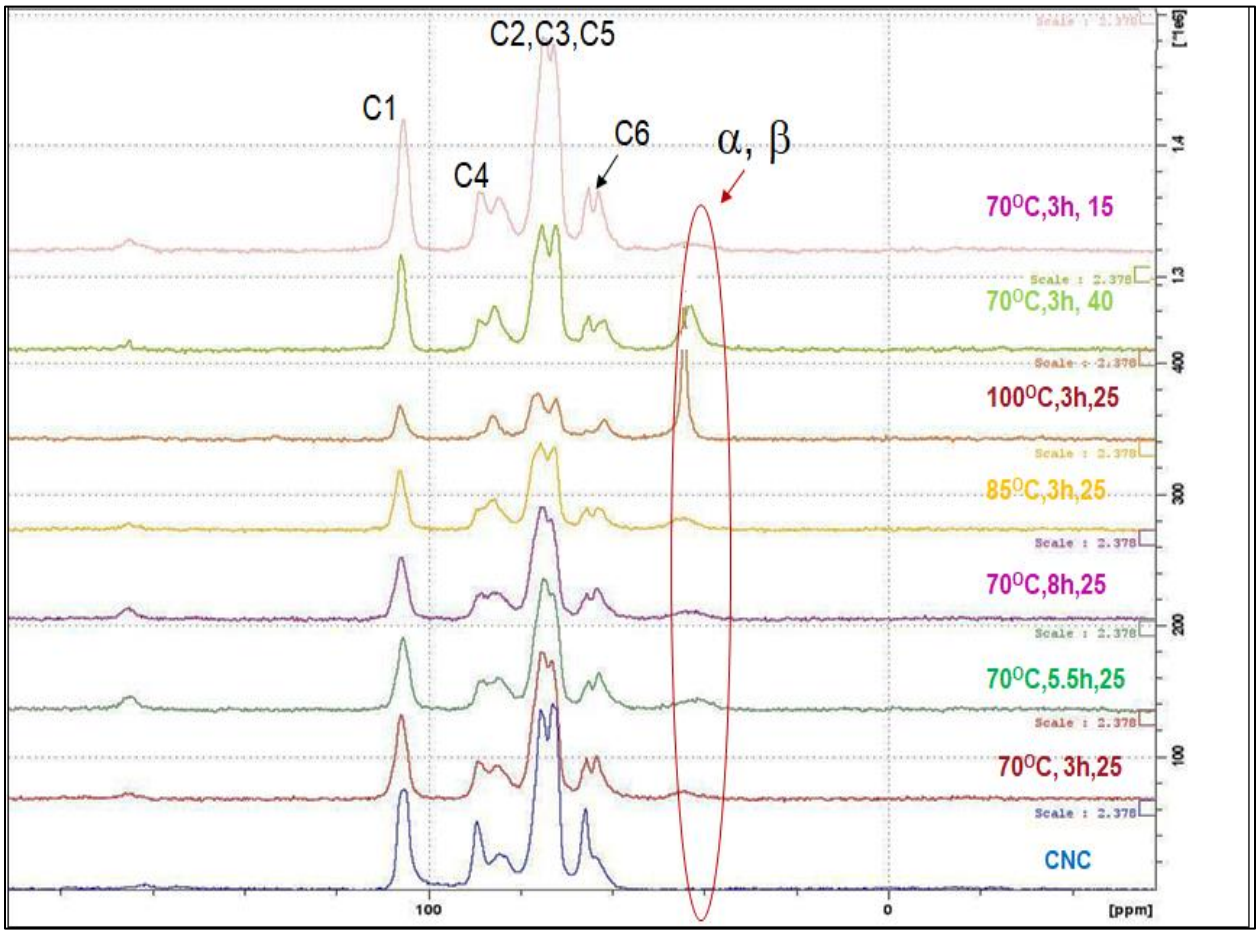

Figure 3.4. ^{13}C NMR of the pristine NCC and the modified NCC at different conditions

After modification, no substantial variation in the C1 signal corresponding to untreated cellulose is evident; however, these spectra show significant changes in the other chemical shifts. In the region from 75 ppm to 71 ppm, related to C2, C3, and C5, there was a decrease in the intensity of the 72-ppm peak. At C4, there was a decrease in intensity of the 89-ppm peak after chemical modification, which indicates a region of higher crystallinity according to the Atalla and VanderHart[26], who analyzed cellulose structure with solid-state ^{13}C NMR spectroscopy [19], [20]. Because of the depolymerization of the crystalline component of the cellulose, the intensity

of the 65-ppm peak decreased. So, these modifications demonstrate ethylenediamine immobilization and the formation of NCC polymer. Furthermore, from 40 ppm to 80 ppm, the presence of the α and β carbons of ethylenediamine was detected in these spectra [25], [29]. A proposed functionalized path based on the ^{13}CNMR results is shown in Figure 3.5.

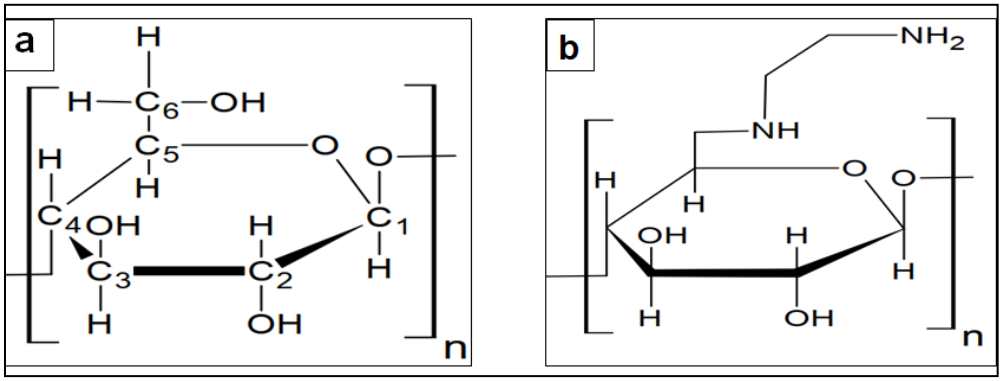

Figure 3.5. a) Cellulose structure b) Proposed functionalized path of reaction of NCC and EDA based on ^{13} CNMR

X-ray diffraction (XRD) patterns of pure NCC and aminated NCCs are shown in Figure 3.6 to investigate changes in the synthesized material's crystallinity. It has been reported that the structure of nanocrystalline cellulose has three characteristic peaks located at $2\theta = 15.54^{\circ}$, $2\theta = 22.90^{\circ}$ and $2\theta = 34.72^{\circ}$, which are related to the crystallographic planes (101), (002) and (040), and corresponding to interplanar distances of 5.64, 3.96 and 2.59 Å respectively[22], [23].

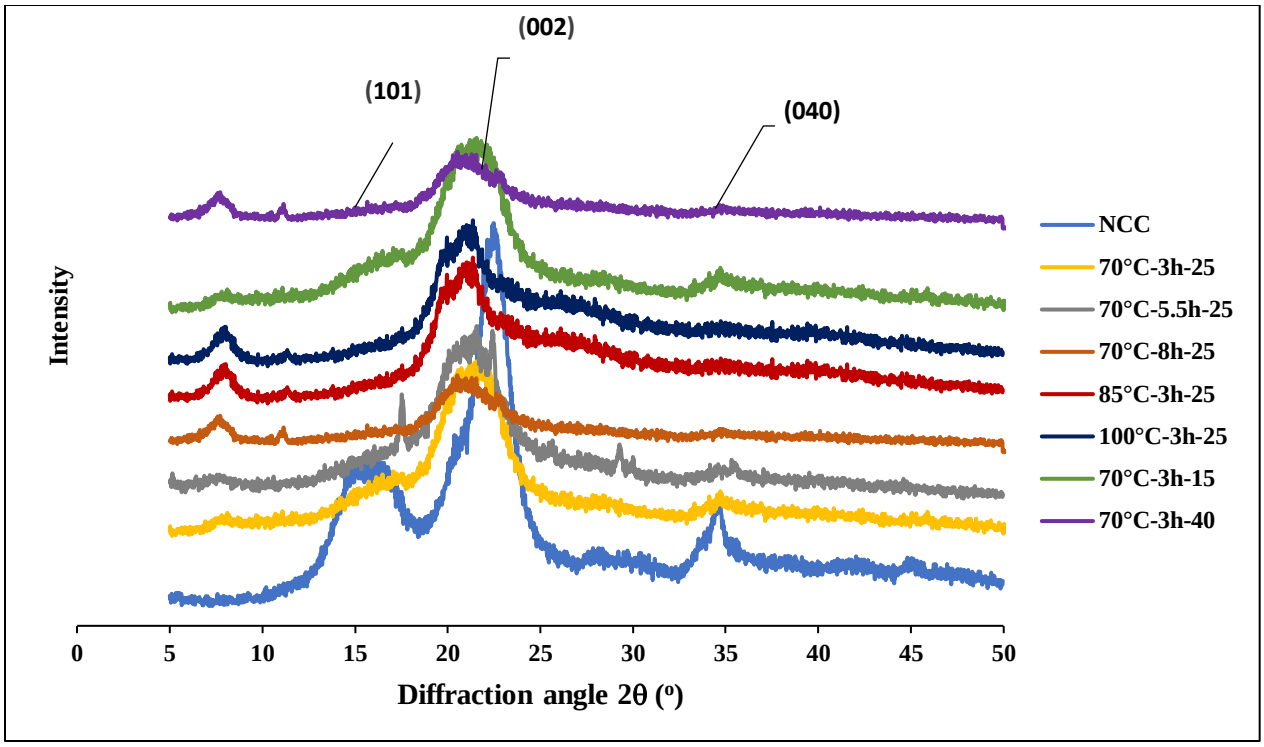

Figure 3.6. XRD spectra of the pristine NCC and the modified NCC at different conditions

When comparing the XRD pattern for EDA-NCCs sorbents to the NCC, no new peak or apparent peak shifting was observed. A decrease in crystallinity being more pronounced in the modified NCCs. These results are coherent with the ^{13}C-NMR analysis. After chemical modification, this decrease in the cellulose crystallinity is attributable to incorporating of amino groups on the cellulose surface. Consequently, the incorporation of amino groups causes changes in polymer's hydrogen inter and intramolecular interactions and its organizational structure, reducing the cellulose's crystallinity following chemical modification[16], [21]. Furthermore, after chemical modification, the NCC crystallinity index (*IC*) was determined by the Segal et al. method [25] to quantify the cellulose crystallinity reduction. As shown in Equation (2) below:

$$IC = [(I_{002} - I_{am})/I_{002}] \times 100 \qquad \text{Eq. 2}$$

Where I_{002} is the peak intensity of the (002) lattice diffraction, and I_{am} is the minimum intensity of diffraction in the same units between (002) and (101) peaks regarding the non-crystalline material in cellulose.

Table 3.2 shows the IC of samples and can see by increasing the time, temperature, and amount of EDA, the crystallinity index is decreased. The reduction in IC is in accordance with the results mentioned above that the EDA modification on the NCC surface causes a disturbance in the hydrogen bonds, hence reducing the crystallinity of the polymers.

Table 3.2 IC of samples

Sample	IC (%)
NCC	80.75
EDA-NCC (70^{o}C, 3hr, 25)	58.41
EDA-NCC (70^{o}C, 5.5hr, 25)	56.33
EDA-NCC (70^{o}C, 8hr, 25)	40.10
EDA-NCC (85^{o}C, 3hr, 25)	53.80
EDA-NCC (100^{o}C, 3hr, 25)	39.46
EDA-NCC (70^{o}C, 3hr, 15)	62.93
EDA-NCC (70^{o}C, 3hr, 40)	53.12

SEM micrographs acquired for the NCC and functionalized- NCC are depicted in Figure 3.7. The modification of cellulose with ethylenediamine generated a modified NCC with nitrogen incorporated into its surface. As expected, there is no noticeable difference in the morphology of the NCC and EDA-NCCs. It can only be seen that with the addition of amines, the cellulose particles, which are in the form of rods or cylinders, are slightly agglomerate.

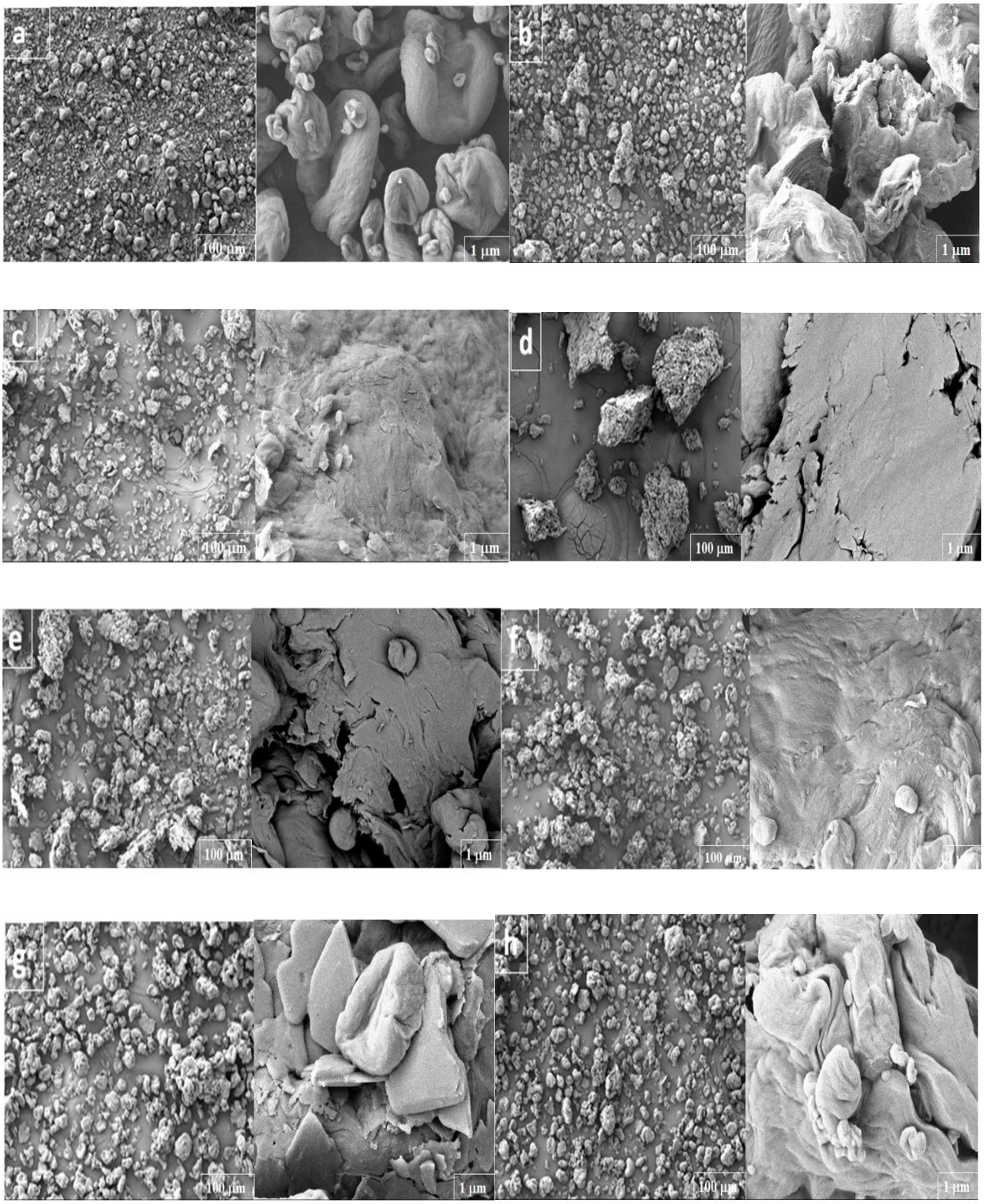

Figure 3.7. SEM of the pristine NCC and the modified NCC at different conditions a) NCC, b) EDA-NCC (70^{o}C, 3hr, 25), c) EDA-NCC (70^{o}C, 5.5hr, 25), d) EDA-NCC (70^{o}C, 8hr, 25), e) EDA-NCC (85^{o}C, 3hr, 25), f) EDA-NCC (100^{o}C, 3hr, 25), g) EDA-NCC (70^{o}C, 3hr, 15), h) EDA-NCC (70^{o}C, 3hr, 40)

The qualitative elemental analysis was performed by EDS to confirm the addition of nitrogen groups on the surface of NCC. Figure 3.8 shows the EDS results for NCC and EDA-NCCs. The peak of Au is due to the use of carbon and gold strip to perform the analysis. On comparing NCC and amine functionalized-NCC, the addition of the N peak confirms the successful addition of EDA on the surface of NCC. However, because of the most common detector designs, nitrogen produces a very weak response making its detection unreliable for most materials. It can be seen, by increasing the amount of EDA on the NCC surface, the N peak intensity increases. However, the results of EDS are not directly quantitative and rather give us an indication of whether the functionalization method was successful.

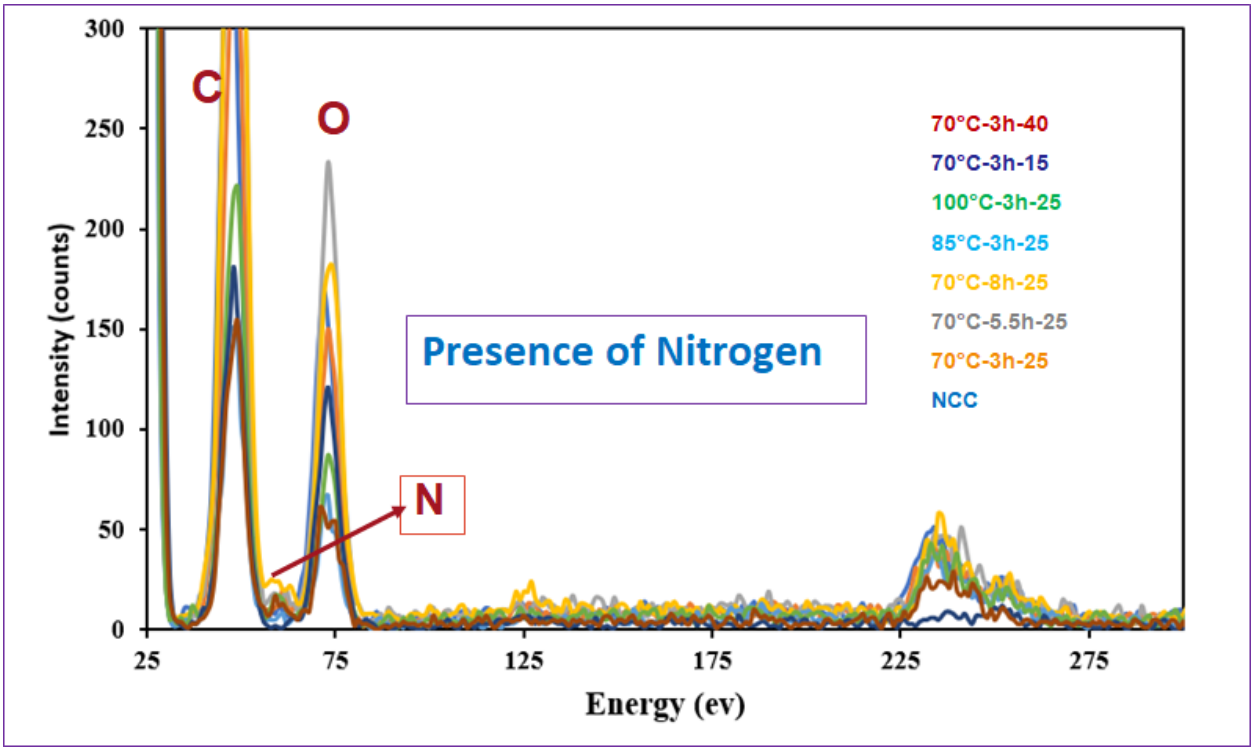

Figure 3.8 EDS analysis of the pristine NCC and the modified NCC at different conditions

Thermogravimetric analysis (TGA) curves of the untreated NCC and modified NCCs are shown in Figure 3.9, and the derivatives of the curves (derivative thermogravimetry (DTG)) are given in Figure 3.10. The curve shows a major decomposition event for pristine cellulose starting at 287^{o}C, with a sudden mass loss of 60%. The NCC then continues to decompose gradually and is entirely decomposed at 574^{o}C. At temperatures between 40^{o}C and 287^{o}C, a mass loss of 4.47% is

equivalent to the water physically adsorbed on NCC's surface. All samples contain moisture as the weight begins dropping immediately upon heating. The thermolysis reaction of cellulose occurs by the cleavage of glycoside bonds (COH, COO, and COC bonds) and by dehydration, decarboxylation, and decarbonylation [20], [22], [23].

The DTG curve from the modified NCCs show three main events of decomposition. The first is related to physisorbed water on the surface of the sorbents. It is observed between 25-60 ^{o}C with a mass loss varying between 4.45-9% for EDA-NCC samples, apart from sample EDA-NCC (100^{o}C, 3hr, 25). This showed a significant mass loss of 30%, indicating that the sample prepared at higher temperatures may have more amine functional groups. The second decomposition event is related to the decomposition of the modified NCC, i.e., decomposition of the amino groups. This event occurs between 60 ^{o}C and 300 ^{o}C, corresponding to a mass loss of 10-50 %, and T_{peak} between 320-340 ^{o}C, attributed to the elimination of NH_3 molecules and the cellulose structure. The third event is related to the decomposition of the cellulose structure [19], [20]. DTG picks (T_{peak} DTG) represents the temperature that occurs the maximum mass loss of each stage for all samples.

These results indicate that the synthesized material is sensitive to temperature, with a possible loss of amine groups at relatively low temperatures. Nevertheless, it also shows that EDA-NCCs are more stable than the NCC at temperatures above 480 ^{o}C. In other words, the immobilization of amino groups on the surface of the cellulose increases the polymer's thermal stability and reduces mass loss at temperatures exceeding 480^{o}C. NCC had a sharp weight loss starting at 320 °C, but the EDA-NCCs decompose at a substantially lower temperature (60°C). This behavior is attributed to the decreased crystallinity associated with the modification reaction, as confirmed by XRD analysis and lower thermal stability than NCC.

As a result of increasing EDA content, the lower thermal stability of polymer in comparison to NCC causes a progressive shift of the TGA degradation curves of the EDA-NCC sorbents toward lower temperatures, and the main degradation temperature of the EDA in the sorbents progressively decreases with increasing EDA content which prepared at a longer time and higher temperature of the reaction.

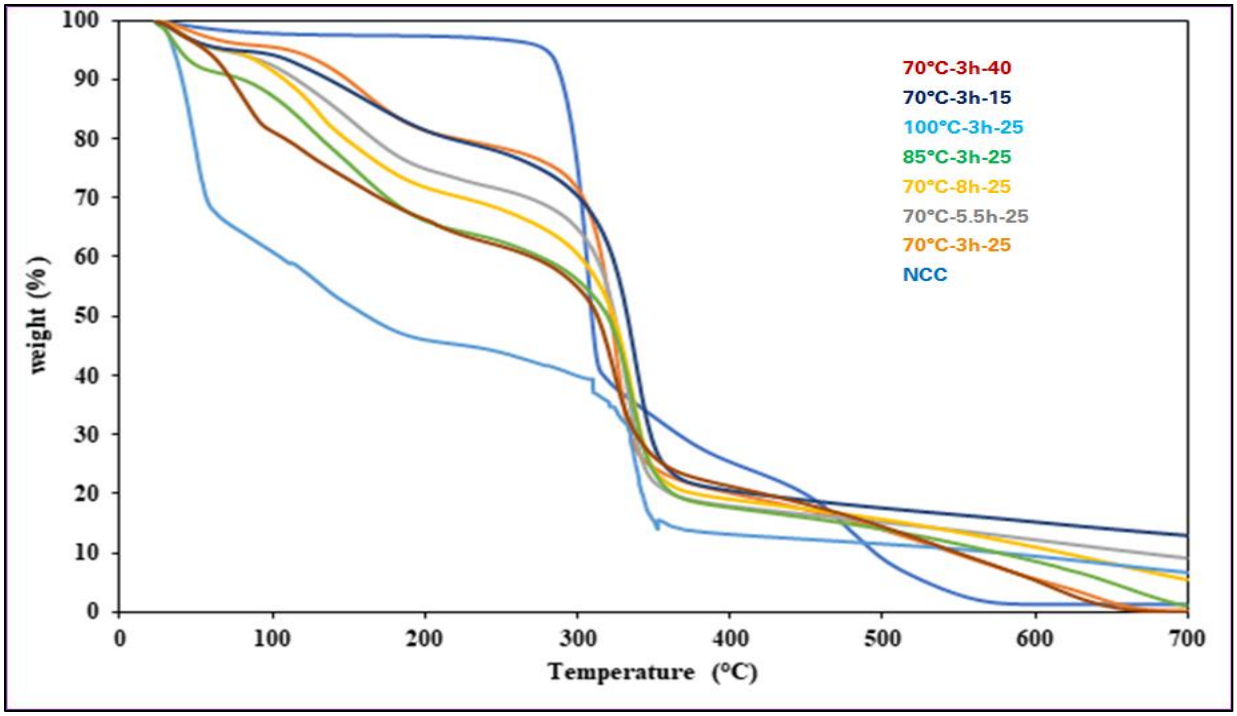

Figure 3.9. TGA results of the pristine NCC and the modified NCC at different conditions

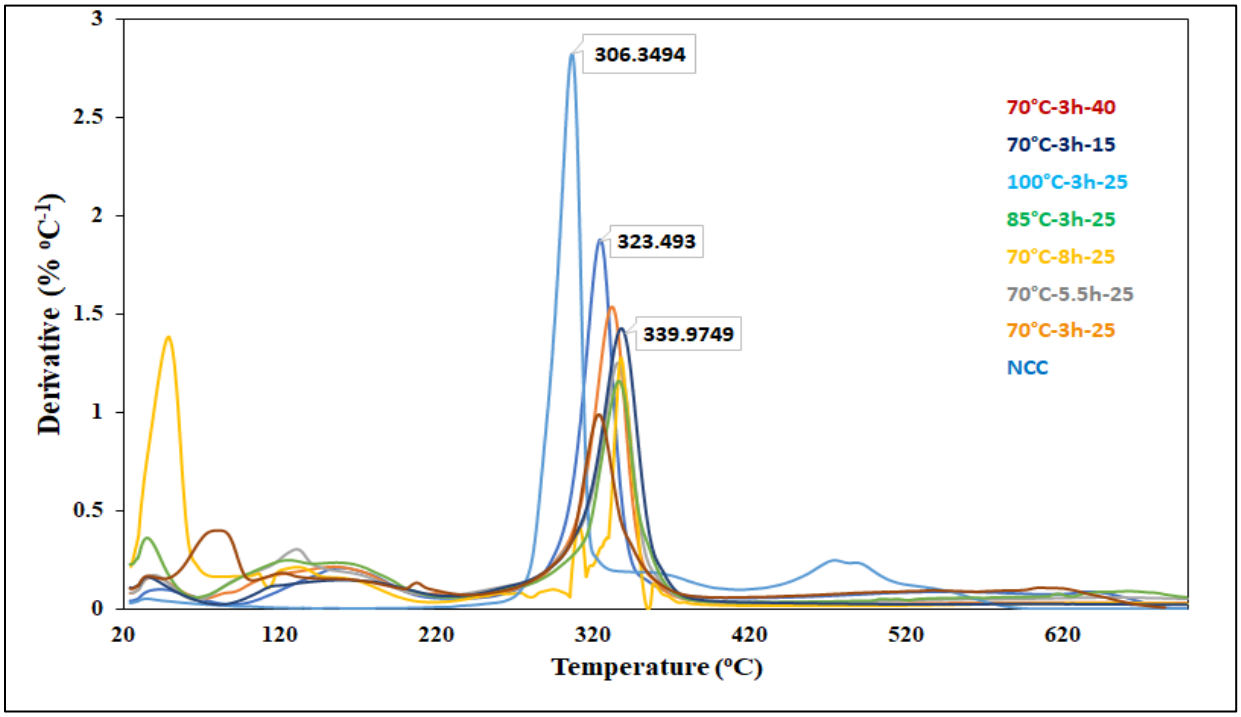

Figure 3.10. Derivatives of the curves (DTG) of the pristine NCC and the modified NCC at different conditions

3.3.2 SO_2 capture studies

It is known that the SO_2 capture capacity of cellulose is a combination of both physical and chemical adsorption. As can be seen from Table 3.3, adsorbents EDA-NCC (70°C, 8hr, 25) and the pristine cellulose (NCC) displayed the highest and lowest SO_2 adsorption capacities of 0.0293 and 0.0013 mg_{SO2}/100 mg sorbent at room temperature and 20 ml/min flow rate respectively. Inspection of the data reveals that the sorbent preparation variables significantly affect the SO_2 adsorption capacity.

Table 3.3. Adsorption capacity of the sorbents at saturation point (Operating conditions: room temperature, atmospheric pressure, and flow rate of 20 ml/min)

Sorbent	Q (mg SO_2/ 100 mg sorbent)
NCC	0.0013
EDA-NCC (70°C, 3hr, 15)	0.0020
EDA-NCC (70°C, 3hr, 25)	0.0037
EDA-NCC (70°C, 3hr, 40)	0.0052
EDA-NCC (70°C, 5.5hr, 25)	0.0054
EDA-NCC (85°C, 3hr, 25)	0.0058
EDA-NCC (100°C, 3hr, 25)	0.0060
EDA-NCC (70°C, 8hr, 25)	0.0293

3.3.3 Effect of amination variables on the SO_2 adsorption capacity

SO_2 breakthrough curves of sorbents prepared at different conditions along with blank studies are shown in Figure 3.11. A blank study was performed for a set of conditions, giving information on the residence time, unsteady state behavior, and maximum concentration that can be measured. The maximum concentration was evaluated to be 25 ppm (slightly different than supplier-provided information) and used to normalized experiments. A steep change from the 0 to the maximum after a short delay time is observed for the blank runs, coherent with the absence of sample.

As shown in Figure 3.11a-c, NCC has a steep change from around 15 minutes, then starts saturating around 38 minutes (and let for 2 hours total). Whereas for EDA-NCC (70°C, 3hr, 25), the saturation

starts around 116.7 mins, and it continues even after 300 mins (5 hrs) with the concentration nears 25 ppm.

For all samples, the change is less steep according to anticipated possible phenomena of capture and mass transfer limitations. The delay in breakthrough time is longer for EDA-NCC (70^{o}C, 8hr, 25) and then EDA-NCC (100^{o}C, 3hr, 25), with less steep and longer time to reach saturation. An analysis of the entire curve shows that the saturation was achieved between 50-250 min for different samples. At the later stages of the curve, there is not much of a difference between the saturation concentration of blank and samples and they have merged towards the end.

Looking at the various samples, SO_2 capture capacity increases as the temperature and time of the ammonia treatment increases. It has been reported that the amount of nitrogen functionalities added to the NCC surface affects the SO_2 adsorption efficiency of modified adsorbents. As can be seen in the figures, in comparison with the NCC, the EDA-NCCs displayed an enhanced ability to adsorb SO_2. The greatest experimental SO_2 adsorption capacity (Table 3), 0.029 mg/100 mg, was obtained for the sample EDA-NCC (70^{o}C, 8hr, 25) that had been modified with EDA at 70°C for 8 hr. Because of the improved surface chemistry, interactions between the acidic SO_2 and the basic nitrogen groups would lead to a greater SO_2 capture. Comparing the results of the prepared samples at different times show that by increasing the synthesis time of the samples, more amine groups probably are deposited on the cellulose surface, which is consistent with the results of TGA.

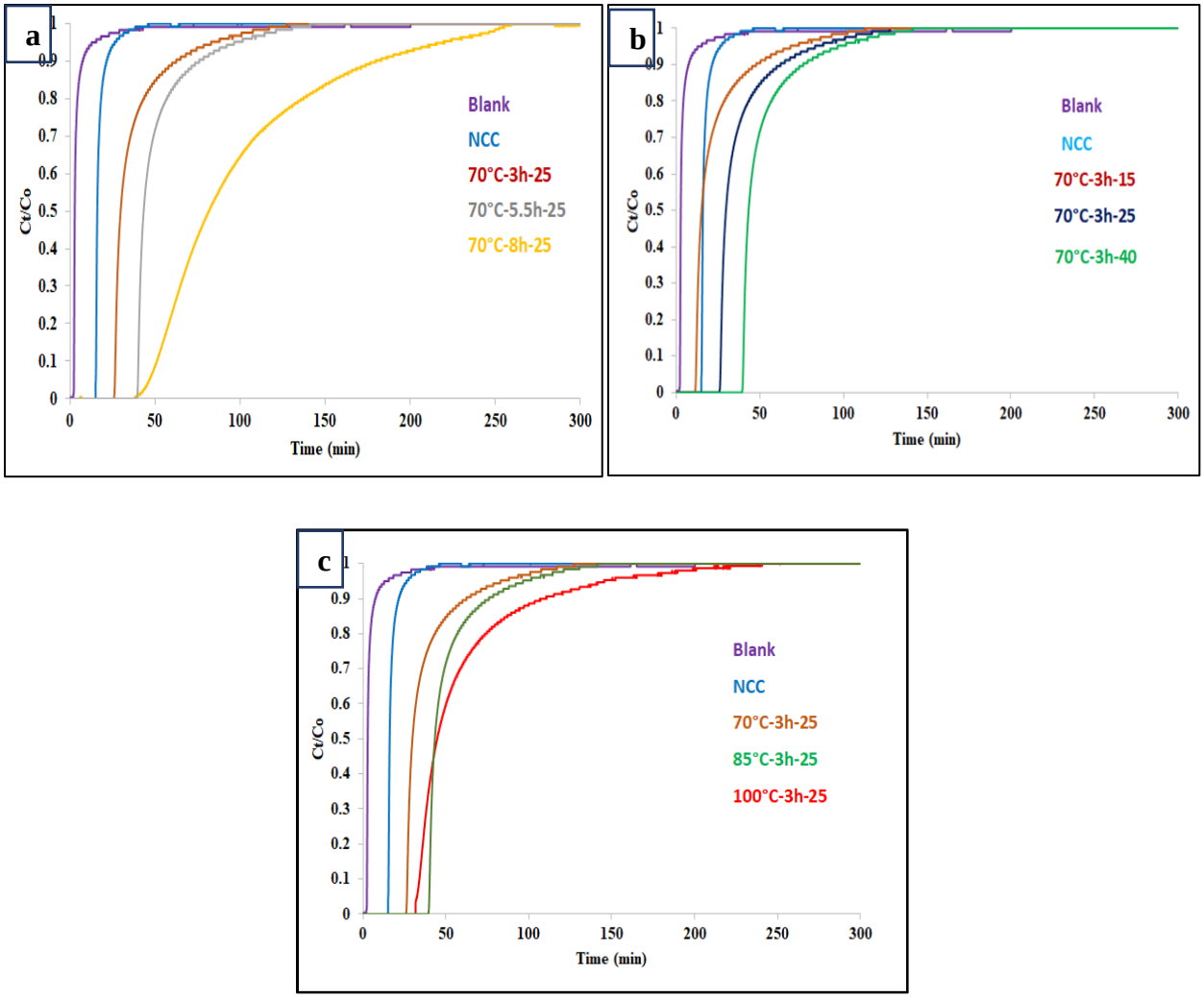

Figure 3.11 Breakthrough curves of sorbents prepared at a) different preparation time b) different EDA/NCC *ratio* c) different preparation temperatures (Operating conditions: room temperature, atmospheric pressure, and flow rate of 20 ml/min)

Note that there is also an increment in the SO_2 uptake with increasing EDA loading in the samples studied, as shown in Figure 3.12. For instance, the SO_2 sorption capacities obtained for EDA-NCC (70^{o}C, 3hr, 25), EDA-NCC (70^{o}C, 3hr, 15), and EDA-NCC (70^{o}C, 3hr, 40) are 0.0037, 0.002, and 0.0052 mg/100 mg, respectively, indicating SO_2 uptake increases significantly with increasing concentration of amine groups in the composite samples.

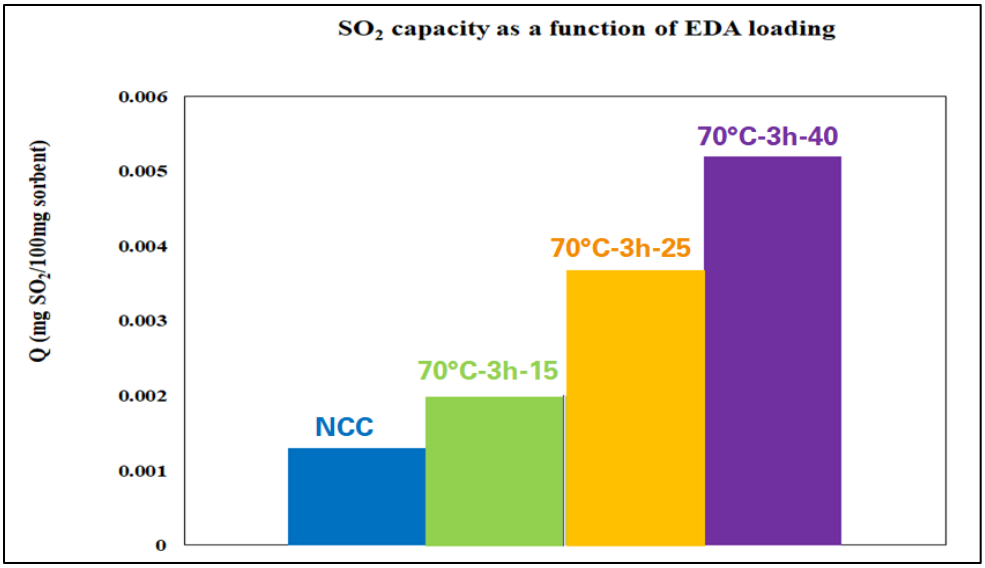

Figure 3.12. SO_2 capacity as a function of EDA loading for modified NCC prepared at 70°C for 3h with variable ratios (Operating conditions: room temperature, atmospheric pressure, and 20 ml/min)

Overall, the sorption capacity increases in the following order for samples studied: NCC< EDA-NCC (70°C, 3hr, 15) < EDA-NCC (70°C, 3hr, 25) < EDA-NCC (70°C, 3hr, 40) < EDA-NCC (70°C, 5.5hr, 25) < EDA-NCC (85°C, 3hr, 25) < EDA-NCC (100°C, 3hr, 25) < EDA-NCC (70°C, 8hr, 25). These results confirmed high sorption between basic amine sites in the EDA-NCCs and acidic SO_2 compared to NCC. This study suggests that the EDA-assisted synthesis leads to the formation of a NCC composite consisting of EDA, and subsequently, these amine groups show high affinity toward SO_2.

3.3.4 Effect of temperature on the breakthrough profile of SO_2 adsorption

The effect of temperature on the breakthrough curves of SO_2 adsorption on EDA-NCC (70°C, 3hr, 25) adsorbent as a case and NCC at feed rate 20 ml min^{-1} is illustrated in Fig 3.13. As shown in this figure, for the flow rate investigated, the SO_2 breakthrough times and adsorption capacities significantly decreased with increasing adsorption temperature for both EDA-NCC and NCC due to the exothermic nature of the adsorption process. The results indicated that the breakthrough curves obtained for NCC show a shorter breakthrough time as temperature increased compared to EDA-NCC. A reduction in breakthrough time was observed with increasing temperature for the EDA-NCC. However, this reduction in breakthrough time was not as significant as that observed for NCC, where physisorption is expected to be dominant. For example, under a feed rate of 20

ml/min^{-1}, EDA-NCC showed a 37% decrease in breakthrough time (from 40 to 25 minutes) when the temperature increased from 20 to 60 °C, whereas the NCC showed a 47% decrease in breakthrough time (from 17 to 9 minutes) over the same temperature range. Similarly, from 20 to 60°C, the capacity of the modified adsorbent decreased less than that of the NCC. An explanation for this observation is that contrary to the anticipated decrease in the physisorption, probably chemisorption through the nitrogen functionalities of EDA-NCC help preservation of the adsorption capacity at elevated temperatures. The results are consistent with those of García et al.[26] and Thote et al[27]. reporting that the breakthrough time and the dynamic CO_2 adsorption capacity of a nitrogen enriched carbon decreased with increasing temperature.

Notably, the slope of the EDA-NCC breakthrough curves was less steep than that obtained for the untreated NCC. In addition, when the temperature increased, the breakthrough profile steepened. Therefore, the mass transfer zone is reduced when the adsorbents are changed, and the temperature is raised. This observation is consistent with the results in which the rate constants increased with increasing adsorption temperature and/or a modified sample.

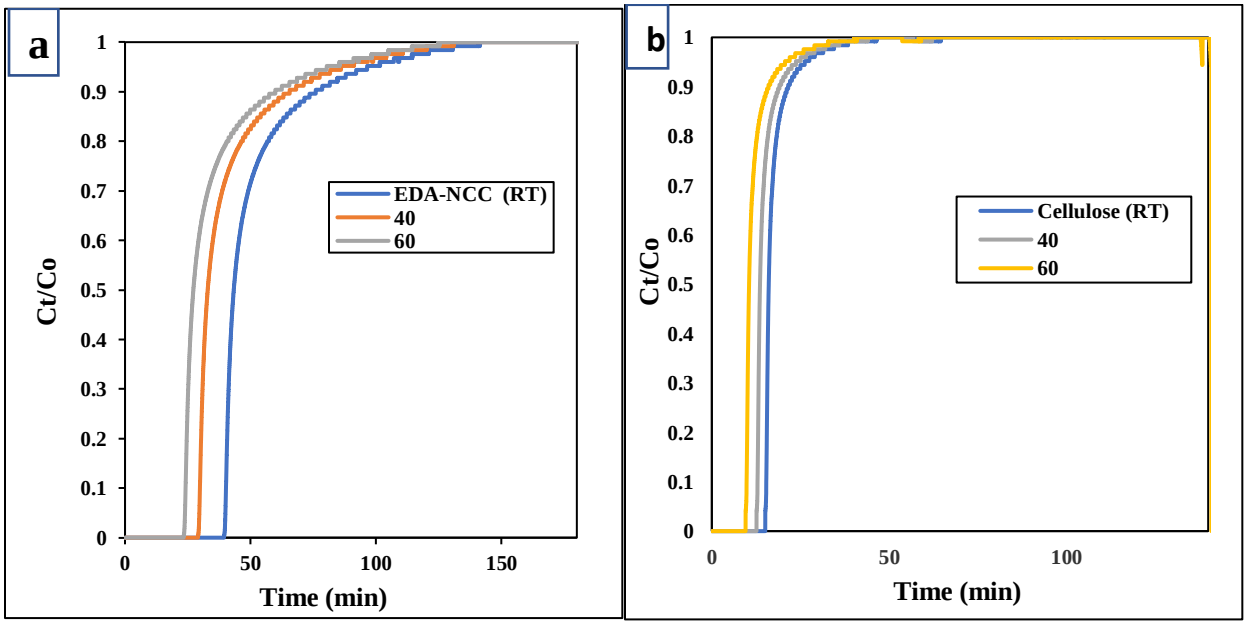

Figure 3.13. a) Breakthrough curves of EDA-NCC (70°C, 3hr, 25) and b) NCC at three different testing temperatures and constant flow rate of 20 ml/min for SO_2 catpure: room temperature, 40 °C, and 60°C

3.3.5 Effect of feed flow rate on the breakthrough curve for the adsorption of SO_2

Fig.3.14 shows the effect of the feed flow rate on the breakthrough curves obtained at room temperature for the EDA-NCC (70^oC, 3hr, 25) adsorbent; this adsorbent was selected just as a base sorbent. This figure shows that as the flow rate increased, a significantly shorter breakthrough and saturation time and a considerably steeper breakthrough curve were achieved over the temperature examined. This finding was reached because more adsorbates enter the bed per unit time when the flow rate increases, causing the breakthrough to occur faster. In addition, a higher Reynolds number with a higher degree of turbulence results from faster feed flow rate and may induce a faster mass transfer zone. Conversely, the slower flow rate was accompanied by the adsorbate molecules' slower transport and led to a prolonged breakthrough time. These observations are in accordance with those reported elsewhere[28], [29]. The use of EDA-NCC adsorbent at 20 °C resulted in a significant decrease in the measured breakthrough time (from 42 to approximately 26 min) when the flow rate increased from 20 to 30 ml min^{-1}. Note that the enhanced breakthrough time or adsorption capacity of the EDA-NCC adsorbent compared with the NCC sample may attribute to chemisorption with the nitrogen surface groups. Since SO_2 molecules have less time to react with N-functionalities as flow rate increases, chemisorption decreases. As a result of these findings, greater feed flow rates cause c_t/c_0 ratio approach to unity slowly than lower feed flow rates at the tail-end section of the breakthrough curves, where the c_t/c_0 ratio approaches 1. Capture capacity at 20 ml/min (0.0057 $mg_{so2}/mg_{\ sorbent}$) was higher than 10 m/min (0.0044 mg/mg); however, it had a little difference with at 30 ml/min (0.0055g mg/mg).

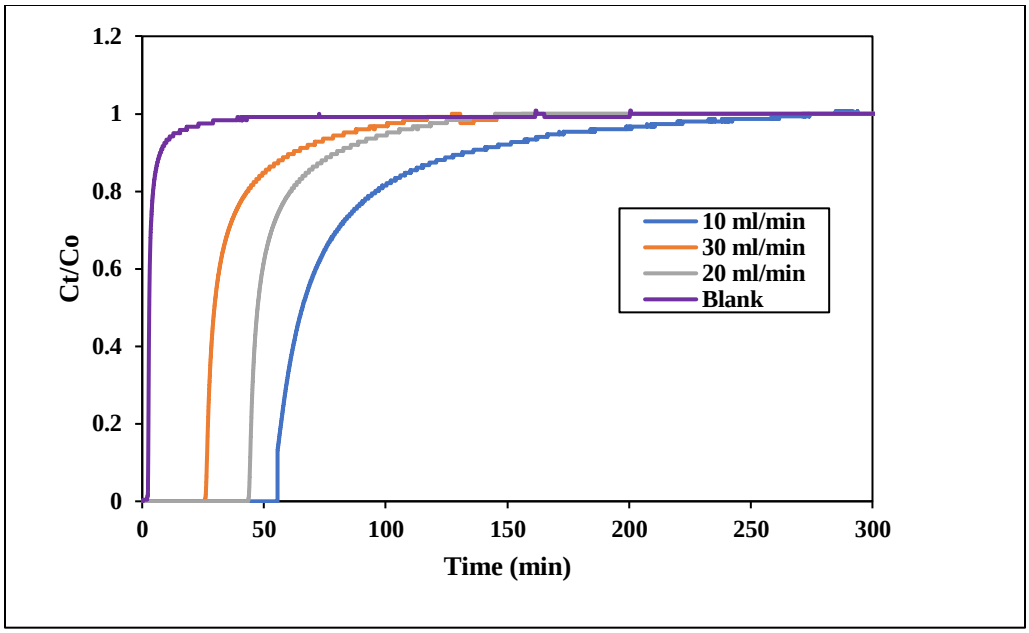

Figure 3.14. Breakthrough curves of sample EDA-NCC (70°C, 3hr, 25), at three different testing flow rates of 10, 20, and 30 ml/min, room temperature, and atmospheric pressure

3.4 Conclusion

Ethylenediamine functionalized-nanocrystalline cellulose was prepared via a green and non-toxic method in which the use of common halogenated solvents to make a good leaving functional group through halogen on cellulose was abandoned. Sorbents were prepared using different functionalization parameters of time, temperature, and EDA contents, then characterized and tested for SO_2 capture application. It is found that the temperature and time used of sorbents preparation significantly influence the capture capacity of sorbents at the same SO_2 test condition; however, the time has a more pronounced impact than temperature and EDA contents. From the FTIR results and the decrease in XRD peak intensity, it was concluded that with increasing temperature and time, more amino functional groups may be deposited on the cellulose surface. As the amount of amine groups increases, more SO_2 gas is adsorbed by the adsorbent. The results were also compared with untreated NCC, and the lower adsorption capacity of NCC was attributed to the assumption that physisorption is predominant between NCC and SO_2. It was concluded that besides physisorption, chemisorption through amine functional groups might be a parameter of increasing the capture capacity of EDA-NCCs. The effects of temperature and flow rate adsorption

operating parameters on breakthrough time were investigated, and it was shown that increasing temperature decrease adsorption capacity. The SO_2 breakthrough times significantly decreased with increasing adsorption temperature for both EDA-NCC and NCC from RT to 60^{o}C due to the exothermic nature of the adsorption process. As the flow rate increased from 10 ml/min to 30 ml/min, a much shorter breakthrough and saturation time, as well as a significantly steeper breakthrough curve, were achieved, as expected with a higher amount reaching the adsorbent in a given time.

3.5 Acknowledgement

The authors sincerely acknowledge the financial support of the Natural Sciences and Engineering Research Council (NSERC) of Canada and thank CelluForce Inc. for providing the unmodified NCC material.

3.6 References

[1] F. Rezaei, A. A. Rownaghi, S. Monjezi, R. P. Lively, and C. W. Jones, "SOx/NOx Removal from Flue Gas Streams by Solid Adsorbents: A Review of Current Challenges and Future Directions," *Energy and Fuels*, vol. 29, no. 9, pp. 5467–5486, 2015, doi: 10.1021/acs.energyfuels.5b01286.

[2] S. O. R. Program, "SO_2 Scrubbing Technologies : A Review," vol. 20, no. 4, pp. 219–228, 2001.

[3] M. A. Hanif, N. Ibrahim, and A. Abdul Jalil, "Sulfur dioxide removal: An overview of regenerative flue gas desulfurization and factors affecting desulfurization capacity and sorbent regeneration," *Environ. Sci. Pollut. Res.*, vol. 27, no. 22, pp. 27515–27540, 2020, doi: 10.1007/s11356-020-09191-4.

[4] L. Yang, X. Jiang, Z. S. Yang, and W. J. Jiang, "Effect of MnSO4on the removal of so2by manganese-modified activated coke," *Ind. Eng. Chem. Res.*, vol. 54, no. 5, pp. 1689–1696, 2015, doi: 10.1021/ie503729a.

[5] X. Song, X. Ma, G. Ning, and J. Gao, "Pitch-Based Nitrogen-Doped Mesoporous Carbon for Flue Gas Desulfurization," *Ind. Eng. Chem. Res.*, vol. 56, no. 16, pp. 4743–4749, 2017, doi: 10.1021/acs.iecr.7b00054.

[6] S. Brunauer, "The Adsorption of Gases and Vapors," *Princet. Univ. Press*, vol. I: Physica.

[7] P. Pullumbi, F. Brandani, and S. Brandani, "Gas separation by adsorption: technological drivers and opportunities for improvement," *Curr. Opin. Chem. Eng.*, vol. 24, pp. 131–142, 2019, doi: 10.1016/j.coche.2019.04.008.

[8] S. Sircar, “Applications of gas separation by adsorption for the future,” *Adsorpt. Sci. Technol.*, vol. 19, no. 5, pp. 347–366, 2001, doi: 10.1260/0263617011494222.

[9] D. Trache, A. F. Tarchoun, M. Derradji, T. Hamidon, N. Masruchin, N. Brosse, M. Hussin, Nanocellulose*: From Fundamentals to Advanced Applications*, vol. 8, no. May. 2020.

[10] N. Mahfoudhi and S. Boufi, “Nanocellulose as a novel nanostructured adsorbent for environmental remediation: a review,” *Cellulose*, vol. 24, no. 3, pp. 1171–1197, 2017, doi: 10.1007/s10570-017-1194-0.

[11] F. L. Bernard, D. Rodrigue, B. B. Polesso, V. V. Chaban, M. Seferin, F.Vecchia, “Development of inexpensive cellulosebased sorbents for carbon dioxide,” *Brazilian J. Chem. Eng.*, vol. 36, no. 1, pp. 511–521, 2019, doi: 10.1590/0104-6632.20190361s20170182.

[12] K. J. Shah and T. Imae, “Selective Gas Capture Ability of Gas-Adsorbent-Incorporated Cellulose Nanofiber Films,” *Biomacromolecules*, vol. 17, no. 5, pp. 1653–1661, 2016, doi: 10.1021/acs.biomac.6b00065.

[13] C. Gebald, J. A. Wurzbacher, P. Tingaut, T. Zimmermann, and A. Steinfeld, “Amine-based nanofibrillated cellulose as adsorbent for CO 2 capture from air,” *Environ. Sci. Technol.*, vol. 45, no. 20, pp. 9101–9108, 2011, doi: 10.1021/es202223p.

[14] J. Tang, J. Sisler, N. Grishkewich, and K. C. Tam, “Functionalization of cellulose nanocrystals for advanced applications,” *J. Colloid Interface Sci.*, vol. 494, pp. 397–409, 2017, doi: 10.1016/j.jcis.2017.01.077.

[15] R. D. S. Bezerra, R. C. Leal, M. da Silva, A. Morais, T. Marques, “Direct modification of microcrystalline cellulose with ethylenediamine for use as adsorbent for removal amitriptyline drug from environment,” *Molecules*, vol. 22, no. 11, 2017, doi: 10.3390/molecules22112039.

[16] L. S. Silva, L.C.B. Lima, F. Silva, J. E. Matos, M. Santos, “Dye anionic sorption in aqueous solution onto a cellulose surface chemically modified with aminoethanethiol,” *Chem. Eng. J.*, vol. 218, pp. 89–98, 2013, doi: 10.1016/j.cej.2012.11.118.

[17] D. J. Trader and E. E. Carlson, “Chemoselective hydroxyl group transformation: An elusive target,” *Mol. Biosyst.*, vol. 8, no. 10, pp. 2484–2493, 2012, doi: 10.1039/c2mb25122a.

[18] E. C. Silva Filho, L. C. B. Lima, K. S. Sousa, M. G. Fonseca, and F. A. R. Pereira, “Calorimetry studies for interaction in solid/liquid interface between the modified cellulose and divalent cation,” *J. Therm. Anal. Calorim.*, vol. 114, no. 1, pp. 57–66, 2013, doi: 10.1007/s10973-012-2868-3.

[19] E. C. da Silva Filho, J. C. P. de Melo, and C. Airoldi, “Preparation of ethylenediamine-anchored cellulose and determination of thermochemical data for the interaction between cations and basic centers at the solid/liquid interface,” *Carbohydr. Res.*, vol. 341, no. 17, pp. 2842–2850, 2006, doi: 10.1016/j.carres.2006.09.004.

[20] E. C. Silva Filho, L. C. B. Lima, F. C. Silva, K. S. Sousa, M. G. Fonseca, and S. A. A. Santana, “Immobilization of ethylene sulfide in aminated cellulose for removal of the divalent cations,” *Carbohydr. Polym.*, vol. 92, no. 2, pp. 1203–1210, 2013, doi: 10.1016/j.carbpol.2012.10.031.

[21] E. C. Da Silva Filho, S. A. A. Santana, J. C. P. Melo, F. J. V. E. Oliveira, and C. Airoldi, “X-ray diffraction and thermogravimetry data of cellulose, chlorodeoxycellulose and aminodeoxycellulose,” *J. Therm. Anal. Calorim.*, vol. 100, no. 1, pp. 315–321, 2010, doi: 10.1007/s10973-009-0270-6.

[22] R. D. S. Bezerra, M. M. F. Silva, A. I. S. Morais, M. R. M. C. Santos, C. Airoldi, and E. C. Silva Filho, “Natural cellulose for ranitidine drug removal from aqueous solutions,” *J. Environ. Chem. Eng.*, vol. 2, no. 1, pp. 605–611, 2014, doi: 10.1016/j.jece.2013.10.016.

[23] L. S. Silva, L. Lima, F. Ferreira, M. Silva, J. Osajima, R. Bezerra, E. Filho, “Sorption of the anionic reactive red RB dye in cellulose: Assessment of kinetic, thermodynamic, and equilibrium data,” *Open Chem.*, vol. 13, no. 1, pp. 801–812, 2015, doi: 10.1515/chem-2015-0079.

[24] J. A. Pavia, D.L.; Lampman, G.M.; Kriz, G.S.; Vyvyan, *Introduction to Spectroscopy*. 2009.

[25] L. Segal, J. J. Creely, A. E. Martin, and C. M. Conrad, “An Empirical Method for Estimating the Degree of Crystallinity of Native Cellulose Using the X-Ray Diffractometer,” *Text. Res. J.*, vol. 29, no. 10, pp. 786–794, 1959, doi: 10.1177/004051755902901003.

[26] S. García, M. V. Gil, C. F. Martín, J. J. Pis, F. Rubiera, and C. Pevida, “Breakthrough adsorption study of a commercial activated carbon for pre-combustion CO2 capture,” *Chem. Eng. J.*, vol. 171, no. 2, pp. 549–556, 2011, doi: 10.1016/j.cej.2011.04.027.

[27] J. A. Thote, K. S. Iyer, R. Chatti, N. K. Labhsetwar, R. B. Biniwale, and S. S. Rayalu, “In situ nitrogen enriched carbon for carbon dioxide capture,” *Carbon N. Y.*, vol. 48, no. 2, pp. 396–402, 2010, doi: 10.1016/j.carbon.2009.09.042.

[28] M. J. Ahmed, A. H. A. K. Mohammed, and A. A. H. Kadhum, “Modeling of Breakthrough Curves for Adsorption of Propane, n-Butane, and Iso-Butane Mixture on 5A Molecular Sieve Zeolite,” *Transp. Porous Media*, vol. 86, no. 1, pp. 215–228, 2011, doi: 10.1007/s11242-010-9617-5.

[29] R. Sabouni, H. Kazemian, and S. Rohani, “Mathematical modeling and experimental breakthrough curves of carbon dioxide adsorption on metal organic framework CPM-5,” *Environ. Sci. Technol.*, vol. 47, no. 16, pp. 9372–9380, 2013, doi: 10.1021/es401276r.

[30] A. Pala, A. Kondorc, S. Mitrad, K. Thua, S. Harishb, B. Baran Saha, " On surface energy and acid–base properties of highly porous parent and surface treated activated carbons using inverse gas chromatography" J. Ind. Eng. Chem., vol 69, pp. 432–443, 2019, doi: .0.1016/j.jiec.2018.09.046.

4 Modifying the surface of Nanocrystalline Cellulose with mixed functional groups: An efficient adsorbent for Sulfur Dioxide Capture

Raheleh Zafari, Clémence Fauteux-Lefebv*

Department of Chemical and Biological Engineering, University of Ottawa, 161 Louis Pasteur St, ON, Canada, K1N 6N5

Abstract

Aqueous amine solutions are organic solvents used for SO_2 capture, but they have well-known operational drawbacks such as producing a lot of waste gas and difficulty in recycling. To overcome these challenges, the support of amines on solid materials emerges as an alternative for SO_2 capture. Cellulose is a versatile and low-cost material that can be used as a support. This study reports the chemical modification of cellulose nanocrystalline (NCC) with citric acid (CA) and ethylenediamine (EDA) and its potential for SO_2 capture. The obtained compounds were characterized by X-ray diffraction (XRD), Fourier Transform Infrared Spectroscopy (FTIR), thermogravimetry analysis (TGA), scanning electron microscopy (SEM), and energy-dispersive microscopy (EDS) analysis to confirm the modification reaction. The presence of carboxylic acid and amine peaks coming from modification with citric acid and EDA respectively approved with FTIR-ATR and proved that incorporation of functional groups on the cellulose's surface was successful. From TGA, thermal stability of modified-NCCs were less than NCC and for CA-NCC was higher than EDA-CA-NCC. Acid-base titration revealed that 83% of hydroxide groups being carboxylate and 92% of supplied carboxyl groups reacted with an amine. The SO_2 capture results indicated that in comparison to NCC and CA modified cellulose, EDA-functionalized NCC shows a higher sorption capacity of 0.003685 $mg_{SO2}/100\ mg_{sorbent}$ at room temperature, atmospheric

pressure, and 20 ml/min flow rate. It concluded that amine groups in EDA-CA-NCC have a crucial role in adsorbing SO_2. However, carboxylic groups in CA-NCC are influential compared to pristine NCC, which gave the lowest adsorption capacity.

Keywords: Nanocrystalline cellulose, Surface modification**,** Mixed-functionalized cellulose

4.1 Introduction

Growing concern regarding the adverse effects of anthropogenic sulfur dioxide (SO_2) emissions on climate change and human health have inspired research into the capture of SO_2 from significant emission sources and the mitigation of the unfettered release of this substantial greenhouse gas into the atmosphere. Fossil fuel-fired power plants account for approximately one-third of worldwide SO_2 emissions due to the combustion of fossil fuels such as petroleum, coal, and natural gas[1]. Therefore, remarkable growth in research activity related to developing, improving, and optimizing efficient separation techniques for removing SO_2 from power-plant flue gas has occurred over the past three decades[2]. There are several different chemical absorption methods for removing SO_2 from industrial gas streams, but amine-based chemical absorption is the most well-established[3]. Due to the high energy needs for regeneration, the absorption process is energy intensive. A low SO_2 loading capacity, extensive corrosion of the process equipment, and toxicity are additional disadvantages of the amine absorption process[4]. A promising option for separating SO_2 from flue gases is adsorption using solid adsorbents reducing the costs associated with the capture step. Other advantages of these solid physical adsorption processes over traditional aqueous amine processes include greater capacity, higher selectivity, more minor regeneration energy requirements, and easier handling. Accordingly, in recent years, various adsorbents, including zeolites[5], metal oxides[6], [7], metal-organic frameworks[8], silicas[9], and carbon materials[10],[11], have been extensively investigated for their application in removing SO_2 from flue-gas streams.

Unfortunately, many of these commercial sorbents remain excessively expensive[12]. This necessitates the development of low-cost SO_2 sorbents. The impregnation of agricultural wastes with amines has been suggested as an alternative for obtaining low-cost sorbents. Bagasse, rice straw, industrial leftovers like mullite and fly ash, as well as other oxygen-rich sorbents, are some

examples.[13]–[16]. Strategies to use residues for SO_2 capture will foster the emergence of green technologies and sustainable development[17]. Notably, however, most of the traditional gas-adsorbents that rely on physisorption have poor adsorption capabilities at relatively low SO_2 concentrations representing a severe drawback for flue gas SO_2 removal using gas adsorption. To enhance SO_2 capture capacity, modifications of adsorbent surface chemical properties by incorporating of nitrogen surface groups have gained much attention in the past few years[18]–[21]. SO_2 is a weak Lewis acid that can interact with electron donors; therefore, the presence of basic nitrogen-containing surface groups is thought to provide adsorbents capable of interacting with SO_2[20].

Samojeden et al.[22] demonstrated that the SO_2 adsorption capacity on an ammonia-treated activated carbon was affected highly by N-containing moieties, and oxygen-containing groups negatively affected SO_2 capture due to their acidic character. Gao et al.[23] observed SO_2 adsorption capacities in N-doped porous carbon are proportional to the nitrogen contents. The sample with 10.2% nitrogen content gave the highest SO_2 adsorption capacity of 48.3 mg/g, 2.95 times higher than non-doped carbon at 25 °C.

Since cellulose is the most abundant natural polymer, low-cost, versatile material, thermodynamically stable, presenting the crystalline structure and numerous hydrogen bonds, and it undergoes functionalization primarily through the hydroxyl groups[24], [25], cellulose materials are one of the most widely proposed adsorbents for pollutant removal in recent years[26], [27] Herein, we investigated the chemical modification of nanocrystalline cellulose (NCC) with Ethylenediamine (EDA) in two steps. First, NCC was functionalized with Citric acid (CA) and carboxylic acid groups created on its surface. Then, EDA was incorporated through a reaction between available carboxylic in CA-modified NCC and amine groups. The final product of the reaction containing amide and amine groups was characterized and tested for SO_2 adsorption. This method created both oxygen and nitrogen groups to find effect of which groups is more pronounce in SO_2 capture.

4.2 Experimental section

4.2.1 Materials

The spray-dried powder form of NCCs is donated by CelluForce Inc. (Windsor, Quebec). The anhydrous citric acid (CA, 99.5% Synth), ethylenediamine, hydrochloric acid (HCl), sodium hydroxide (NaOH), ethanol (CH_3CH_2OH, 99%), and phenolphthalein were all laboratory grades, purchased from Sigma-Aldrich and used as purchased. Distilled water was used to wash the adsorbents.

4.2.2 Cellulose modification

Ethylenediamine-functionalized cellulose was prepared using a two-steps methodology. In the first step, NCC was modified with citric acid (CA-NCC) and then functionalized with ethylenediamine (EDA-CA-NCC). For CA-modified, the cellulose was poured into a flask containing 0.6 M aqueous solution of CA (at a ratio of 1 g cellulose to 10 ml CA). This solution was stirred for 0.5h at room temperature. The temperature was then increased up to 120°C and kept constant for 1.5h under stirring. After cooling, the cellulose was washed with distilled water to remove any excess of CA, dried at 55°C for 24h, and preserved in a desiccator.[28].

The amine functionalization reaction is described in detail elsewhere[29]. In reflux under N_2 atmosphere, 1 g of CA- modified cellulose was added to the amine dissolved (molar ratio COOH/amine=1/1/) in 15 mL of dimethylformamide (DMF). The mixture was stirred at 40°C for 2 h. The material was separated by filtration, repeatedly washed with distilled water and ethanol, and dried at 55°C for 24 h. A schematic of the proposed functionalization reaction is displayed in Figure 4.1.

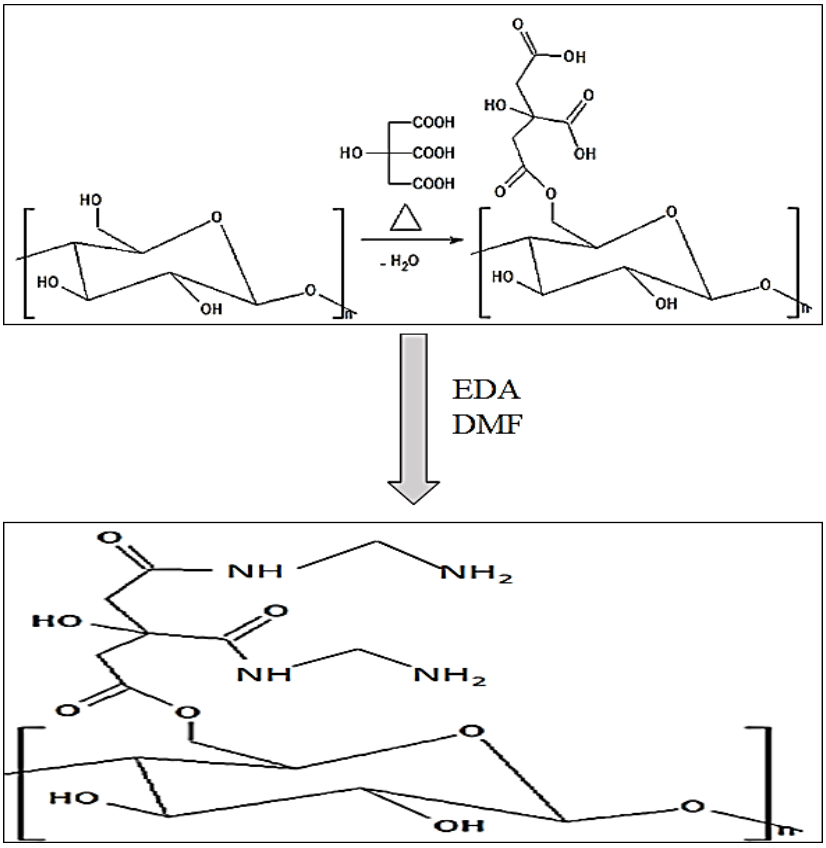

Figure 4.1 Schematic of EDA functionalization of NCC in two steps

4.2.3 Characterizations

Samples were characterized using Attenuated Total Reflection-Fourier Transform Infrared Spectroscopy (ATR-FTIR) (Nicolet 6700 FTIR (Thermo Scientific)), and a diamond crystal is applied to acquire the spectra. All scans are recorded at the resolution of 4 cm^{-1} in a range of wave numbers between 400 and 4000 cm^{-1}. X-ray diffraction (XRD, Rigaku Ultima IV Diffractometer) is used to study the crystallinity structure of the samples. The XRD analysis was carried out at room temperature using Cu Kα radiation (λ=1.5418 Å) at 40 kV and 44 mA. The 2θ range of 5° to 50° is covered with 0.02° step width and 1°/min scan speed. Morphology and elemental analysis of samples are characterized by scanning electron microscopy coupled with EDS (SEM-EDS). Images were taken from the top surface using the Zeiss Gemini SEM 500 and were analyzed at different magnifications. Thermogravimetric Analysis (TGA) was carried out on Pyris 1 TGA (Perkin Elmer) to provide information about the structural stability of compounds with temperature

changes. The temperature of all samples was scanned over a range from 25 to 700 °C at a heating rate of 10 °C/min. Nitrogen is given at a flow rate of 10 mL/min to avoid sample oxidation. Back Acid–base titration was used to quantify the amine groups (mol/mg) introduced into the modified cellulose using NaOH and HCl as a titrant and phenolphthalein used as an indicator. 0.03 g of cellulose were treated with 10 mL of 0.01 M NaOH solution in an Erlenmeyer for 1 h under constant stirring. Soon after that, the materials were separated by single filtration, and three aliquots of obtained solution were titrated with 0.01 M HCl until a level off pH reaches. Likewise, 0.03 g of sample was suspended in 10 mL of 0.01 M NaOH solution for CA-NCC. The mixture was titrated with 0.01 M HCl until a level off pH reaches. For EDA-CA-NCC, 0.03 g of sample was suspended in 10 mL of 0.01 M HCl solution, and the mixture was titrated against 0.01 M NaOH.

4.2.4 SO_2 capture experiments

The experimental breakthrough apparatus shown in Figure 4.2 consists of a quartz tube 45 cm in length and 2.5 mm in internal diameter packed with the adsorbent sample. Two quartz wool were placed at the bottom and top of the sample to retain the adsorbent particles in the bed. 50 mg sample is put in the reactor with an adsorbent length bed of approximately 20 mm. Before entering the tube, the gas flow rate was regulated using a rotameter to attain a constant total flow of 20 ml/min**.** Continuous monitoring of the SO_2 concentration at the tube exit was performed using an SO_2 analyzer. The temperature was measured using a thermocouple with an accuracy of ±1 K located inside the solids bed. A SO_2 detector, Drager Pac 600, attached at the outlet of the quartz tube, detected the amount of SO_2 not captured by the prepared material and recorded the SO_2 concentration at a minute interval. Because SO_2 can be harmful even at low concentrations, the setup is placed within a fume hood. Before each run, the sorbent was purged for 30 min online in pure argon at room temperature and a flow rate of 15 ml/min under atmospheric pressure. Then, Ar is stopped and, the SO_2/Ar (35 ppm SO_2 in Ar) is fed at the inlet of the quartz tube at a specific volumetric flow rate to be tested, considering argon is inert [38]. First, SO_2/Ar mixture was fed through an empty tube containing no traces of the sorbent material, followed by a run where powdered NCC from the supplier was placed in the tube then the synthesized sorbents were tested. Between each run, argon gas (Ar) is fed to purge the system. The system reached saturation when the outlet concentration read on the Drager detector was constant or until the effluent concentration was equal to the feed concentration, i.e., $c_t/c_0=1$. The data is exported from the USB to an Excel

file via Gas Vision Software. The maximum concentration was evaluated as 25 ppm (slightly different from supplier-provided information, which was 35 ppm because of the experimental errors). Experiments with blank samples showed that the reactor system was inert in adsorbing gas. Because the amount of outlet SO_2 gas quickly reached 25 ppm and did not change after a long time. It indicates that the whole system is ineffective in adsorbing gas.

The SO_2 Capture capacity is determined from below equation 1:

$$q = \frac{[(\int (Ci - Co) dT) \times volumetric\ flowrate]}{Mass\ of\ material} \qquad \text{Equation.1}$$

Where Q is adsorption capacity (mg_{SO2}/mg adsorbent) and C_i and C_0 are the amounts of SO_2 at the inlet and outlet, respectively, and *t* is time. A detailed description of the calculations is given in Appendix 1. The flow rate of the reaction was varied from 10 mL/min to 30 mL/min, and the mass of material was taken as 50 mg.

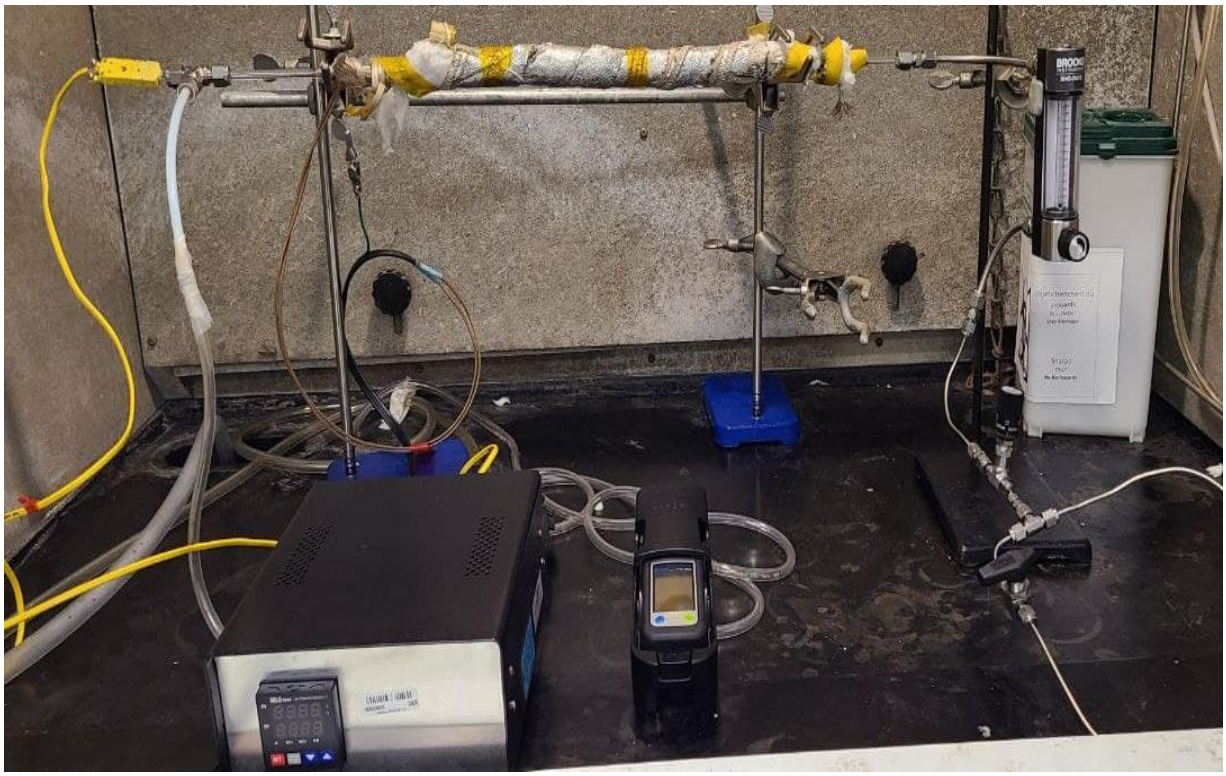

Figure 4.2 Schematic of SO_2 testing capture set-up

4.3 Results and discussion

Physicochemical Characterization

4.3.1 Attenuated Total Reflection-Fourier Transform Infrared Spectroscopy (ATR-FTIR)

Fourier transform infrared spectroscopy (Figure 4.3) was used to investigate the presence of primary amine, amide, and carboxylic acid groups in EDA functionalized NCC. The infrared spectra of NCC showed broadband located at 3330 - 3340 cm^{-1}, attributed to the stretching of the OH groups, the band near 2920 cm^{-1} related to C-H stretching, band at 1160 cm^{-1} corresponding to C-O-C asymmetrical stretching, broadbands around 1050 cm^{-1} and 890 cm^{-1} related to the C-H and C-O stretching vibration of the cellulose structure[30]. By comparing cellulose and citric acid-modified cellulose spectra, we identified a strong band at 1740 cm^{-1} attributed to the carboxylic acid in the citric acid structure. This indicates the introduction of citric acid into the cellulose chain[31]. A reduction in the intensity of 1740 cm^{-1} related to the carboxyl group absorption band was observed due to the chemical modification with amines. A new band at 1454 cm^{-1}, characteristic of the symmetric bending of primary amines (NH_2) and at 2869 cm^{-1} corresponding to the CH_2 stretching modes of the amine chains observed for EDA-CA-NCC[32]. An evident shoulder at 3286 cm^{-1} may be attributed to amide N-H stretching vibrations[32]. The distinctive N-H peak between 3500 and 3200 cm^{-1} was hidden by the high O-H absorption of cellulose, thus hindering the viewing of the absorption bands related to the amino groups.

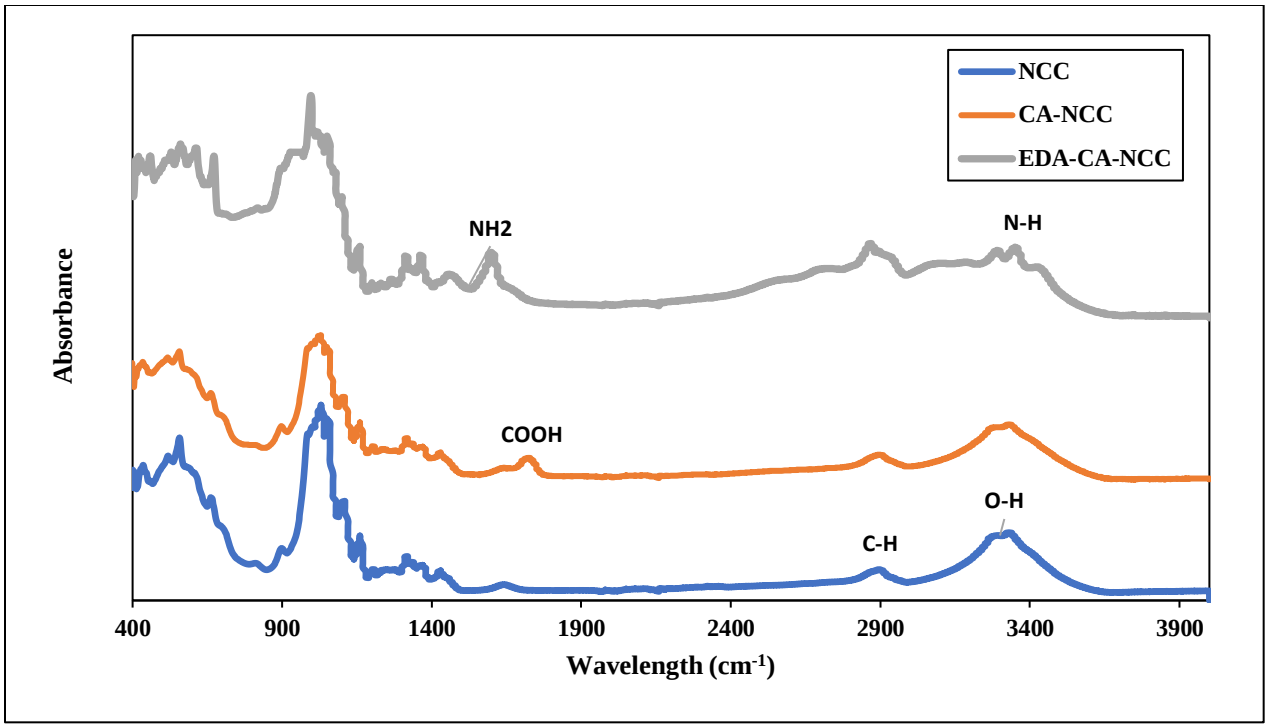

Figure 4.3. ATR-FTIR of NCC, CA-NCC, and EDA-CA-NCC

4.3.2 X-Ray Diffraction (XRD)

Figure 4.4 shows the X-ray diffraction profiles of the cellulose and modified cellulose samples. It has been reported that the structure of nanocrystalline cellulose has three characteristic peaks located at $2\theta=15.54^{\circ}$, $2\theta=22.90^{\circ}$ and $2\theta=34.72^{\circ}$, which are related to the crystallographic planes (101), (002) and (040) [33], [34], respectively and consistent with the XRD pattern provided in Figure 4.4. When comparing the XRD pattern for EDA-CA-NCC to the NCC, no new peak or peak shifting was observed, confirming that the insertion of functional groups to the NCC surface happened on the crystal surfaces and did not affect the crystal structure of untreated NCC. The crystalline regions and ordered structure of NC are formed due to the intense hydrogen interaction; therefore, the incorporation of amino groups on the cellulose surface causes changes in those interactions, modifying its structure and decreasing the crystallinity after chemical modification. Furthermore, to quantify the cellulose crystallinity after chemical modification, the cellulose crystallinity index (*IC*) was determined by the method proposed by Segal et al. as shown in Equation below[35]:

$$IC = [(I_{002} - I_{am})/I_{002}] \times 100 \qquad \textit{Equation 2}$$

Where I_{002} is the peak intensity of the (002) lattice diffraction, and I_{am} is the minimum intensity of diffraction in the same units between (002) and (101) peaks regarding to the non-crystalline material in cellulose. It found that after modification, IC% decreases from 80.75 for NCC to 68.8% for EDA-CA-NCC.

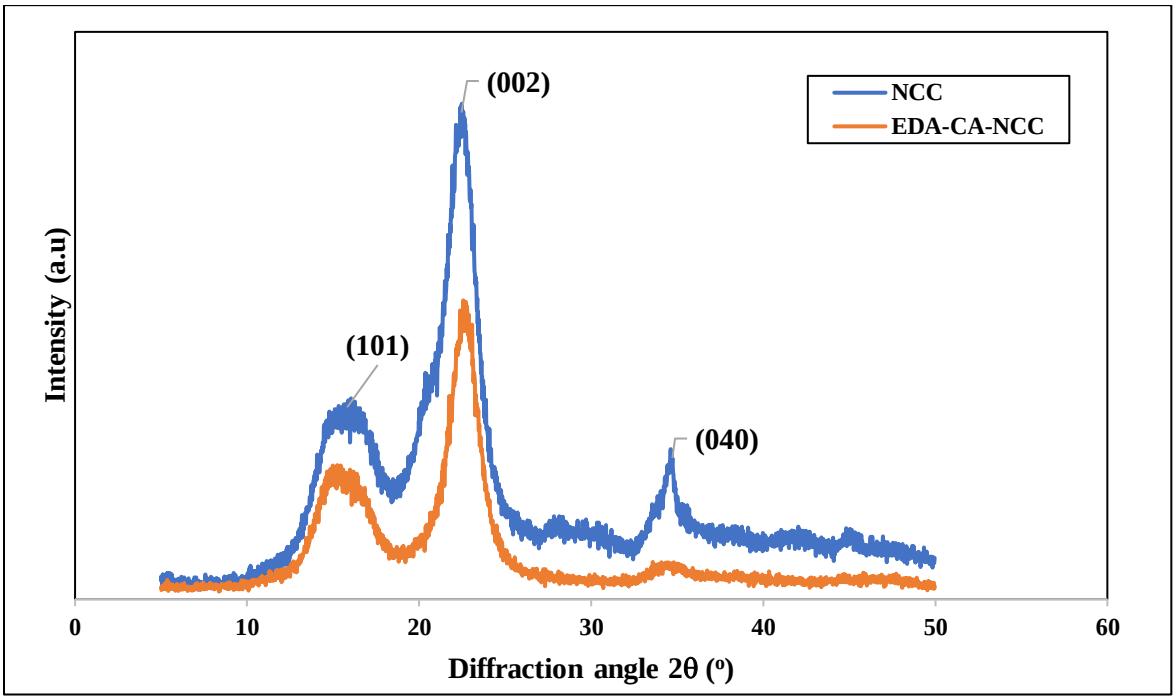

Figure 4.4. XRD of NCC and EDA-CA-NCC

4.3.3 Thermogravimetric Analysis (TGA)

Figure 4.5 presents TGA and DTG (derivative thermogravimetry**)** curves obtained for samples. Samples showed two thermal events. The first weight loss was around 4.5-6.4% and attributed to water vaporization in the 100 to 150°C range. For NCC, the second weight loss was attributed to cellulose degradation, in which 54% cellulose was probably degraded and converted into gas. The thermolysis reaction of cellulose occurs by the cleavage of glycoside bonds (COH, COO, and COC bonds) and by dehydration, decarboxylation, and decarbonylating[37]. As it can be seen the second mass loss for EDA-CA-NCC started at the same temperature as NCC but, at a higher temperature

than CA-NCC, which indicate that the reaction of carboxylic groups with amine groups increases thermal stability[37]. Degradation temperatures for CA-NCC is at T_{onset} = 157°C, and for both NCC and EDA-CA-NCC at T_{onset} =256°C. T_{onset} is where a deflection is first observed from the established baseline prior to the thermal event. The weight loss for NCC and EDA-CA-NCC is ≅73% and for CA-NCC ≅ 53%. At higher temperatures, the modified samples present higher thermal stability than cellulose.

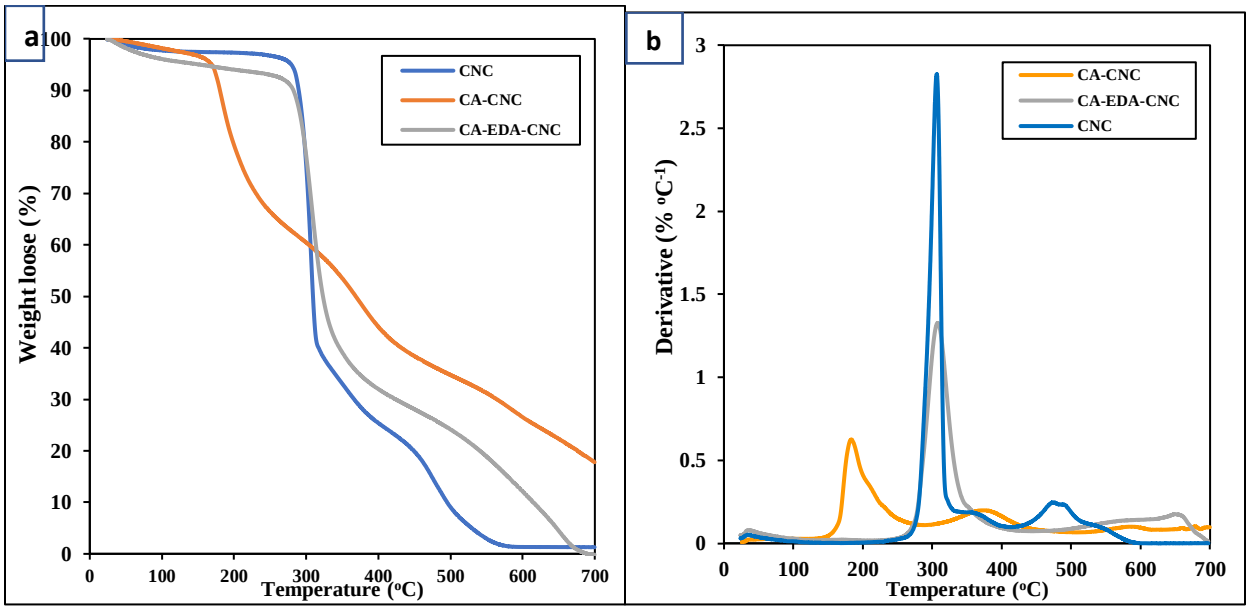

Figure 4.5. a) TGA results of the samples and b) Derivatives of the curves (DTG)

4.3.4 Scanning electron microscopy (SEM) and Energy dispersive spectroscopy (EDS)

SEM micrographs acquired for the NCC and functionalized- NCC is depicted in Figure 4.6. EDA modified cellulose showed similar morphology and no noticeable difference in the morphology to that demonstrated by the NCC. It can only be seen that with the addition of amines, the cellulose particles, which are in the form of rods or cylinders, are slightly agglomerates. EDS performed the elemental analysis to confirm the deposition of EDA on the surface of NCC. Figure 4.7 shows the EDS of the NCC and CA-EDA-NCC. The analysis was performed on the specific regions and not on the overall surface of the samples. However, the results of EDS are not precise and give us an indication of if we were able to functionalize NCC with EDA, we can have a comparative result

and verify whether our method was successful or not. In EDS, the addition of the N peak confirms the successful acquisitions of EDA on the surface of NCC.

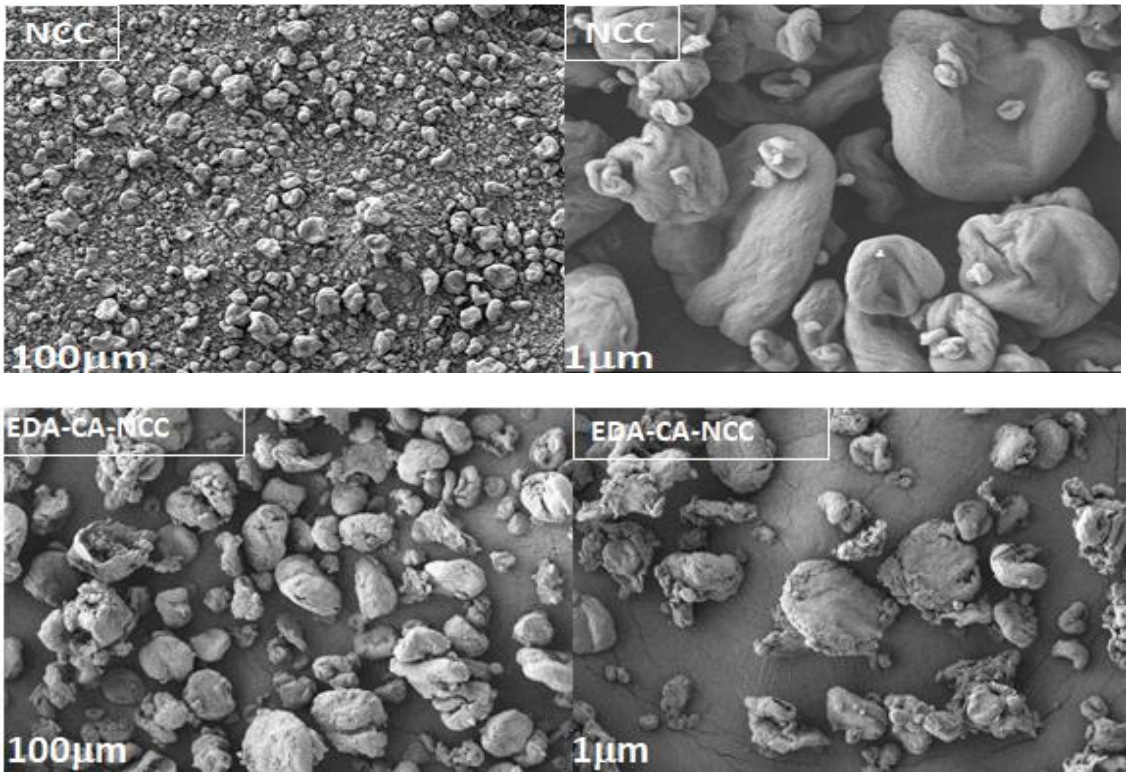

Figure 4.6. SEM of NCC and EDA-CA-NCC

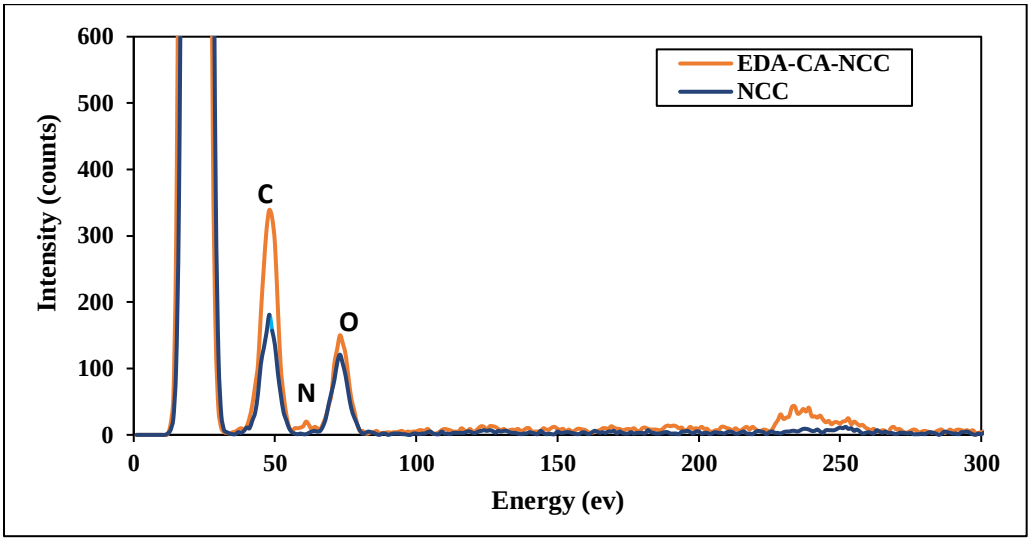

Figure 4.7. EDS analysis of NCC and EDA-CA-NCC

4.3.5 Quantification of amine using acid-base titration

Endpoint titration was used to measure the quantity of amine added to the cellulose. Equations 3-5 show the reaction between HCl and NaOH with the samples. From the titration of remaining of NaOH after reaction with NCC, we can obtain moles of carboxylic acid. Also, by titration of the remaining of HCl after reaction with CA-NCC, we can obtain the amount of EDA incorporated into EDA-CA-NCC (mmol/g) based on the calculation in the Appendix.

$$\text{Cellulose} - \text{OH} + 2\text{NaOH} \rightarrow \text{Cellulose} - O^{-}Na^{+} + H_2O + NaOH \qquad Equation\ 3$$

$$\text{Titration of remaining NaOH} + \text{HCl} \rightarrow \text{NaCl} + H_2O$$

$$\text{Cellulose} - \text{COOH} + 2\text{NaOH} \rightarrow \text{Cellulose} - COO^{-}Na^{+} + H_2O + NaOH \qquad Equation\ 4$$

$$\text{Titration of remaining NaOH} + \text{HCl} \rightarrow \text{NaCl} + H_2O$$

$$\text{Cellulose} - \text{COOH} + 2\text{HCl} \rightarrow \text{Cellulose} - COOH_2^{+}Cl^{-} + HCl \qquad Equation\ 5$$

$$\text{Titration of remaining HCl} + \text{NaOH} \rightarrow \text{NaCl} + H_2O$$

Using equation, the determined concentration of carboxylic functions of the CA-NCC sample was calculated to be 1.90 ± 0.12 mmol/g of CA-NCC, which equates to 83% of hydroxide groups being carboxylate. The concentration of the loaded amine was 1.73 mmol/g, indicating that 92% of supplied carboxyl groups were reacted.

4.4 Gas sorption measurements

Figure 4.8 presents the experimental results for SO_2 sorption at atmospheric pressure, room temperature, and 20 ml/min flow rate for the synthesized materials. A blank study was performed, giving information on the residence time, unsteady state starting behavior, and maximum concentration that can be measured. A steep change from 0 to the maximum after a short delay is observed for the blank run, coherent with the absence of a sample. For the NCC, the change is the same as the blank; however, reaching saturation happened long and with delay. The curve for CA-NCC and EDA-CA-NCC is less steep according to anticipated possible phenomena of capture and

mass transfer limitations. An analysis of the entire curves shows that the saturation for CA-NCC and EDA-CA-NC was achieved at about 116-196 min, however for NCC, saturation occurred at 45 min. As can be seen, the breakthrough time for NCC starts in 2 minutes after the SO_2 injection. This delay is due to the long passage of gas to reach the detector. For NCC and CA-NCC, the breakthrough time started at around 15 minutes, and for EDA-CA-NCC happened in 28 minutes after the reaction.

Note that the amine-functionalized sample (EDA-CA-NCC) presented higher sorption values when compared with the citric acid-modified cellulose and untreated cellulose. According to study of Sandra Einloft et al.,[29] their simulation results indicated that for citric acid-modified cellulose, CO_2 adsorb through only the physisorption due to electrostatic interactions. However, chemisorption occurs for samples functionalized with NH and NH_2 groups[21], [29]. Their result can assume that the same phenomena probably happen for SO_2 since both gases are acidic in nature. The sorption results at 20°C were 0.0056 mg_{SO2} /100 $mg_{sorbent}$ for the Cellulose enriched with EDA (contains amide and amine functional groups), which was higher than that obtained for CA-EDA (0.0023 mg $_{SO2}$/100mg sorbent) and lower than the sorption values obtained for the sample contains only EDA (0.029345 mg/100 $mg_{sorbent}$) which was prepared at 70^{o}C for 8 hr and EDA/NCC=25 in chapter 3.

This shows that the SO_2 adsorption capacity on ammonia-treated cellulose is affected highly by N-containing moieties and oxygen-containing groups have relatively less effect on SO_2 capture due to their acidic character. Comparing the results with the previous part showed that incorporating oxygen groups and reducing basic properties of sorbent by incorporating carboxylic and amide groups have a significant effect on reducing capture capacity.

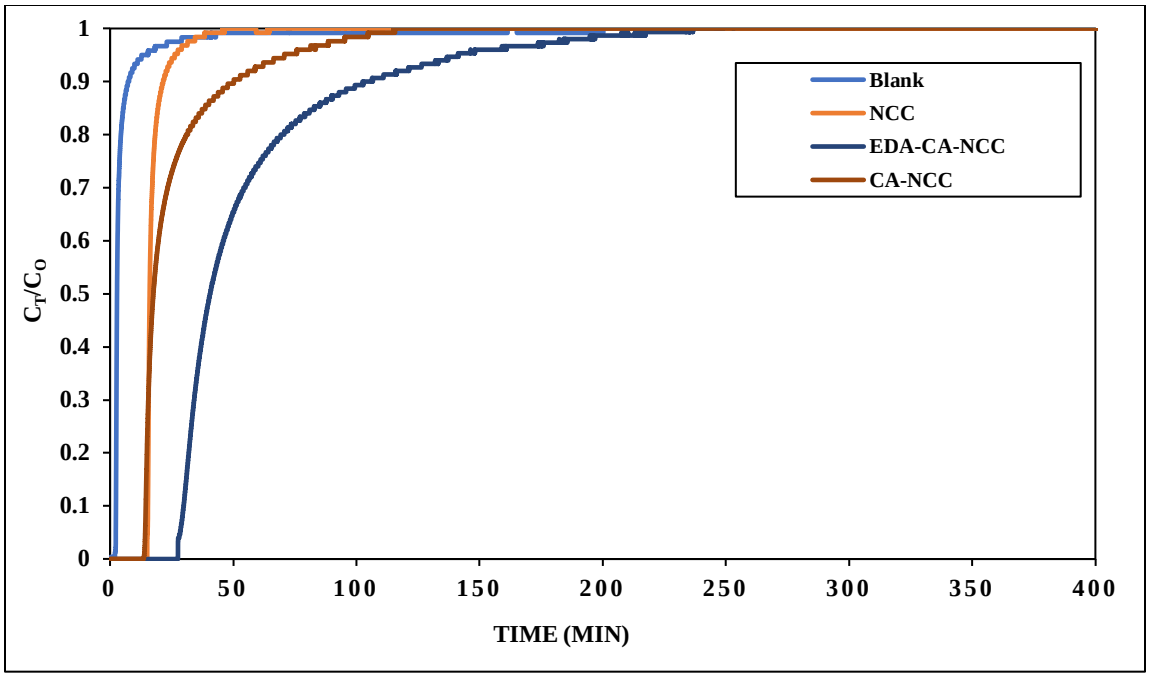

Figure 4.8 Breakthrough curves of NCC, CA-NCC, and EDA-CA-NCC at room temperature, atmospheric pressure, and flow rate of 20 ml/min

4.5 Conclusion

The chemical modification of nanocrystalline cellulose with citric acid and ethylenediamine was performed. The compounds were examined for their potential as sorbents for SO_2 capture. The experimental results revealed an increase in sorption capacity in the order of NCC< CA-NCC< CA-EDA-NCC. NCC's poor performance was due to the absence of alkalinity in this case and a relatively weak attraction of the SO_2 molecule to the cellulose surface. The performance of CA-NCC is inferior to that of EDA-CA-NCC, probably because the carboxylic group cannot chemically bind SO_2 in the -NH-NH_2 configuration. The presence of different functional groups was not the primary parameter where SO_2 uptake was concerned; the type of introduced surface groups that made a difference in basic and acidic properties of sorbents was possibly a critical parameter affecting difference in capture capacities.

4.6 Acknowledgement

The authors thank CelluForce Inc. for providing the unmodified NCC material and gratefully acknowledge the financial support of the Natural Sciences and Engineering Research Council (NSERC) of Canada.

4.7 References

[1] F. Rezaei, A. A. Rownaghi, S. Monjezi, R. P. Lively, and C. W. Jones, "SOx/NOx Removal from Flue Gas Streams by Solid Adsorbents: A Review of Current Challenges and Future Directions," *Energy and Fuels*, vol. 29, no. 9, pp. 5467–5486, 2015, doi: 10.1021/acs.energyfuels.5b01286.

[2] E. Sugawara and H. Nikaido, "EIA energy outlook 2020," *Antimicrob. Agents Chemother.*, vol. 58, no. 12, pp. 7250–7257, 2019.

[3] S. O. R. Program, "SO_2 Scrubbing Technologies : A Review," vol. 20, no. 4, pp. 219–228, 2001.

[4] M. A. Hanif, N. Ibrahim, and A. Abdul Jalil, "Sulfur dioxide removal: An overview of regenerative flue gas desulfurization and factors affecting desulfurization capacity and sorbent regeneration," *Environ. Sci. Pollut. Res.*, vol. 27, no. 22, pp. 27515–27540, 2020, doi: 10.1007/s11356-020-09191-4.

[5] A. Khaleque, M. M. Alam, M. Hoque, Sh. Mondal, J. B. Haider, "Zeolite synthesis from low-cost materials and environmental applications: A review," *Environ. Adv.*, vol. 2, no. August, p. 100019, 2020, doi: 10.1016/j.envadv.2020.100019.

[6] U. Tumuluri, M. Li, B. G. Cook, B. Sumpter, S. Dai, and Z. Wu, "Surface Structure Dependence of SO2 Interaction with Ceria Nanocrystals with Well-Defined Surface Facets," *J. Phys. Chem. C*, vol. 119, no. 52, pp. 28895–28905, 2015, doi: 10.1021/acs.jpcc.5b07946.

[7] H. Wu, W. Cai, M. Long, H. Wang, Zh. Wang, Ch. Chen, X. Hu, X. Yu, "Sulfur Dioxide Capture by Heterogeneous Oxidation on Hydroxylated Manganese Dioxide," *Environ. Sci. Technol.*, vol. 50, no. 11, pp. 5809–5816, 2016, doi: 10.1021/acs.est.5b05592.

[8] C. Reviews, "Introduction to Metal − Organic Frameworks," pp. 673–674, 2012.

[9] Y. Mathieu, M. Soulard, J. Patarin, and M. Molière, "Mesoporous materials for the removal of SO_2 from gas streams," *Fuel Process. Technol.*, vol. 99, pp. 35–42, 2012, doi: 10.1016/j.fuproc.2012.02.005.

[10] D. J. Babu, D. Puthusseri, F. Kühl, Sh. Okeil, M. Bruns, M. Hampe, J. chneider, "SO_2 gas adsorption on carbon nanomaterials: A comparative study," *Beilstein J. Nanotechnol.*, vol. 9, no. 1, pp. 1782–1792, 2018, doi: 10.3762/bjnano.9.169.

[11] U. Narkiewicz, A. Pietrasz, I. Pełech, and W. Arabczyk, “Removal of SO 2 from gases on carbon materials,” *Polish J. Chem. Technol.*, vol. 14, no. 1, pp. 41–45, 2012, doi: 10.2478/v10026-012-0057-6.

[12] K. J. Shah and T. Imae, “Selective Gas Capture Ability of Gas-Adsorbent-Incorporated Cellulose Nanofiber Films,” *Biomacromolecules*, vol. 17, no. 5, pp. 1653–1661, 2016, doi: 10.1021/acs.biomac.6b00065.

[13] I. Dahlan, G. U. I. M. Mei, A. H. Kamaruddin, A. R. Mohamed, and K. T. Lee, “REMOVAL OF SO_2 AND NO OVER RICE HUSK ASH (RHA)/ CaO-SUPPORTED METAL OXIDES 2 . Materials and Methods,” *Sci. Technol.*, vol. 3, no. 2, pp. 109–116, 2008.

[14] S. Gupta and N. H. Tai, “Carbon materials as oil sorbents: A review on the synthesis and performance,” *J. Mater. Chem. A*, vol. 4, no. 5, pp. 1550–1565, 2016, doi: 10.1039/c5ta08321d.

[15] D. Liu, B. Li, J. Wu, and Y. Liu, “Sorbents for hydrogen sulfide capture from biogas at low temperature: a review,” *Environ. Chem. Lett.*, vol. 18, no. 1, pp. 113–128, 2020, doi: 10.1007/s10311-019-00925-6.

[16] M. B. Shakoor, A. Shafaqat, R. Muhammad, A. Farhat, B. Irshad, “A review of biochar-based sorbents for separation of heavy metals from water,” *Int. J. Phytoremediation*, vol. 22, no. 2, pp. 111–126, 2020, doi: 10.1080/15226514.2019.1647405.

[17] M. S. Shafeeyan, W. M. A. W. Daud, A. Houshmand, and A. Shamiri, “A review on surface modification of activated carbon for carbon dioxide adsorption,” *J. Anal. Appl. Pyrolysis*, vol. 89, no. 2, pp. 143–151, 2010, doi: 10.1016/j.jaap.2010.07.006.

[18] X. Yu, J. Hao, Z. Xi, T. Liu, Y. Lin, and B. Xu, “Investigation of low concentration SO_2 adsorption performance on different amine-modified Merrifield resins,” *Atmos. Pollut. Res.*, vol. 10, no. 2, pp. 404–411, 2019, doi: 10.1016/j.apr.2018.08.015.

[19] M. L. Gray, Y. Soong, K. J. Champagne, H. Pennline, J. P. Baltrus, R.W. Stevens, R. Khatri, S.S.C. Chuang, T. Filburn, “Improved immobilized carbon dioxide capture sorbents,” *Fuel Process. Technol.*, vol. 86, no. 14–15, pp. 1449–1455, 2005, doi: 10.1016/j.fuproc.2005.01.005.

[20] Y. Zhi, Y. Zhou, W. Su, Y. Sun, and L. Zhou, “Selective adsorption of SO2 from flue gas on triethanolamine-modified large pore SBA-15,” *Ind. Eng. Chem. Res.*, vol. 50, no. 14, pp. 8698–8702, 2011, doi: 10.1021/ie2004658.

[21] T. T. N. Bachelor and P. Toochinda, “Development of low-cost amine-enriched solid sorbent for CO_2 capture,” *Environ. Technol. (United Kingdom)*, vol. 33, no. 23, pp. 2645–2651, 2012, doi: 10.1080/09593330.2012.673014.

[22] B. Samojeden and T. Grzybek, “The influence of nitrogen groups introduced onto activated carbons by high- or low-temperature NH3 treatment on SO_2 sorption capacity,” *Adsorpt. Sci. Technol.*, vol. 35, no. 5–6, pp. 572–581, 2017, doi: 10.1177/0263617417702153.

[23] F. Sun, J. Gao, X. Liu, Y. Yang, and S. Wu, "Controllable nitrogen introduction into porous carbon with porosity retaining for investigating nitrogen doping effect on SO_2 adsorption," *Chem. Eng. J.*, vol. 290, pp. 116–124, 2016, doi: 10.1016/j.cej.2015.12.044.

[24] R. S. Varma, "Biomass-Derived Renewable Carbonaceous Materials for Sustainable Chemical and Environmental Applications," *ACS Sustain. Chem. Eng.*, vol. 7, no. 7, pp. 6458–6470, 2019, doi: 10.1021/acssuschemeng.8b06550.

[25] J. Tang, J. Sisler, N. Grishkewich, and K. C. Tam, "Functionalization of cellulose nanocrystals for advanced applications," *J. Colloid Interface Sci.*, vol. 494, pp. 397–409, 2017, doi: 10.1016/j.jcis.2017.01.077.

[26] S. Hokkanen, A. Bhatnagar, and M. Sillanpää, "A review on modification methods to cellulose-based adsorbents to improve adsorption capacity," *Water Res.*, vol. 91, pp. 156–173, 2016, doi: 10.1016/j.watres.2016.01.008.

[27] L. Wojnárovits, C. M. Földváry, and E. Takács, "Radiation-induced grafting of cellulose for adsorption of hazardous water pollutants: A review," *Radiat. Phys. Chem.*, vol. 79, no. 8, pp. 848–862, 2010, doi: 10.1016/j.radphyschem.2010.02.006.

[28] B. Zhu, T. Fan, and D. Zhang, "Adsorption of copper ions from aqueous solution by citric acid modified soybean straw," *J. Hazard. Mater.*, vol. 153, no. 1–2, pp. 300–308, 2008, doi: 10.1016/j.jhazmat.2007.08.050.

[29] F. L. Bernard, D. Rodrigues, B.B. Polesso, V.V. Chaban, M.Seferin, F.D. Vacchia, S. Einloft, "Development of inexpensive cellulosebased sorbents for carbon dioxide," *Brazilian J. Chem. Eng.*, vol. 36, no. 1, pp. 511–521, 2019, doi: 10.1590/0104-6632.20190361s20170182.

[30] N. Johar, I. Ahmad, and A. Dufresne, "Extraction, preparation and characterization of cellulose fibres and nanocrystals from rice husk," *Ind. Crops Prod.*, vol. 37, no. 1, pp. 93–99, 2012, doi: 10.1016/j.indcrop.2011.12.016.

[31] P. De Cuadro, B. Tiina K. Katri, R. Mehedi, K. Eero, V. Tapani, H. Mark, "Cross-linking of cellulose and poly(ethylene glycol) with citric acid," *React. Funct. Polym.*, vol. 90, pp. 21–24, 2015, doi: 10.1016/j.reactfunctpolym.2015.03.007.

[32] C. H. Yu, C. H. Huang, and C. S. Tan, "A review of CO2 capture by absorption and adsorption," *Aerosol Air Qual. Res.*, vol. 12, no. 5, pp. 745–769, 2012, doi: 10.4209/aaqr.2012.05.0132.

[33] R. D. S. Bezerra, M. M. F. Silva, A. I. S. Morais, M. R. M. C. Santos, C. Airoldi, and E. C. Silva Filho, "Natural cellulose for ranitidine drug removal from aqueous solutions," *J. Environ. Chem. Eng.*, vol. 2, no. 1, pp. 605–611, 2014, doi: 10.1016/j.jece.2013.10.016.

[34] L. S. Silva, L.C.B. Lima, F. Ferreira, M.S. Silva, J. Osajima, R.D.S. Bezerra, E. F. Silva, "Sorption of the anionic reactive red RB dye in cellulose: Assessment of kinetic,

thermodynamic, and equilibrium data," *Open Chem.*, vol. 13, no. 1, pp. 801–812, 2015, doi: 10.1515/chem-2015-0079.

[35] L. Segal, J. J. Creely, A. E. Martin, and C. M. Conrad, "An Empirical Method for Estimating the Degree of Crystallinity of Native Cellulose Using the X-Ray Diffractometer," *Text. Res. J.*, vol. 29, no. 10, pp. 786–794, 1959, doi: 10.1177/004051755902901003.

[36] E. C. Silva Filho, L. C. B. Lima, F. C. Silva, K. S. Sousa, M. G. Fonseca, and S. A. A. Santana, "Immobilization of ethylene sulfide in aminated cellulose for removal of the divalent cations," *Carbohydr. Polym.*, vol. 92, no. 2, pp. 1203–1210, 2013, doi: 10.1016/j.carbpol.2012.10.031.

[37] E. C. da Silva Filho, J. C. P. de Melo, and C. Airoldi, "Preparation of ethylenediamine-anchored cellulose and determination of thermochemical data for the interaction between cations and basic centers at the solid/liquid interface," *Carbohydr. Res.*, vol. 341, no. 17, pp. 2842–2850, 2006, doi: 10.1016/j.carres.2006.09.004.

[38] A. Pala, A. Kondorc, S. Mitrad, K. Thua, S. Harishb, B. Baran Saha, " On surface energy and acid–base properties of highly porous parent and surface treated activated carbons using inverse gas chromatography" J. Ind. Eng. Chem., vol 69, pp. 432–443, 2019, doi: .0.1016/j.jiec.2018.09.046.

5 CONCLUSIONS AND RECOMMENDATIONS

5.1 Conclusions and general discussion

The research goal was to develop an adsorbent to capture SO_2 at relatively low temperatures. To improve SO_2 adsorption capacity, modifications of the chemical properties of nanocrystalline cellulose surface were performed by incorporating amine surface groups using Ethylenediamine. Since SO_2 is a weak Lewis acid that can interact with electron donors; therefore, the presence of basic nitrogen-containing surface groups provided adsorbents capable of interacting with SO_2 via electrophilic-nucleophilic interaction.

Nanocellulose crystalline was selected since it is the most abundant natural polymer, low-cost, versatile material, and sustainable, thermodynamically stable, presenting the crystalline structure and numerous hydrogen bonds. It undergoes functionalization primarily through the hydroxyl groups.

Ethylenediamine functionalized-NCC was prepared via a green and non-toxic method. The use of halogenated solvents to make a good leaving functional group through halogen on cellulose was abandoned, then characterized and tested for SO_2 capture application. Sorbents were prepared at different reaction conditions of time, temperature, and EDA contents. It is found that temperature and time of sorbents preparation significantly influence the capture capacity of sorbents, and the effect of time was pronounced than temperature and EDA contents. From the FTIR results and the decrease in XRD peak intensity, it was concluded that with increasing temperature and time, more amino functional groups may be deposited on the cellulose surface. As the amount of amine groups increases, more SO_2 gas is adsorbed by the adsorbent. The results were also compared with NCC and concluded that lower adsorption capacity of NCC is probably because of physisorption, in the event that besides physisorption, chemisorption through amine functional groups could be a key parameter of increasing capture capacity. The effect of temperature and flow rate on SO_2 capture capacity was investigated. The results showed that increasing temperature has adversely affected capture capacity as the adsorption is exothermic. Also, an enhancement in flow rate resulted in a significant decrease in breakthrough time due to faster movement of the mass transfer zone.

The two-step chemical modification of NCC with citric acid followed by ethylenediamine was also performed. This method created both amide and amine functional groups on the NCC surface. The potential of the obtained compounds for use as sorbents for SO_2 capture was evaluated. The experimental results revealed that the increase in sorption capacity in the order of NCC< CA-NCC< EDA-CA-NCC. The performance of CA-NCC is inferior to that of EDA-CA-NCC; this is probably because the carboxylic group cannot chemically bind SO_2 in the -NH-NH_2 configuration. In turn, separating -NH- and -NH_2 by one methylene group results in a more decent SO_2 capture.

By comparing the SO_2 capture results of EDA-NCC prepared in one step (chapter 3) and EDA-CA-NCC prepared in two steps (chapter 4), we found that EDA-NCC has a higher capture capacity. The capture capacity results at RT and flow rate 20 ml/min indicated that capacity of 0.0056 mg_{SO2} /100 $mg_{sorbent}$ for the Cellulose enriched with EDA (contains amide and amine functional groups) is higher than that obtained for CA-EDA (0.0023 mg SO_2/100mg sorbent) and lower than the sorption values obtained for the sample contains only EDA (0.029345 mg/100 $mg_{sorbent}$) which was prepared at 70^{o}C for 8 hr and EDA/NCC=25 in one step. This was possibly due to the differences in the type of introduced surface groups. Because in EDA-CA-NCC, besides amine groups, we have carboxylic and amide groups, which have less basic strength than amine groups, and the SO_2 adsorption capacity on an ammonia-treated NCC was affected highly by N-containing moieties and oxygen-containing groups negatively affected SO_2 capture due to their acidic character.

5.2 Recommendations for Future Work

The application of cellulose as a gas adsorbent with efficient removal of acid gas was investigated through this study; however, further efforts are still required to modify and/or design the cellulose structure at a molecular level, improve the adsorption capacity, regenerate the cellulose, and separate the adsorbate. The recommendations for future work based on the results of this dissertation are summarized below:

1) In this investigation, the incoming gas was pure SO_2. However, in real-world situations, such as natural gas or industrially produced gas, the stream like CO_2 fractions differ and are along with certain pollutants. As a result, to evaluate interference/competition effects,

it is advisable to introduce feed gas that is similar to the actual condition at the same operating temperature and pressure.

2) Water content is commonly coupled with natural/produced gas, and it can affect adsorption. As a result, the influence of H_2O on SO_2 adsorption should be considered.
3) When compared to pristine cellulose, the obtained results showed that an optimal amount of nitrogen functionalization can improve adsorption capacity. As a result, it is recommended that a technique be used to manage nitrogen loading to maximize adsorption capacity.
4) In this project, the reaction time was a maximum of 8 hours, which gave the best gas adsorption result. Further study of the effect of longer time on the functionalization of cellulose is needed and in order to know the amount of amine groups, elemental analysis should be used.
5) Due to time constraints, the desorption characteristics study was limited in this study. Additional research into cellulose regeneration and SO_2 sequestration is still needed. The effect of several parameters on functionalized NCC regeneration, such as temperature, time duration, cycle numbers, and purging gas, could be an intriguing area for future research.
6) Molecular dynamic (MD) software is frequently used to simulate complex systems that consider atom position over time. The author recommends using MD to consider a system's space and time evolution involving millions of atoms.

6 Appendix

Capture Capacity Calculations

The SO_2 capture capacity was calculated using the following formula:

The ($\int C_i$ - C_o) dT term was calculated by subtracting the area under the curve of the blank and sample and the calculation sequence was followed:

Area under $Blank$ curve – Area under $Sample$ curve = $Amount\ Adsorbed\ (ppm.\ min)$

The area under the curve was calculated with the help of area under the curve using Trapezoidal rule using recorded concentration with time from the SO_2 detector:

$$Area\ under\ the\ curve = \sum_{t=0}^{t=(t-1)} \{0.5 \times (y_2 + y_1) \times (x_2 - x_1)\} = a.ppm.min$$

Multiplying the amount adsorbed with the flow rate during the reaction:

$$a.ppm.min \times f\frac{ml}{min} = (a \times f)ppm.ml$$

Applying the unit conversion:

$$= (a \times f)ppm.ml \times 10^{-6} \frac{\frac{mol\ SO_2}{mol}}{ppm} \times \frac{mol}{22400\ ml} \times \frac{64\ g\ SO_2}{mol\ SO_2}$$

Dividing the above equation with the mass of sample taken m = 50 mg

$$= \frac{(a \times f) \times 10^{-6} \times 64\ g\ SO_2}{22400} \times \frac{1000\ mg}{g} \times \frac{1}{50\ mg\ sample} \times 100$$

$$= [(a \times f) \times (5.714 \times 10^{-6})] \frac{mg}{100\ mg\ sorbent}$$

This is the final equation obtained.

Acid-Base Titration Calculation

$$\text{Hydroxyl content}\left(\frac{mmol}{\text{g NCC}}\right) = \frac{(C_{NaOH} \times V_{NaOH}) - (C_{HCl} \times V_{HCl})}{\text{mass of NCC}} = \frac{(0.01 \times 10) - (0.01 \times 3.2)}{0.03}$$
$$= 2.27\ mmol/g$$

$$\text{Carboxylic acid content}\left(\frac{mmol}{\text{g CA} - \text{NCC}}\right) = \frac{(C_{NaOH} \times V_{NaOH}) - (C_{HCl} \times V_{HCl})}{\text{mass of CA} - \text{NCC}}$$
$$= \frac{(0.01 \times 10) - (0.01 \times 4.3)}{0.03} = 1.90\ mmol/g$$

$$\text{Amine content}\left(\frac{mmol}{\text{g EDA} - \text{CA} - \text{NCC}}\right) = \frac{(C_{HCl} \times V_{HCl}) - (C_{NaOH} \times V_{NaOH})}{\text{mass of CA} - \text{NCC}}$$
$$= \frac{(0.01 \times 10) - (0.01 \times 4.8)}{0.03} = 1.73\ mmol/g$$

Where C_{NaOH} is the concentration of the NaOH solution (mol/L), C_{HCl} is the concentration of the HCl solution (mol/L), V_{NaOH} is the volume of the NaOH solution, and V_{HCl} is the volume of HCl solution.